

THE ROLE OF MAGNESIUM IN CONCRETE DETERIORATION

**Final Report
November 1994**

Iowa DOT HR-355

**Submitted to the Project Development Division
of the Iowa Department of Transportation
and
The Iowa Highway Research Board**

**Robert D. Cody, Paul G. Spry,
Anita M. Cody, and Guo-Liang Gan
Department of Geological and Atmospheric Sciences
Iowa State University
Ames, IA 50011**

DISCLAIMER

The contents of this report do not represent a warranty on the products used on behalf of the State of Iowa, Iowa State University, Iowa Department of Transportation, Highway Research Board, or the authors. The opinions, findings, and conclusions expressed in this publication are those of the authors and not necessarily those of the Highway Division or Project Development Division of the Iowa Department of Transportation. The responsibility for the use of information in this report remains with the user. This report is for information purposes and is made available with the understanding that it will not be cited without the permission of the authors.

TABLE OF CONTENTS

	Page No.
LIST OF PLATES	vi
LIST OF FIGURES	vii
LIST OF TABLES	viii
ABSTRACT	ix
INTRODUCTION	1
DETERIORATION OF IOWA CONCRETES	1
MAGNESIUM AS A POTENTIAL CAUSE OF CONCRETE DETERIORATION	2
OBJECTIVES OF RESEARCH	3
<p style="text-align: center;">PART I. THE CHEMICAL CHARACTERISTICS OF IOWA HIGHWAY CONCRETES CONTAINING DOLOMITE COARSE AGGREGATE</p>	
RESEARCH PROCEDURES	5
COLLECTION OF HIGHWAYS CONCRETE	5
GENERAL PROCEDURES AND INSTRUMENTATION	5
GENERAL CHARACTERISTICS OF IOWA HIGHWAY CONCRETE	7
CRYSTALLINITY AND CRYSTAL SIZE OF THE DOLOMITE AGGREGATES	7
CHEMICAL COMPOSITION OF DOLOMITE AGGREGATES	8
CEMENT PASTE	11
CHEMICAL COMPOSITION OF COARSE AGGREGATE/PASTE INTERFACE	12
NON-DURABLE CONCRETES	12
Reaction Rim Development	12
Electron Microprobe Analysis of Non-Durable Concrete	
Reaction Rims	14
DURABLE CONCRETES	17
Rim Development and Electron Microprobe Analyses	17

	Page No.
DISCUSSION	18
CAUSES OF CONCRETE DETERIORATION	18
POSITIVE, NEGATIVE, AND NEUTRAL REACTION	
RIMS IN CONCRETE	19
RIM DEVELOPMENT SEQUENCES	20
COMPARISON OF RIM SEQUENCES	21
MECHANISM OF DEDOLOMITIZATION-INDUCED CONCRETE	
DETERIORATION	22
The Alkali-Dolomite Reaction	22
Volume Changes Resulting from Dedolomitization	23
SIGNIFICANCE OF REACTION RIMS IN IOWA	
DOLOMITE AGGREGATE CONCRETES	25
MAGNESIUM AND CONCRETE DETERIORATION	28
PART II. EXPERIMENTAL STUDY OF THE DETERIORATION OF IOWA HIGHWAY CONCRETE	
INTRODUCTION	29
EXPERIMENTAL METHODS	30
STARTING MATERIALS	30
EXPERIMENTS	30
Wet/Dry (W/D) Experiments	31
Freeze/Thaw (F/T) Experiments	31
Continuous Immersion	31
End of Experiment Procedures	31
EXPERIMENTAL RESULTS	32
X-RAY DIFFRACTION ANALYSES OF TREATED CONCRETES	32
EFFECTS OF WATER	32
EFFECTS OF MAGNESIUM CHLORIDE SOLUTIONS	33
Deterioration of Concretes	33
Experimentally Induced Rim Formation	34
EFFECTS OF CALCIUM CHLORIDE SOLUTIONS	35
Deterioration of Concretes	35
Experimentally Induced Rim Formation	35
EFFECTS OF SODIUM CHLORIDE SOLUTIONS	36

DISCUSSION	37
GENERAL OBSERVATIONS	37
SIGNIFICANCE OF EXPERIMENTAL RESULTS	38
PART III. GENERAL CONCLUSIONS AND RECOMMENDATIONS	
GENERAL CONCLUSIONS	40
ULTIMATE CAUSE OF CONCRETE DETERIORATION	40
DIRECT CAUSE OF CONCRETE DETERIORATION	41
ALKALI-DOLOMITE REACTIONS AND THE NATURE OF COARSE AGGREGATES	42
ROLE OF MAGNESIUM IN CONCRETE DETERIORATION	43
ROLE OF ROCK SALT DEICERS IN ACCELERATING DETERIORATION	44
RECOMMENDATIONS	44
ACKNOWLEDGMENTS	45
APPENDIX. REPRESENTATIVE ELECTRON MICROPROBE ANALYSES OF CARBONATE AGGREGATE IN IOWA CONCRETE (Under Separate Cover)	46
REFERENCES	47
PLATES	51
FIGURES	107

LIST OF PLATES

Plate Number	Page No.
PART I	
I. Core samples of Iowa high concrete.	53
II. SEM micrographs of non-durable and durable concretes	57
III. SEM and light micrographs of concretes.	61
IV. Light and SEM micrographs of Smith quarry concrete and Paralta quarry concrete.	65
V. Light and SEM micrographs of Paralta concrete and Smith quarry concrete.	69
VI. Light and SEM micrographs of durable Mar-Jo Hills and Sundheim quarry concretes.	73
VII. Light and SEM micrographs of durable Mar-Jo Hills and Sundheim and non-durable Smith quarry concretes.	77
PART II	
VIII. Experimentally-produced deterioration of Iowa concretes.	81
IX. Experimentally-produced deterioration of concrete containing Smith, Garrison, Sundheim, and Mar-Jo Hills dolomite coarse aggregate.	85
X. Experimental deterioration of concretes and micrographs of treated materials.	89
XI. Experimental deterioration of concretes. Light and SEM micrographs of concretes containing Paralta and Smith aggregate.	93
XII. Experimental deterioration of concretes. Light micrographs of aggregate-paste interfaces, durable Mar-Jo Hills aggregate concrete.	97
XIII. Experimental deterioration of concretes. SEM and light micrographs of Mar-Jo Hills and Garrison aggregate concretes.	101
XIV. Experimental deterioration of concretes. Light and SEM micrographs of concrete containing Paralta aggregate.	105

LIST OF FIGURES

Figure Number	Page No.
PART I	
Fig 1. Electron microprobe traverse across non-durable concrete containing Smith quarry aggregate.	109
Fig 2. EDAX element maps of Smith quarry concrete.	111
Fig 3. Electron microprobe traverse across non-durable concrete containing Smith quarry aggregate.	113
Fig 4. EDAX element maps of Smith quarry concrete.	115
Fig 5. EDAX element maps of Paralta quarry concrete.	117
Fig 6. Electron microprobe traverse across non-durable concrete containing Paralta quarry concrete.	119
Fig 7. Electron microprobe traverse across non-durable Smith quarry concretes.	121
Fig 8. EDAX element maps of non-durable Smith quarry concrete.	123
Fig 9. EDAX element maps of non-durable Smith quarry concrete.	125
Fig 10. Electron microprobe traverse across durable concrete containing Mar-Jo Hills quarry aggregate.	127
Fig 11. Electron microprobe traverse across durable concrete containing Sundheim quarry aggregate.	129
Fig 12. EDAX element maps of durable concrete containing Sundheim quarry aggregate.	131
Fig 13. Electron microprobe traverse across durable concrete containing Sundheim quarry aggregate.	133
Fig 14. Electron microprobe traverse across durable concrete containing Mar-Jo Hills quarry aggregate.	135
Fig 15. Electron microprobe traverse across durable concrete containing Sundheim quarry aggregate.	137
Fig 16. Fig 16. EDAX element maps for concrete containing Mar-Jo Hills quarry aggregate.	139
Fig 17. EDAX element maps for concrete containing Smith quarry aggregate.	141
PART II	
Fig 18. Experimental decomposition of concrete. EDAX element maps of concrete containing Garrison quarry aggregate after wet/dry cycling in Ca solution.	143
Fig 19. Experimental decomposition of concrete. Electron microprobe traverse across concrete containing Paralta quarry aggregate after wet/dry cycling in Ca solution.	145
Fig 20. Experimental decomposition of concrete. EDAX element maps of concrete containing Paralta quarry aggregate after wet/dry cycling in Ca solution.	147
Fig 21. Experimental decomposition of concrete. EDAX of high magnification of area shown in Fig 20.	149
Fig 22. Experimental decomposition of concrete. Electron microprobe traverse of concrete containing Paralta quarry aggregate after freeze/thaw cycling in Ca solution.	151

Figure Number	Page No.
Fig 23. Experimental decomposition of concrete. Electron microprobe traverse of concrete containing Smith quarry aggregate after wet/dry cycling in Ca solution.	153
Fig 24. Experimental decomposition of concrete. Electron microprobe traverse of concrete containing Mar-Jo Hills quarry aggregate after wet/dry cycling in Ca solution.	155
Fig 25. Experimental decomposition of concrete. Electron microprobe traverse of concrete containing Mar-Jo Hills quarry aggregate after freeze/thaw cycling in Ca solution.	157
Fig 26. Experimental decomposition of concrete. Electron microprobe traverse of concrete containing Mar-Jo Hills quarry aggregate after freeze/thaw cycling in Mg solution.	159
Fig 27. Experimental decomposition of concrete. EDAX element maps of concrete containing Mar-Jo Hills quarry aggregate after wet/dry cycling in Mg solution.	161
Fig 28. Experimental decomposition of concrete. EDAX element map of concrete containing Mar-Jo Hills quarry aggregate after wet/dry cycling in Mg solution.	163
Fig 29. Experimental decomposition of concrete. Electron microprobe traverse of concrete containing Paralta quarry aggregate after wet/dry cycling in Mg solution.	165
Fig 30. Experimental decomposition of concrete. EDAX element maps of concrete containing Garrison quarry aggregate after wet/dry cycling in Mg solution.	167
Fig 31. Experimental decomposition of concrete. Electron microprobe traverse of concrete containing Paralta quarry aggregate after wet/dry cycling in Na solution.	169
Fig 32. Experimental decomposition of concrete. EDAX element maps concrete containing Paralta quarry aggregate after wet/dry cycling in Na solution.	171

LIST OF TABLES

Table Number	Page No.
I. Core Locations, Service Records, and Aggregate Sources	4
II. Chemical Composition of Dolomite Aggregate (Electron Microprobe Data)	10
III. Chemical Composition of Dolomite Aggregate (Iowa DOT Chemical Analysis Data, Average)	11
IV. A Summary of Concrete Experiments	33

ABSTRACT

for the final report on HR 355:

The Role of Magnesium in Concrete Deterioration

Robert D. Cody

Paul G. Spry

Anita M. Cody

Guo-Liang Gan

Concretes with service lives of less than 15 years and those with lives greater than 40 years were studied with petrographic microscope, scanning electron microscope, and electron microprobe to determine why these two groups of concrete exhibit such different degrees of durability under highway conditions. Coarse aggregate used in both types of concrete were from dolomite rock, but investigation revealed that that dolomite aggregate in the two groups of concretes were much different in several respects. The poorly-performing aggregate is fine-grained, has numerous euhedral and subhedral dolomite rhombohedra, and relatively high porosity. Aggregate from durable concrete is coarse-grained, tightly interlocked crystal fabric, anhedral dolomite boundaries, and low porosity. Aggregate in short service life concrete was found to have undergone pervasive chemical reactions with the cement which produced reaction rims on the boundaries of coarse aggregate particles and in the cement region adjacent to aggregate boundaries. Textural and porosity differences are believed to be chiefly responsible for different service lives of the two groups of concrete.

The basic reaction that has occurred in the short service life concretes is between coarse aggregate and cement is an alkali-dolomite reaction. In the reaction dolomite from the aggregate reacts with hydroxide ions from the cement to free magnesium ions and carbonate ions, and the magnesium ions precipitate as brucite, $Mg(OH)_2$. Simultaneously with this reaction, a second reaction occurs in which product carbonate ions react with portlandite from the cement to form calcite and hydroxide ions. Crystal growth pressures of newly formed brucite and calcite together with other processes, e.g. hydration state changes of magnesium chloride hydrates, lead to expansion of the concretes with resultant rapid deterioration.

According to this model, magnesium from any source, either from reacting dolomite or from magnesium road deicers, has a major role in highway concrete deterioration. Consequently, magnesium deicers should be used with caution, and long-term testing of the effects of magnesium deicers on highway concrete should be implemented to determine their effects on durability

INTRODUCTION

DETERIORATION OF IOWA CONCRETES

Premature failures of concrete in highways are due predominantly to deterioration of joints and cracks. This deterioration is generally referred to as D-cracking, which has been defined as "cracking in a slab surface in a pattern that appears first in an orientation parallel to transverse and longitudinal joints and cracks, continues around corners, and may progress into the central area of the slab" (Girard et al. 1982). This type of portland cement concrete pavement deterioration was first recognized in Iowa's primary road system in the late 1930s. Since 1960, extensive research into the mechanism of D-cracking, and methods of preventing and reducing D-cracking, has been conducted. Marks and Dubberke's (1982) research revealed that most D-cracking in Iowa results predominantly from freeze/thaw failure in the coarse aggregate. Based on this finding, Iowa began using ASTM C666 Method B, "Freezing in Air - Thawing in Water" to evaluate the durability of concrete. The basic tests currently used in Iowa to evaluate the quality of coarse aggregate for concrete, are abrasion by AASHTO T96 and a 16-cycle water-alcohol freeze/thaw test (Marks and Dubberke 1982). These tests effectively exclude argillaceous materials and have been a part of the standard specifications for 40 years (Dubberke and Marks 1987a).

Since 1978, considerable research at the Iowa DOT has focused on the pore system of limestones used as coarse aggregate in concrete and its relationship to freeze/thaw failure (Myers and Dubberke 1980; Dubberke 1983). Their results showed that most non-durable aggregate exhibit a predominance of pore sizes in the 0.04 - 0.2 μm (micron) radius range, and aggregates that do not exhibit a predominance of these pore sizes are generally less prone to freeze/thaw deterioration. Pitt et al. (1989) revealed similar results — aggregates exhibiting the best performance tend to have the fewest pores in the size range 0.05 - 0.5 μm radius. In 1978, the Iowa Pore Index Test was adapted as a standard test (Myers and Dubberke 1980). The Iowa Pore Index Test is a very simple test utilizing a

modified pressure meter as a test apparatus. A known volume of oven-dried coarse aggregate is immersed in water at the base of the pressure meter. The volume of water injected into the aggregate under a constant 35 psi pressure during the period between 1 and 15 minutes after the application of this pressure is referred as the pore index. The available test results show that limestone aggregate with pore indexes of 27 ml are susceptible to freeze/thaw D-cracking deterioration (Myers and Dubberke 1980; Marks and Dubberke 1982).

Although these tests have been relatively effective in yielding durable concrete, exceptions continue to occur and which result in rapid deterioration of recently constructed pavements. This suggests that there should be other factors that contribute to the rapid deterioration of highways. Probable factors influencing concrete service life are chemical reactions of various types between coarse aggregate and the paste which weaken aggregate-paste bonds. One such reaction involves coarse aggregate composed of clay-rich carbonate rocks. Reactions between aggregate and paste result in rims with increased silica concentrations on the outer margins of the aggregate. This feature is referred to as rim silification (Bisque and Lemish 1958; Mather 1974). Another reaction involves concretes containing certain types of dolomite aggregate. Many concretes containing this type of aggregate have undergone reactions that result in rims with reduced magnesium, this reaction has been described as the alkali-carbonate reaction (Mather 1974; Tang et al. 1991; Poole 1981; Poole and Sotiropoulos 1980). There is also evidence that deicing salt applications may accelerate concrete deterioration, especially for concretes containing coarse aggregates that have undergone adverse reactions with the paste (Dubberke and Marks 1985).

MAGNESIUM AS A POTENTIAL CAUSE OF CONCRETE DETERIORATION

One of the potentially deleterious chemical reactions between coarse aggregate and paste involves magnesium. Two contradictory conclusions have been proposed for the role

of magnesium in concrete deterioration. Observations made by personnel of the Iowa DOT seem to indicate that magnesium released into the portland cement concrete paste from certain types of dolomite aggregate particles may play a role in the deterioration of Iowa highway concrete (Dubberke, Myers, and Rippe, pers. comm. 1992). Alternatively, several experimental studies seem to indicate that magnesium chloride is a safer and more effective road deicer than rock salt and that its use might be beneficial for use on Iowa highways (Sayward 1984; Pitt et al. 1989; Cargill Co., pers. comm. 1992).

OBJECTIVES OF RESEARCH

The main objective of the current research is to investigate the role of magnesium, which may be introduced into the paste, either from dedolomitization of dolomite coarse aggregate, or from surface-applied magnesium deicers, in the deterioration of Iowa highway concrete. A second objective is to investigate the effects of deicer salt applications on Iowa concretes to determine if magnesium deicers might be less damaging than rock salt, NaCl.

These objectives were accomplished by:

1. Determining the chemical changes that have occurred during deterioration of selected Iowa highway concretes which contain coarse dolomite aggregate from different quarries and geologic formations, and relating these changes to the degree of concrete deterioration.
2. Comparing the chemical changes and characteristics of durable highway concretes having service lives greater than 40 years to those of non-durable concretes which deteriorate significantly after less than 12 years. Both durable and non-durable types contain coarse aggregates which are primarily dolomite.
3. Conducting laboratory experiments to investigate the chemical reactions between magnesium chloride and concrete aggregate-paste, and the effects of these reactions on the deterioration of Iowa concretes which contain dolomite coarse aggregate.

This report of investigations will be presented in three parts. Part I will focus on the chemical characteristics of durable and non-durable Iowa highway concretes, and the major mineralogical and physical characteristics of these two groups of concrete. Part II will deal with experimental studies on the effects of deicer salts on Iowa highway concretes. Part III will present general conclusions on the role of magnesium in highway concrete deterioration.

In the following sections, the term concrete refers to the mixture of portland cement, fine aggregate, and coarse aggregate; paste or cement will be used to indicate the portland cement paste, as distinguished from the fine and coarse aggregates which occurs within the paste; and aggregate, coarse aggregate or dolomite aggregate will be used for the coarse dolomite aggregate used in the concretes.

Table I. Concrete Core Locations, Service Records, and Aggregate Sources

Sample Number	Location of Core	Aggregate Source	Service Record
1	US 63, just north of Buckingham	Smith quarry (Basal Coralville Member, Cedar Valley Formation, Devonian)	12 years
2	US 151, near intersection with IA 13. NE of Cedar Rapids	Paralta quarry (Otis Member, Wapsipinicon Formation, Devonian)	8 years
3	US 218, near intersection with IA 8, east of Vinton	Garrison quarry (Basal Coralville Member, Cedar Valley Formation, Devonian)	15 years
4	US 20, west of Dubuque	Sundheim quarry (Hopkinton Formation, Silurian)	> 40 years
5	E 29, 1/2 mile east of US 65	Ames gravel pit (Skunk river gravels, recent)	8 years
6	E 29 at junction with US 65	Ames gravel pit (Skunk river gravels, recent)	8 years
7	US 52, south of Dubuque	Mar-Jo Hills quarry (Stewartville Member, Galena Formation, Ordovician)	> 40 years

**PART I. THE CHEMICAL CHARACTERISTICS
OF IOWA HIGHWAY CONCRETES CONTAINING
DOLOMITE COARSE AGGREGATE**

RESEARCH PROCEDURES

COLLECTION OF HIGHWAY CONCRETE

Four-inch diameter cores of Iowa highway concrete with different dolomite aggregate sources, service records, and quarry locations were obtained from Iowa highways 20, 29, 52, 63, 65, 151, and 218 by personnel of the Iowa Department of Transportation (Table I, Figs. Ia - If). The coarse aggregates were derived from the Ames gravel pit, and the Smith, Paralta, Garrison, Sundheim, and Mar-Jo Hills quarries (Table I; Plt I). These concretes show a wide variety of service records which, at least partly, are a result of the different coarse aggregate sources.

GENERAL PROCEDURES AND INSTRUMENTATION

The 4-inch diameter cores were first cut longitudinally, and the cut surface was visually inspected and photographed (Plt I). One-half of the core was then cut into small rectangular blocks, approximately 1/2" x 1/2" x 1". Polished thin-sections were made from these blocks and examined by transmitted light utilizing standard polarizing microscope techniques, but the great variety of aggregate particles precluded a detailed mineralogical analysis of coarse aggregates in the samples. Detailed studies emphasized the chemistry of the aggregate/paste interface, as a potential indicator of adverse chemical reactions between dolomite aggregate and paste. Most compositions were obtained with an electron microprobe and a scanning electron microscope (SEM) with energy dispersive x-ray (EDAX) capability. Emphasis was placed on the aggregate/cement paste interface to determine if compositional variations occur within the aggregate particles near their

contact with the paste, because paste-initiated reactions with the dolomite aggregate should commence at that location. X-ray diffraction (XRD) methods were also used to supplement electron microprobe and SEM/EDAX data.

Electron probe microanalysis for Ca, Mg, Si, Na, K, Al, and Fe each reported as oxides, were performed using an automated ARL-SEMQ electron microprobe housed in the Department of Geological and Atmospheric Sciences at Iowa State University. This instrument has wavelength and energy dispersive spectrometers, as well as secondary and backscattered imaging capabilities. Operating conditions included an accelerating voltage of 20 kV and a sample current of 15 nA on a Faraday cup. On-line ZAF corrections employed the PRSUPR program utilizing the method of Donovan et al. (1992). When running profiles across the dolomite aggregate/cement past interface, relatively wide, 10 - 25 μm , steps were first used. The distance between analysis points was later reduced to 1.0 - 5.0 μm in order to minimize the possibility of missing important mineral matter by using step increments that were too large. Over 20,000 data points were obtained by electron microprobe techniques.

Most of the SEM/EDAX studies were conducted using a Hitachi S-2460N instrument, a reduced-vacuum scanning electron microscope located in the Department of Civil Engineering at ISU. An accelerating voltage of 15 kV was used. This instrument has a great advantage compared to conventional SEM in that the reduced vacuum and lack of sample coating reduce the possibility of sample dehydration due to high vacuum. High magnification EDAX area mapping were performed for Si, Al, K, O, Ca, Mg, S, Cl, and Fe. A few samples were examined with the Department of Botany Jeol JSM-35 scanning electron microscope. X-ray diffraction studies with performed a Philips XRG-3100 powder diffractometer in the Department of Geological and Atmospheric Sciences. An accelerating voltage of 30 kV and a current of 20 mA were used.

GENERAL CHARACTERISTICS OF IOWA HIGHWAY CONCRETE

For the purposes of this report, the seven highway concrete cores obtained from the Iowa DOT were divided into two groups based on their service records. The first group consisted of durable concretes which contained coarse aggregate from the Sundheim and Mar-Jo Hills quarries, and the second group was comprised of non-durable concretes containing aggregate from Smith, Paralta, and Garrison quarries, and from the Ames gravel pit. Aggregate sources included rocks of Ordovician (Mar-Jo Hills quarry), Silurian (Sundheim quarry), Devonian (Smith, Paralta, Garrison quarries), and Recent (Ames gravel pit) ages.

With the exception of the Ames gravel, most of coarse aggregate was dolomite with minor amounts of limestone particles present in several of the concretes. The Ames gravel consisted of shale, granite, dolomite, and limestone particles reflecting the diverse source rocks of the gravel. After an initial study, the Ames quarry aggregate was eliminated from further consideration because it was not possible to determine whether chemical alteration of the aggregate occurred before or after deposition of the gravel, or as a result of chemical reactions with the paste.

In the following discussion, illustrative electron microprobe traverses and high-magnification SEM EDAX area maps are shown in Figures 1 - 17. Photographs of cut concrete cores are shown in Plate I, thin-sections and SEM photographs of representative materials are shown in Plates II - VII. Compositional data for traverses across dolomite aggregates are listed in an Appendix which is published under separate cover.

CRYSTALLINITY AND CRYSTAL SIZE OF THE DOLOMITE AGGREGATES

Both petrographic and SEM studies revealed significant differences in the nature of the coarse dolomite aggregate used in the two groups of concrete. In the non-durable

concrete, a major percent of aggregate particles consists of fine-grained dolomite with abundant void spaces between poorly-formed dolomite crystals. Dolomite crystals in non-durable concrete aggregates typically fall within the diameter of 0.005 to 0.05 mm. A representative example is shown in SEM photograph, Plt IIe. In this photograph of Paralta quarry dolomite, the abundant small particles and void spaces, the abundance of subhedral and euhedral dolomite crystals, and the scarcity of tightly interlocking crystals are evident. In durable materials, by contrast, dolomite crystals are extremely well-crystallized and consist of large tightly-intergrown dolomite crystals. Typically these large crystals are anhedral because of the interlocking fabric. Individual dolomite crystals typically have maximum diameters between about 0.05 and 0.50 mm with the majority of crystals near 0.50 mm in size. A representative SEM photograph of durable concrete dolomite aggregate from the Sundheim quarry is shown in Plt IIIf. This photograph shows the closely interlocked nature of dolomite crystals without euhedral crystal forms, and the lack of pores and small discrete particles. Plates IIa - c show SEM and visible-light photographs of the Paralta quarry concrete, a non-durable concrete with service life of about 8 years, whereas Plates IIId-f show similar photographs of Sundheim quarry concrete that has a service life in excess of 40 years.

It was also observed that the fine grain size of the non-durable concrete dolomite aggregate allowed it to react more vigorously with dilute, 10% (by volume), HCl than the coarser-grained aggregate in durable concretes.

CHEMICAL COMPOSITION OF DOLOMITE AGGREGATES

Microprobe and SEM/EDAX analyses indicated that dolomite aggregates in durable and non-durable concretes contain approximately 30 wt % CaO and 20 wt % MgO concentrations which are characteristic of normal dolomite. Theoretical CaO is 30.41 wt % and MgO is 21.86 wt %, with a ratio of CaO/MgO of 1.3911. For the dolomite aggregates analyzed by microprobe, all averaged more calcium than the theoretical values.

Average ratios ranged from $\text{CaO/MgO} = 1.483$ in the Sundheim dolomite to $\text{CaO/MgO} = 1.775$ in the Smith quarry aggregate (Table II). Detailed micro-analysis, however, showed that the high CaO/MgO ratios did not result from an abundance of calcite crystals intergrown with the dolomite. Very little consistent differences in minor elements were observed for durable concrete aggregate compared to those from non-durable concretes. For example, the Mar-Jo Hill quarry, which produced long service life concrete has very low FeO compared to aggregate from Smith, Garrison, and Paralta quarries which produce non-durable concretes, but the Sundheim rock, which also produces durable aggregate had much more FeO than the Mar-Jo Hills aggregate and nearly as much as the Smith, Garrison, and Paralta aggregate.

Bulk analyses by the Iowa DOT (Table III) show similar results, with CaO/MgO ratios in the range of 1.339 for Paralta quarry dolomite and 1.796 for Smith dolomite. Their analyses also found no consistent FeO differences for aggregate producing either durable or non-durable concretes. Their values were consistently higher in Al_2O_3 and SiO_2 . It should be pointed out, however, that the DOT analyses are from whole rocks which include impurity minerals such as quartz and clay minerals, whereas the electron microprobe data are more selective and can usually avoid these impurities. Very tiny mineral inclusions such as clay minerals, however, may be occasionally encountered by the electron beam, and may influence the analytical results

Electron microprobe analysis profiles of calcium and magnesium are rarely perfectly uniform across a dolomite aggregate particle, even though the particle appears to consist entirely of intergrown dolomite crystals (Figs 1, 3, 6, 7, 10, 11, 13-15). Averaged over several 10s of microns, calcium and magnesium concentrations are essentially constant within an aggregate interior, but over shorter distances the concentration profiles exhibit irregular peaks and valleys. If the short-distance variations in magnesium were caused by small calcitic crystals within the dolomite mass, then there should be an increase in calcium corresponding to a magnesium decrease. This correspondence often occurs,

Table II. Chemical Composition of Dolomite Aggregate (Electron Microprobe Data)

Aggregate source	No. Anal.		FeO	K ₂ O	CaO	SiO ₂	Al ₂ O ₃	MgO	SrO	BaO	MnO	Na ₂ O	CO ₂	TOTAL
Smith	168	Min	0.24	0.10	25.12	0.11	0.04	16.93	0.07	0.10	0.13	0.09	46.80	99.49
		Max	2.55	0.41	34.29	3.79	1.01	23.09	0.22	0.33	0.33	0.35	48.47	100.89
		Ave	0.48	0.15	31.04	0.66	0.21	19.57	0.13	0.23	0.20	0.17	47.37	100.21
		S.Dev.	0.28	0.05	1.26	0.59	0.15	0.78	0.03	0.05	0.04	0.05	0.27	0.36
Paralta	172	Min	0.26	0.09	25.69	0.08	0.03	15.69	0.07	0.12	0.14	0.10	46.54	99.02
		Max	3.17	0.24	35.56	2.94	1.57	20.92	0.20	0.44	0.80	0.25	48.25	100.86
		Ave	0.59	0.12	31.01	0.61	0.16	19.10	0.13	0.24	0.21	0.16	47.41	99.76
		S.Dev.	0.45	0.03	1.52	0.60	0.23	1.01	0.03	0.05	0.07	0.03	0.31	0.49
Garrison	20	Min	0.09	0.00	27.90	0.00	0.00	17.56	0.00	0.00	0.00	0.00	45.86	99.00
		Max	2.35	0.20	35.12	2.77	0.67	21.21	0.00	0.00	0.26	0.13	47.53	100.92
		Ave	0.40	0.02	33.30	0.43	0.06	18.76	0.00	0.00	0.02	0.04	46.86	99.89
		S.Dev.	0.48	0.05	1.59	0.73	0.15	0.86	0.00	0.00	0.06	0.04	0.38	0.57
Mar-Jo Hills	64	Min	0.00	0.00	29.97	0.00	0.00	19.32	0.00	0.00	0.00	0.00	45.74	99.58
		Max	0.64	0.18	32.23	2.87	0.56	21.35	0.00	0.03	0.07	0.10	47.86	100.77
		Ave	0.15	0.01	31.56	0.26	0.03	20.67	0.00	0.00	0.01	0.01	47.42	100.10
		S.Dev.	0.10	0.04	0.37	0.55	0.09	0.26	0.00	0.00	0.01	0.02	0.35	0.36
Sundheim	218	Min	0.23	0.09	27.16	0.07	0.03	18.17	0.07	0.11	0.11	0.09	47.20	99.07
		Max	0.56	0.64	31.58	3.55	1.05	21.76	0.21	0.39	0.26	0.33	48.61	100.91
		Ave	0.32	0.13	30.20	0.38	0.12	20.37	0.13	0.24	0.18	0.14	47.56	99.76
		S.Dev.	0.05	0.06	0.61	0.45	0.12	0.53	0.02	0.05	0.02	0.03	0.16	0.41

and usually both MgO and SiO₂ typically increase when CaO decreases. Sometimes, however, there is poor correspondence between excess calcium and reduced magnesium. Most of the short-distance variations in MgO/CaO are due to boundary effects where the microprobe beam stopped fortuitously at a boundary between adjacent dolomite crystals, although presumably, there may also be small regions within dolomite crystals that may be depleted in either magnesium or calcium without replacement of the ion sites by the other cation. Some of the variations may also result from small inclusions of other minerals.

Because the silicon, aluminum, and potassium contents in both durable and non-durable concrete aggregates show strong positive correlation with each other, they indicate the presence of a mineral (or minerals) containing these three elements in abundance.

Clay minerals, and particularly K-rich illite, are the most probable minerals because of their common occurrence in Paleozoic carbonate rocks.

Table III. Chemical Composition of Dolomite Aggregate
(Iowa DOT Chemical Analysis Data, Average)

Aggregate Source	No. Anal.	FeO**	K ₂ O	CaO	SiO ₂	Al ₂ O ₃	MgO	SrO	P ₂ O ₅	MnO	S	CO ₂	TiO ₂	TOTAL
Sundheim	3	0.15	0.20	30.41	2.56	0.49	20.11	0.01	0.01	0.02	0.03	45.82	0.03	99.83
Mar-Jo Hills	13	0.33	0.28	30.75	2.73	0.41	19.48	0.01	0.09	0.05	0.04	45.40	0.00	99.57
Smith	5	0.34	0.14	32.72	1.74	0.40	18.24	0.00	0.02	0.00	0.35	45.59	0.02	99.56
Paralta	8	0.23	0.06	29.47	0.59	0.11	22.01	0.01	0.01	0.03	0.04	47.15	0.01	99.72
Garrison	9	0.62	0.13	32.13	1.57	0.36	18.38	0.01	0.01	0.03	0.66	45.28	0.01	99.19

**FeO is converted from Fe₂O₃ of Iowa DOT Analyses.

CEMENT PASTE

Micro-fractures and larger fractures are much more common in the non-durable pastes than in the durable concretes. Often the fractures parallel aggregate/paste boundaries, however, many fractures apparently are also randomly oriented. Common types of micro-fractures in non-durable concrete containing Smith quarry and Paralta quarry aggregates are shown in Plt IIa and Plt IIb respectively. In Plt IIa the longer fracture is subparallel to the dolomite/paste boundary, but the smaller tributary fracture is at a high angle to the boundary. A very narrow fracture also cross-cuts the boundary at a steep angle. In Plt IIb the major fractures are also subparallel to the dolomite/paste interface, but subsidiary cracks are perpendicular to that boundary. Although less common than in the non-durable concretes, micro-cracks also occur in durable concretes, as shown in Plt IIc of concrete containing Mar-Jo Hills dolomite aggregate.

The cement paste shows major textural differences between durable and non-durable concretes. Small concentric-laminated, spherical bodies are common in the durable concrete pastes (Plt IIIa), whereas they are almost lacking in the non-durable pastes. These bodies are composed of hydrated cement phases. In the non-durable paste, abundant highly-fractured spherical to subspherical mineral grains without concentric structures occur (Plt IIIb). These grains also are probably a portland cement mineral phase, but their appearance is strikingly different than those in the durable concretes.

CHEMICAL COMPOSITION OF COARSE AGGREGATE/PASTE INTERFACE

NON-DURABLE CONCRETES

Reaction Rim Development

In non-durable concretes, those containing coarse aggregate from Smith, Paralta, and Garrison quarries, both the coarse aggregate particles and the cement paste adjacent to the aggregate particles often exhibit discolored rims along the interface between the two phases. Five zones, or regions, can be distinguished: [1] unaltered dolomite interior (Zone A of Figures and Plates), [2] and [3] two reactions rims along the dolomite aggregate margins (Zones B and C), [4] a reaction rim in the concrete paste adjacent to a dolomite aggregate particle (Zone D), and [5] unaltered portland cement paste (Zone E).

These reaction rims, from the unaltered dolomite rock phase toward the unaltered portland cement paste are:

[1] a *dark dolomite rim* (Zone B, Figs 1 - 7; Plates III - Va, b)- a relatively thick, typically 100 -300 μm wide, dark-colored, dirty-appearing rim which occurs at or near the outer margin of the coarse aggregate particles. This rim is much darker than the interior, presumably unaltered, dolomite. Fewer dolomite crystals are visible within the rim compared to the dolomite interior, so that some of the crystals may have dissolved or been

absorbed by growth of other crystals during rim development. In aggregates where this rim is directly in contact with the paste, micro-fractures parallel to the boundary are common, and the outermost part of the dark dolomite rim is much less porous than the dolomite interior.

[2] a *light-colored dolomite rim* (Zone C, Figs 1, Plate IIIc - IIIe) - a much narrower, typically 20 - 50 μm wide, unstained, cleaner-appearing, light-colored rim which is located outside the dark dolomite rim, and which is in contact with the cement paste. Where absent, the dark rim occurs in contact with the paste. The light-colored dolomite rim is typically much lighter in color than the unaltered dolomite. Usually dolomite within the light rim is less porous and exhibits fewer and smaller intercrystalline voids than the unaltered dolomite interior or the dark dolomite rim. Abundant micro-fractures occur at the margin between the light and dark dolomite rims, and often the cracks parallel the dolomite/paste interface.

[3] a *light-colored paste rim* (Zone D, Figs 11 -17, Plates III - Va, b)- a relatively thick, light-colored rim which occurs in the portland cement paste adjacent to the outer margin of the dolomite aggregate. It is typically much lighter in color than the darker and dirtier-appearing, presumably unaltered, paste which occurs farther away from the dolomite aggregate. Although small micro-fractures may occasionally occur within the light paste rim, most fractures occur within the paste outside the light-colored rim.

Representative photographs of rim development are shown in Plates IIIc - IVb. The related electron microprobe traverses and SEM/EDAX element maps are shown in Figs 1-7. Plt IIIc and d are color petrographic microscope views of Smith quarry aggregate and adjacent paste showing rim development. Plt IIIc-d photographs show the aggregate-rim contact in plane-polarized light and between crossed-polarizers, respectively. These two photographs show all three reaction rims (Zone B, C, and D). Note that the major difference in color of the light-colored paste rim (Zone D) compared to the darker, apparently unaltered paste (Zone E) is especially evident in Plt IIIId. The dark dolomite

rim is best seen in plane polarized light of Plt IIIc. An SEM photograph of the same area of the concrete is given in Plt IIIe. The SEM view shows the lower porosity which is typical of the light-colored dolomite rim (Zone C) compared to the interior dolomite (Zone A), and the light color of the paste reaction rim (Zone D). Plts IIIf and IVa,b are views of another Smith quarry aggregate/paste interface. Similar views of non-durable concrete containing Paralta quarry aggregate are shown in Plts IVc, d, e, f. This concrete lacks the light-colored dolomite rim.

Within the same concrete core, each of the rims may vary in thickness and other characteristics, and one or more rims may be missing depending on the specific aggregate particle. Dark and light-colored dolomite rims are best observed with a petrographic microscope in plane-polarized light. In SEM images, the dark and light dolomite rims can be distinguished from the dolomite interior by differences in porosity. These two rims are usually poorly visible when viewed between crossed-polarizers or with the SEM. The light-colored paste rim, zone D, can best be seen when observed between crossed polarizers, and with SEM images. Although the majority of dolomite aggregates have reaction rims, a few aggregate particles do not exhibit reaction rims. The non-rimmed aggregates may occur adjacent to those with well-developed rims.

Electron Microprobe Analysis of Non-Durable Concrete Reaction Rims

Considerable variation in chemical composition across the interface between aggregate and paste is apparent in EDAX area-maps and in microprobe profiles (Fig 1 - Fig 9, Plates IIIc - V) of many samples. Various combinations of rim sequences may occur on different aggregate particles.

Type I Rim Sequence. This reaction rim sequence is developed on aggregates and paste in which all of the above described reaction rims occur: both the dark and light dolomite rims and the light portland cement paste rim (Plt IIIc,d,e,f and Plt IVa,b). An electron microprobe traverse across a non-durable concrete containing Smith quarry

aggregate illustrates the chemical composition of the three reaction rims and the apparently unaltered paste and dolomite aggregate interior (Fig 1). In the profile, Fig 1a, CaO remains essentially constant, with minor irregularly spaced peaks and valleys, throughout the dolomite interior (Zone A) and the inner dark dolomite rim (Zone B). The dark dolomite rim may have less compositional variability, but the difference probably is insignificant, and there is no consistent changes within the dark dolomite rim compared to the dolomite aggregate interior. MgO shows similar compositional variations, but with fewer and smaller irregularities than CaO. The small variation is characteristic of dark dolomite rims developed on aggregate containing both the dark and the light dolomite rims. Changes in CaO or MgO content typically occur only in the outer light-colored dolomite rim

In the outer, light-colored dolomite rim, there is a distinct increase in CaO and a corresponding decrease in MgO compared to the dolomite interior and the dark dolomite rim. Undoubtedly, these chemical differences result from magnesium loss by dedolomitization within the dolomite aggregate immediately adjacent to the paste. The composition differences of the light-colored dolomite rim is confirmed by high-magnification EDAX maps (Fig 2)

Other element profiles are shown in Fig 1b (FeO and Al₂O₃) and in Fig 1c (K₂O and Na₂O). In Figs 1a, b, and c, a small potassium aluminosilicate inclusion, probably illite clay, within the aggregate is reflected by the sharp SiO₂, K₂O, and Al₂O₃ peaks located near the 200 μm marker. None of these elements shows significant differences in concentration throughout the dolomite, so that reaction rim dedolomitization appears to effect only CaO and MgO, as shown by both the microprobe traverses and SEM/EDAX mapping.

Within the paste, CaO shows great variability throughout the light-colored paste rim, but is often higher than in the unaltered paste. The increase in CaO within the light-colored inner paste rim is probably due to precipitation of CaCO₃ (calcite) since this is a

product typical of dedolomitization in concretes (Tang et al. 1991). $\text{Ca}(\text{OH})_2$ (portlandite) may also be present in the CaO-rich zone. MgO typically decreases across the dolomite/paste interface, and is much lower in the paste. However, there is no clearly defined difference in MgO in the light-colored paste rim and the presumably unaltered cement which is located farther from the dolomite/paste interface. Within the paste, MgO may increase locally.

There are slightly greater MgO, K_2O , Na_2O , Al_2O_3 and FeO concentrations in the light-colored paste rim compared to the unaltered cement (Figs 1a, b, c, and Fig 2). Na_2O correlates strongly with K_2O , and Al_2O_3 correlates with FeO in the cement paste, which indicates that most of the Al and Fe exist within the same unknown mineral phases, which are probably not clay minerals. The high Mg and O concentrations shown in EDAX maps indicate that the Mg probably exists as brucite crystals (Figs 2 and 4), another common product of dedolomitization in concretes (Tang et al. 1991).

Type II Rim Sequence. This sequence is found in those aggregate particles lacking the light-colored dolomite rim, and is evident on a second aggregate particle in the Paralta quarry concrete core (Fig 3, Plt IVc-f and Va-f). Our analyses reveal this type of aggregate is most common in the non-durable concretes studied here. In the sample containing Paralta quarry aggregate, the dark dolomite rim is thick and well-defined both visually and chemically (zone B, Fig 6). The microprobe traverse reveals a significant increase in CaO with a corresponding decrease in MgO within the dark dolomite rim compared with the unaltered interior dolomite (Fig 6). Both Na_2O and K_2O (Fig 3b), and Al_2O_3 (Fig 3c) often increase within the dark rim, whereas FeO often remains almost constant from aggregate interior through to the dark dolomite rim.

Some aggregate particles in the non-durable concrete exhibit no reaction rims. In this respect these aggregate particles more closely resemble aggregate particles in durable highway concretes than those in non-durable concretes. For aggregates with well-developed

reaction rim sequences, the rims usually are variable in width and occasionally do not continue completely around the entire coarse aggregate particle.

DURABLE CONCRETES

Rim Development and Electron Microprobe Analyses

Durable concretes typically show considerable differences in reaction rim development and abundance when compared to non-durable materials. The most common type of interface between dolomite aggregates and paste shows no apparent reaction rims in either the dolomite or the paste (Figs 10 -13, and Plt VIaf). Electron microprobe traverses indicate that CaO and MgO typically are much more uniform and with smaller localized compositional irregularities than is typical in non-durable concretes. Only rarely are reaction rims evident and there is usually a very sharp chemical boundary between aggregate and paste with little, if any, chemical gradation. Within dolomite aggregate, the concentration of minor elements, FeO, K₂O, and Na₂O show almost no variation along the traverse, and the SiO₂ concentration is uniformly low unless a quartz grain is encountered. The paste itself is chemically very similar to that of the unaltered non-durable paste (Zone E). A few brucite grains occur in the paste as indicated by small Mg- and O-rich spots shown on EDAX maps (e.g. Fig 12).

In a few aggregate grains discolored reaction rims can be seen at the interface of both dolomite aggregate and cement paste (Figs 14 -15; Plates VIIa-f). These rims resemble those found in the non-durable concretes. Dark or light dolomite rims may be visible, but both rims do not typically occur together. Often these rims, particularly the thin, light dolomite rims, are discontinuous and extend only partly around an aggregate particle.

For dolomite aggregate with reaction rim development, compositions from electron microprobe traverses are quite uniform throughout the dolomite interior. Figure 14 shows a concrete sample containing dolomite aggregate from the Mar-Jo Hills quarry. In this aggregate particle, the dark dolomite rim shows much more variation in CaO, MgO, K₂O,

and Na_2O content than the dolomite interior. In electron microprobe traverses, profiles may exhibit sharp but irregular increases in CaO with corresponding decreases in MgO . For some aggregates exhibiting light-colored dolomite rims, there is almost no change in CaO and MgO until the extreme outer edge of the rim at which there is a pronounced increase in CaO with a corresponding decrease in MgO (Fig 15).

For the cement surrounding rimmed coarse aggregate, there are essentially the same chemical characteristics as for non-durable concrete pastes. Typically there is a light-colored paste rim surrounding the dolomite aggregate, and occasionally there may be a slight enrichment in K_2O and Na_2O in this rim zone.

DISCUSSION

CAUSES OF CONCRETE DETERIORATION

In the concretes studied in the present research, there are many similarities between concretes with long service lives, such as those containing Sundheim and Mar-Jo Hills quarry aggregate, and those with short service lives, such as those with coarse aggregate from the Paralta, Smith, and Garrison quarries. The differences in durability among the various concretes depends primarily on the physical differences between the dolomite aggregate. It is well-known that coarse aggregates used in concrete have a major role in affecting service life, primarily by their relative stability within the highly alkaline, calcium- and silica-rich, portland cement environment. Certain types of rock aggregate undoubtedly react with the paste with a resultant weakening of the bond between the exterior surfaces of aggregate particles in contact with the paste. Some of these reactions will be discussed in the next section.

POSITIVE, NEGATIVE, AND NEUTRAL REACTION RIMS IN CONCRETE

Various rim types formed by chemical reactions between alkali elements from the cement and carbonate aggregates have been described, but they may be summarized into three broad groups based on their relative solubility compared to the interior of the aggregate (Mather 1974; Poole and Sotiropoulos 1980; Poole 1981):

1. Reactions with non-dolomitic carbonate rocks. The reaction exhibits negative rims – the reaction rim zone dissolves more rapidly in dilute HCl and is left with a lower relief than the interior part of the aggregate.

2. Reactions with dolomite or highly dolomitic carbonate rocks. The visible reaction rims within the aggregate are dissolved at about the same rate as the unrimmed area, and they are neutral rims.

3. Reactions with impure fine-grained dolomitic limestone containing interstitial calcite and clay. Mather (1974) subdivided these reactions into two sub-types, dedolomitization reactions with negative rims, and rim-silicification reactions with positive rims which are left in high relief after dilute HCl treatment.

Poole (1981) pointed out that the difference in rim solubility (positive, neutral and negative rims) appears to be associated with the concentration of silica in the rim zone of the aggregate. The processes for both silicified rim development and non-silicified rim development reactions were believed to be similar – essentially a dedolomitization process.

In the present investigation, there seem to be two rim types. The first, and most common are neutral rims. After immersion in 3.8% HCl for a few hours, the coarse aggregate typically is reduced below the level of the paste, and the dissolved dolomite surfaces are essentially flat without depression or elevation in the region immediately adjacent to the paste. These aggregates clearly have rims that dissolve at about the same rate as the dolomite interior. In a few aggregates, however, there is a marked depression adjacent to the concrete relative to the rest of the aggregate surface elevation. These rims

are negative rims which are more soluble than the dolomite interior because they are less dolomitic. Both types of rims were common in aggregate producing non-durable concretes.

RIM DEVELOPMENT SEQUENCES

As early as 1958, Lemish et al. identified a reaction rim sequence consisting of two rims at the aggregate-paste interface: a darker inner rim occurring within the aggregate and outlining its outer edge, and an outer rim of light gray material occurring in the cement paste surrounding the affected aggregates. The inner rim showed a concentration of opaque materials and interstitial silica or silicate materials, and the material in the outer rim was believed to be calcium hydroxide. Bisque and Lemish (1958) found that the inner reaction rims were silicified and selectively formed on aggregate containing clay, a high percent of insoluble residue, high magnesium content, and higher concentration of silica. Reaction rims were not observed in pure limestone aggregates. The inner rim material from affected concrete was marked by a decrease in magnesium content, a marked increase in insoluble residue (with 85% - 90% SiO_2), and a slight increase in calcium content. Hydrochloric acid leaching of the concretes left the inner rim zone standing high in relief, and the outer rim of cement paste adjacent to the rimmed aggregate was more rapidly attacked by hydrochloric acid than the paste beyond the outer rim or adjacent to unrimmed aggregate particles. They also found that effective porosity of the aggregate rim zone was decreased markedly as compared to that of unaffected aggregate, and aggregates which lacked clay did not grow siliceous rims in the laboratory experiments. The possible mechanism for this silicification was postulated as "tying together" of clay-size particles in the calcitic matrix by silicon ions (Bisque 1959; Bisque and Lemish 1960).

Poole (1981), and Poole and Sotiropoulos (1978, 1980) observed a sequence of three reaction rim zones at the dolomite aggregate - cement paste interface: zone A - a dark zone in the aggregate extending inward from the margin of the aggregate with an irregular and gradational inner margin; zone B - a light zone in the cement paste immediately adjacent

to the aggregate which is only present around some of the grains, and zone C – a dark zone in the cement paste with a gradational outer margin beyond zone B. The total width of these reaction rims increases slightly with time, and zone C diminishes with time as the width of zone B increases. Zone A was Mg-poor, and Ca- and Si-rich compared with the unaltered interior part of dolomite aggregate. The overall composition of zone B was Si-poor, Ca-rich and, possibly Mg-rich, when compared to the cement paste beyond zone C. Zone C sometimes had a higher SiO₂ content.

COMPARISON OF RIM SEQUENCES

The present research has revealed a similar, but somewhat different, sequence of reaction rims associated with dolomite coarse aggregate in non-durable Iowa concretes. The sequence is unaltered dolomite aggregate interior → a dark-colored dolomite reaction rim → a light-colored dolomite reaction rim → light-colored cement reaction rim → dark, presumably unaltered, cement paste. By comparing between this rim pattern and the patterns described by Lemish et al. (1958) and Poole et al. (1981), it is clear that the dark dolomite reaction rim corresponds to the darker inner rim observed by Lemish, and to zone A in Poole's observations. The light-colored cement reaction rim seems to correspond to the light outer rim in Lemish's rim pattern, and zone B of Poole's rim sequence. Zone C described by Poole et al. (1981) is missing from the concretes studied in the present research. A reasonable explanation for the absence of zone C is that it has diminished with time. Poole et al. (1981) found their equivalent zone slowly disappeared over time, and the Iowa concretes we studied have been in service for many years. The light-colored dolomite reaction rim of the present research was not described by either Lemish et al. (1958) or Poole et al. (1981). A possible reason for this is that our light-colored dolomite rim represents the end product of a reaction between dolomite aggregates and cement paste.

MECHANISM OF DEDOLOMITIZATION-INDUCED CONCRETE DETERIORATION

The Alkali-Dolomite Reaction

There can be little doubt from the electron microprobe profiles and EDAX maps that the rims observed in concretes containing Smith, Paralta, and Garrison quarry dolomites result from chemical reactions between concrete paste and dolomite aggregates related to dedolomitization of the outer margins of the aggregate. Through these reactions, magnesium is released and then migrates into the cement phase. Reactions involving magnesium and cement have been determined by previous studies to be deleterious to concrete durability. In spite of abundant research, however, the question remains as to the precise cause of deterioration of concretes containing dedolomitized aggregate. The majority of researchers have concluded that deterioration is caused by changes resulting from dedolomitization. Most studies have concluded that there is a significant volume increase associated with the reactions, but the precise cause of the expansion is uncertain and is the subject of considerable disagreement.

If we consider the simplest reaction which converts dolomite into calcite



Calcium is derived from the paste, and magnesium is released from the dolomite and diffuses into the paste. This reaction will be accompanied by almost a 14% volume increase, providing the calcium and magnesium ions are free to migrate into and out of the site of dedolomitization.

If, however, we consider a much more likely reaction in which dolomite is attacked by alkali derived from the high pH portland cement and which results in the formation of brucite, calcite, and carbonate ions:



we find there is nearly a 5% decrease in volume. This reaction is generally referred to as the alkali-carbonate reaction (Hadley 1961, 1964; Lemish and Moore 1964; Sherwood and

Newlon 1964; Swenson and Gillott 1964, 1967; Gillott 1964, 1978; Gillott and Swenson 1969; Carles-Gibergues et al. 1989; Tang et al. 1986, 1989, 1991; Deng and Tang 1993). In the present investigation a better term is alkali-dolomite reaction because the coarse aggregate is composed almost entirely of dolomite. The reaction is considered to be the fundamental reaction involving dedolomitization in the highly alkaline portland cement concrete environment. In addition, carbonate released from dedolomitization may react with portlandite, $\text{Ca}(\text{OH})_2$ to regenerate the hydroxide and maintain a highly alkaline environment:



In spite of the small volume decrease accompanying reaction (2) there seems little doubt that dedolomitization actually results in a volume increase. Expansion was observed in experiments of Tang et al. (1988) after they soaked concrete in highly alkaline solutions. This expansion is considered to be the major cause of concrete deterioration accompanying dedolomitization of coarse dolomite aggregate.

Volume Changes Resulting from Dedolomitization

Two contradictory hypotheses have been proposed to explain the observed expansion associated with the alkali-carbonate reactivity: the first proposes an indirect mechanism which assigns a trigger role to dedolomitization and invokes other factors as responsible for expansion (Swenson and Gillott 1964, 1967; Gillott 1964, 1978; Gillott and Swenson 1969), whereas the second invokes a direct mechanism which attributes excessive expansion to the attack of the alkali upon the dolomite (Hadley 1961, 1964; Sherwood and Newlon 1964; Deng and Tang 1993; Tang et al. 1986, 1989, 1991),

Because the sum of the volume of solid products in reaction (2) is less than that of the reactants, Gillott and his colleagues proposed an indirect mechanism for expansion in which the expansivity of certain dolomitic rocks is due to development of a swelling pressure resulting from wetting of previous unwetted clay or clay-size minerals. Wetting is

facilitated by dedolomitization which produces access channels for moisture (Gillott 1964, 1978; Swenson and Gillott 1964, 1967; Gillott and Swenson 1969). This proposed mechanism involves two steps: (a) attack by cement alkali on the dolomite (dedolomitization) which opens micro-cracks allowing water and solution to penetrate into the rock and (b) moisture uptake by the dry clay with development of expansive forces due to surface hydration and build-up of hydrous double-layers surrounding the clay minerals.

In contrast, other researchers considered the alkali-carbonate reaction as the direct cause of the associated expansion even though alkali carbonate reactions should reduce volume. Sherwood and Newlon (1964) suggested that complex hydrated double salts of large unit size caused the experimentally-observed increase in solid volume. Hadley (1961) postulated a different cause. His measurements on a single crystal of dolomite during experimentally-induced dedolomitization disclosed a slight expansion of 0.15% after 100 days. In addition to expansion of the individual dolomite crystals during dedolomitization, Hadley (1964) postulated that expansion also results from osmotic forces because the alkali - carbonate solution at the reacting dolomite crystal may differ in concentration and nature from the solution in the pores. The differences in flow tendencies of the two solutions through interstitial clay may lead to the build-up of a swelling pressure.

Tang and his colleagues proposed another mechanism - they hypothesized that the network of clay disseminated throughout impure dolomite furnishes channels through which H_2O , K^+ , Na^+ , and OH^- migrate into the interior of the reactive rock (Tang et al. 1986, 1989, 1991; Deng and Tang 1993). They concurred that dedolomitization causes a reduction in volume, but they also pointed out that the reaction products of dedolomitization, calcite and brucite, were fine-grained and enclosed many voids. By including the void volume, their calculation revealed an increase in the overall volume of the solid skeleton plus voids during dedolomitization.

SIGNIFICANCE OF REACTION RIMS IN IOWA DOLOMITE AGGREGATE CONCRETES

The following characteristics of the concretes studied here are summarized:

(1) Non-durable Iowa concretes exhibit better developed and more abundant reaction rims than the durable Iowa concretes. These reaction rims are commonly located near the interface between dolomite aggregate and paste. The less abundant coarse limestone aggregate which occurs in some of the concretes do not have the same reaction rims, indicating that the reactions responsible for deterioration of the highway concretes studied in this current research are dolomite-specific. In addition, non-durable concretes are far more deteriorated and contain more cracks or micro-cracks than durable concretes. The only major and consistent differences between durable and non-durable concretes apparently are the coarse aggregates used in making the concretes, so that dedolomitization reactions must be the primary cause of deterioration.

(2) The most complete sequence of rims includes an inner dark dolomite rim, and outer light-colored dolomite rim, and an inner light-colored Portland cement paste rim.

(3) The light-colored paste rim is rich in Ca, but poor in other elements (Si and Mg etc.). The overall composition of this rim zone is more calcitic in non-durable concretes than in durable concretes.

(4) No obvious differences in composition occur between the dolomite aggregate interior and the dark dolomite reaction rim (or the inner part of this rim when the light-colored dolomite rim is absent), but a pronounced increase in CaO and a corresponding decrease in MgO, sometimes accompanied by a slight increase in SiO₂ are observed in the light-colored aggregate rim or in the outer part of the dark dolomite rim when the light-colored rim is absent.

(5) The light-colored dolomite rim, or the outer part of the dark reaction rim when the light rim is missing, has a lower porosity than the dolomite interior, and some interstitial spaces have been filled with Ca-rich materials and Mg- and O-rich materials.

The Ca-rich material is chiefly calcite although minor amounts of portlandite may also be present, and the Mg- and O-rich material is brucite.

(6) In non-durable concretes, brucite occurs in dark dolomite reaction rims, throughout the light-colored paste rim, and into dark cement paste, and its abundance is slightly higher in the dark cement paste than in the lighter paste. Brucite concentrations are often much lower in the dolomite aggregate rims than in the paste. Due to the small size of brucite in the dolomite reaction rims, brucite may be missed during electron microprobe traverses.

(7) Alkali elements, potassium, sodium, and calcium, are often concentrated in the dark cement paste. In some samples they are also enriched in the lighter-colored paste rim.

(8) Dolomite aggregate particles in all concrete studied varied in the degree of rim development. Rim development was much more abundant in non-durable concretes, but some concretes had three rims, two in the dolomite and one in the paste. Other aggregates had only two rims, one in the dolomite and one in the paste. Although most of the aggregates in durable concretes lacked rim development, a few particles had reaction rims in the paste and either a dark or a light-colored rim in the dolomite. Variability in rim development appears to indicate that dolomite aggregate particles vary in susceptibility to dedolomitization reactions promoted by contact with the paste. Such variable reactivity is to be expected because coarse aggregate used in concrete is usually a blend of dolomite from several horizons in a quarry.

Reaction rims developed after pouring of the concrete as a result of chemical reactions between the calcium-rich, highly alkaline, cement paste, and the dolomite crystals occurring at or near the interface between the paste and dolomite aggregate. Dedolomitization of reactive dolomite aggregate has occurred abundantly in non-durable Iowa concretes aggregate, and to a minor extent in durable concretes, by an alkali-carbonate reaction. Dolomite in these reactive aggregates has reacted with alkali derived from the cement, with formation of calcite, brucite, and alkali carbonate. Clay minerals or other

clay-size minerals in dolomite aggregate may provide channels for the migration of alkali ions- and OH-bearing solutions, thus promoting the reaction. Most of the neoformed calcite is precipitated along the interface where it contributes to the formation of light-colored dolomite reaction rims in which calcite replaces dolomite crystals. Some of the light-colored dolomite rim neoformed calcite also fills intercrystalline spaces between dolomite crystals or within voids created by dissolution of dolomite crystals. It thereby reduces the porosity of the dolomite reaction rim. Magnesium ions released by dedolomitization diffuse outward into the cement where they precipitate as brucite crystals in the light-colored paste rim. Magnesium also diffuses inward into the dolomite aggregate, and may be precipitated as brucite in voids containing neoformed calcite. Small but measurable amounts of silicon ions also diffuse into the dark dolomite reaction rim from the siliceous paste, although some of the silicon in the dark dolomite rim may result from redistribution of clay-derived silicon. Alkali elements diffuse outward into the dark cement paste. The alkali elements often accumulated in the light-colored cement zone, and these elements may represent regeneration of alkali according to reaction (3).

The current research extends the work of Gillot et al. (1975) who concluded that alkali-carbonate reactions were most common in dolomitic limestones, in which isolated dolomite rhombohedra are surrounded by calcite. These rocks also contained abundant clay and clay minerals, and typically were not very porous. Because the reactive rocks were mixtures of dolomite and calcite, the term alkali-carbonate-rock reaction was appropriate. In contrast, the Iowa concrete aggregates studied in the present research were considerably different than those implicated by Gillot (1975). The reactive coarse aggregate in the non-durable Iowa concretes are composed almost entirely of dolomite without much calcite. These dolomite rocks exhibited relatively high porosity and did not consistently contain significantly higher clay concentrations than non-reactive dolomites used in durable concretes.

MAGNESIUM AND CONCRETE DETERIORATION

Although several studies have supported the conclusion that expansion of dedolomitized coarse carbonate aggregate is important in causing concrete deterioration, there still remains the question as to whether magnesium ions released by dedolomitization may also play a role in reducing concrete service life. Newly-released magnesium undoubtedly leads to brucite precipitation in the concrete paste, and brucite growth may itself create crystal growth pressures which lead to expansion and deterioration. For example, Winkler and Singer (1972) conclude that growing gypsum and halite crystals may exert pressures in excess of 2000 atm, so that analogous pressures may be expected to develop from growth of brucite in concrete voids. In addition, there may be adverse chemical reactions between magnesium and the paste, analogous to the effects of sulfate ions on concrete. Oberste-Pathberg (1985) mixed magnesium chloride into cement paste and found the concrete rapidly deteriorated, perhaps partly due to magnesium reactions with the paste. An understanding of the effects of magnesium on concrete is especially pertinent at this time because magnesium chloride and/or calcium magnesium acetate (CMA) have been proposed as road deicers and substitutes for rock salt.

The next section, Part II, will explore the effects of immersing concrete in magnesium chloride solution under different environmental conditions. For comparison, the effects of concrete immersion in distilled water, calcium chloride, and sodium chloride solutions will also be investigated in order to provide comparison.

PART II. EXPERIMENTAL STUDY OF THE DETERIORATION OF IOWA HIGHWAY CONCRETE

INTRODUCTION

The primary objective of the experiments was to evaluate the effects of magnesium-rich solutions on concrete deterioration under different physical and chemical conditions. The experiment were intended to determine if magnesium contributes to highway concrete deterioration, and whether or not magnesium chloride or calcium magnesium acetate may be suitable substitutes for NaCl as deicers on Iowa highways.

Another objective was to determine whether reaction rims on dolomite aggregate and portland cement paste could be induced by saturating concretes with calcium-rich solutions. Ca-rich brines at relatively high temperatures might promote rapid dedolomitization. If so, then newly-produced reaction rims could be compared to ones produced during aging of concretes under highway conditions. Experiments would provide additional insights concerning dedolomitization processes in highways.

A third objective was to evaluate the common deicer salts sodium chloride, calcium chloride, and magnesium chloride, for their relative effects on concrete durability.

The experimental procedures were developed to explore a wide range of physical and chemical conditions in order to evaluate the importance of those conditions on concrete stability in the presence of chemical substances that are or may be used as highway deicing salts. Distilled water and solutions of calcium chloride, magnesium chloride, and sodium chloride were tested in the experiments. The solutions were maintained at 60°C (140°F) to enhance chemical reactions, the rate of which usually is increased by higher temperatures. On the upper surfaces of Iowa highways, 60°C temperatures might well develop during very hot, sunny summer days.

One set of experiments involved continuous immersion of concrete in each of these solutions simulating conditions in which highway concrete is completely and

continuously saturated. Such conditions might occur within porous highway concrete slabs when brines within the slabs contain enough deicer concentrations to reduce vapor pressure of the solutions below that of the air above the slab.

Another set of experiments involved cycles alternating between total immersion in solutions and complete drying of the concretes. Two different drying temperatures, 60°C and 90°C (194°F) were used to determine if extremely high temperatures would have greater destructive effects than more normal 60°C temperatures.

A third set of experiments involved cycles alternating between total immersion in solutions and freezing. Two different freezing temperatures, 0°C (32°F) and -70°C (-94°F) were tested. The lower temperature was far colder than any Iowa winter temperature and was used to insure freezing of all deicer solutions, whereas a higher freezing temperature of 0°C was used to more closely simulate winter highway temperatures at some depth within the concrete slab where concentrated salt solutions will not completely freeze.

EXPERIMENTAL METHODS

STARTING MATERIALS

The concrete cores Nos. 1 - 7 as discussed in the previous section were used for experiments. Table I gives highway location of the cores, and quarry source and geologic age of the coarse aggregate. Each core was sliced in half longitudinally, and cut into small rectangular blocks about 1/2" x 1/2" x 1" which weighed between 7 and 11 g.

EXPERIMENTS

All solutions were made with double-distilled deionized water and ACS certified chemicals. Because of the strong possibility of mold and bacteria growth in the solutions during the extended experiments, all contained 0.01% sodium azide for their control. Experiments were conducted with 0.75 or 3.0M CaCl₂·2H₂O, MgCl₂·6H₂O, and NaCl. A few experiments were performed with magnesium acetate and with magnesium nitrate to

determine the importance of anionic composition on concrete deterioration. Distilled water was used as a control in evaluating the destructive effects of salt solutions. A concrete block from each core was immersed in 100 ml of each solution. Blocks and solutions were then sealed in cleaned polymethylpentene (PMP) containers and stored in a constant temperature oven at 60°.

Wet/Dry (W/D) Experiments

Concrete blocks were immersed in 60°C solutions for 132 hours, removed from the solution, dried at 90° or 60°C for 24 hours, air cooled to 25°C, rinsed for 1 minute in distilled water to remove surface salts, returned to their immersion solutions at 25°C, and again stored at 60°C for 132 hours. Cycles continued until significant deterioration of some samples developed. Longer term experiments would have caused severe crumbling of the material, and difficulty in making sections for analysis.

Freeze/Thaw (F/T) Experiments

Samples were removed from the 60°C immersion solutions after 132 hours, air cooled to 25°C, frozen for 24 hours at either 0°C or at -70°C, air warmed to 25°C, returned to the 25°C solutions, and stored at 60°C for 132 hours. Cycling was continued for 222 days or until deterioration of some samples had developed.

Continuous Immersion (CI) Experiments

Concrete blocks in sealed containers were constantly immersed for 222 days at 60°C.

End of Experiment Procedures

Samples were rinsed for 1 min in distilled water, dried at room temperature, and visually inspected to determine patterns of deterioration. Representative samples were then

photographed, thin-sections and polished sections were made and studied by petrographic microscopy, SEM, EDAX element mapping, and electron microprobe. It should be noted that photographs and electron microprobe traverses were obtained with cut and polished concrete blocks, so that the horizontal surfaces used for views and analyses were never directly in contact with brines during experiments. The concrete paste is relatively porous and permeable so that solutions penetrated into the concrete blocks during experiments, and reacted with paste and aggregate phases.

EXPERIMENTAL RESULTS

X-RAY DIFFRACTION ANALYSES OF TREATED CONCRETES

Samples of untreated and concretes treated by wet/dry cycling were analyzed with XRD to determine possible mineral changes caused by experiments (Table IV). With calcium and sodium chloride solutions, all major XRD peaks and most of the minor peaks of the untreated concrete were retained during wet/dry cycling, although their intensities changed. A few new peaks, which were impossible to identify because of the complexity of the spectra, appeared after treatments. Probably most of these peaks are due to soluble salt and salt hydrate precipitation although some may be due to more complex mineral phases formed during brine treatments interaction with cement phases. Magnesium chloride wet/dry experiments produced fundamental changes in cement mineralogy in both durable and non-durable concretes. Most of the major XRD peaks produced by the cement paste after treatments were completely different than those of the untreated paste, and only a few of the minor peaks of untreated paste survived the experiments.

EFFECTS OF WATER

None of the experiments with distilled water produced damage to the concrete blocks.

Table IV A Summary of Concrete Experiments

Experiment Type	NaCl	MgCl ₂	CaCl ₂	H ₂ O
F/T, 3 M, -70°C/25°C/60°C, 9 cycles	NC	NC	NC	NC
W/D, 3 M, 60°C/90°C, 4 cycles	NC	Paste: brown color and decomposes Aggr.: NC	Paste: cracks at paste/aggr. interface Aggr.: NC	NC
W/D, 3 M, 60°C/60°C, 6 cycles	NC	Paste: brown color and severe decomposition Aggr.: NC	Paste: cracks at paste/aggr. interface Aggr.: NC	NC
Soak only, 3 M, 60°C, 222 days	Paste: slight brown color Aggr.: NC	Paste: dark brown color and cracks at paste/aggr. interface Aggr.: NC	Paste: brown color and cracking or initial cracking Aggr.: NC	NC
W/D, 0.75 M, 60°C/60°C, 16 cycles	NC	Paste: brown rim in paste around aggr. Aggr.: cracking	Paste: decomposition at paste/aggr. interface, some cracks Aggr.: cracking	NC
F/T, 0.75 M, 0°C/25°C/60°C, 16 cycles	Paste: pale brown color, Aggr.: NC	Paste: slightly brownish and slight crumbling Aggr.: NC	Paste: corners crumble, some cracks Aggr.: NC	NC

Aggr. = aggregate; NC = no change

EFFECTS OF MAGNESIUM CHLORIDE SOLUTIONS

Deterioration of Concretes

Concrete deterioration was especially severe with magnesium chloride treatments (Plts VIIIa-f; IXe-f, Xa). The most severe crumbling and dark brownish cement paste discoloration occurred during wet/dry cycling. Both durable and non-durable concretes were equally affected. Cracking of both paste and aggregate occurred during wet/dry cycling as shown in Plt XIIIa-b of the durable concrete containing Mar-Jo Hills quarry

dolomite. Often the dolomite aggregate was cracked near its outer margin. These cracks are oriented either parallel to or at high angles to the dolomite/paste interface. Some of the cracks and other voids have been filled or lined with a sequence of newly-precipitated minerals. For example, concrete containing Mar-Jo Hills aggregate developed a complex three-layered mineral crack filling (Plt XIIIa-b). White calcite precipitated immediately adjacent to the walls of the openings. Farther away from the crack walls, a later-stage intermediate layer of brucite and magnesium chloride precipitated over the calcite layer, and finally was covered by the latest precipitates consisting of very fine-grained, poorly consolidated minerals containing Fe, Mg, O, Cl, S, and Al. These elements indicate mineral phases such as aluminum hydroxide, magnesium chloride hydrates, brucite, and silicates. EDAX area maps of these crack-filling minerals are shown in Figures 27 and 28. The cement paste, as expected, was enriched in magnesium and depleted in calcium and silicon when compared to untreated concretes (Fig 26).

Experimentally Induced Rim Formation

In the non-durable concrete, reaction rims in both dolomite aggregate and paste were observed after experiment treatments, but the observed rims were present in the samples before treatment, as discussed in Part I. Evidence for this conclusion is that rim sequences and electron microprobe traverses are similar to those of untreated concretes. Minor effects of magnesium chloride treatments appear to be superimposed on the earlier rims which have been slightly modified by brine contact. Experimentally superimposed rim modifications include: (1) voids within the dark dolomite rims that were filled with brucite and magnesium chloride; (2) light-colored paste rims that were reduced in calcium and increased in magnesium compared to the equivalent rims of untreated concretes (Figs 29); and (3) voids and pores in the cement paste rims that were filled with magnesium chloride precipitates.

In durable concretes no reaction rims formed in either coarse aggregate or PCC paste as a result of magnesium chloride treatments.

EFFECTS OF CALCIUM CHLORIDE SOLUTIONS

Deterioration of Concretes

Next in severity to magnesium-induced concrete deterioration is calcium chloride treatment. In the concretes treated with calcium chloride solutions, concrete deterioration was mainly by crack development and brownish discoloration of the cement paste. These effects were especially evident during wet/dry cycling (Plts VIIIa-f, IXb-d). In general, cracks were much better developed in the paste than in the coarse dolomite aggregate. Many of the cracks occurred adjacent to the outside of aggregate boundaries, and were chiefly oriented parallel or subparallel to the interface (Plts VIIIa-f, IXb-d, Xe). Only a few cracks occurred precisely at the aggregate/paste interface. Cracks and voids were often partially or completely filled with neoformed mineral matter, which EDAX maps revealed to be calcium chloride-rich, as expected, with significant amounts of Al at some locations (Fig 18).

Experimentally Induced Rim Formation

One of the goals of the experiments was to determine if dedolomitization occurred as a result of treatment with concentrated calcium brines at relatively high temperatures. Unlike with magnesium chloride treatments, experiments with calcium chloride produced new, highly visible, reaction rims at the margins of coarse aggregates in non-durable concretes under both wet/dry and freeze/thaw conditions (Plts Xf, XIa-e). Concretes containing Paralta aggregate were especially susceptible to new rim development. Evidence for new rim formation is their different chemistry compared to rims formed under highway conditions (older rims). Interpretation of chemical data obtained by electron microprobe analysis is complex for new rims because they were superimposed on older

rims which developed by reactions between aggregate and concrete paste in the highway environment. Consequently, rim chemistry of the new rims is a blend of earlier rim composition and experimentally-induced new rim alteration.

New rims resemble older rims in general appearance, but the new rims differ from older ones in that (1) the new rims are much wider than the older rims, and (2) the outermost region of new rims shows an increase in MgO and corresponding decrease in CaO whereas old rims exhibit the reverse chemical changes. Old rims were usually preserved, and much of their original chemical signature is still evident after treatment with calcium solutions.

An increase in the magnesium content of dolomite rims after treatment with calcium chloride solutions was unexpected and its precise cause is unclear. A probable explanation is that elevated magnesium values of dolomite rims may result from slightly enhanced dedolomitization of porous and permeable aggregate interior. With greater calcium chloride-induced dedolomitization in the aggregate interior, the aggregate rim will appear magnesium-rich. Differential dedolomitization might be caused by lower porosities of rim dolomite compared to interior dolomite. Observations on untreated concrete, as discussed in Part I, revealed that outermost dolomite rims had very low porosity. Lower porosities render access to the aggregate interior dolomite more difficult for the dedolmitizing solutions, and result in reduced dedolomitization.

Unlike the abundant new rim development in non-durable concretes, no new rims were apparent in durable concretes subjected to continuous immersion, wet/dry, or freeze/thaw cycling in calcium chloride solutions.

EFFECTS OF SODIUM CHLORIDE SOLUTIONS

Under the same experimental conditions in which magnesium chloride and calcium chloride solutions were highly destructive, sodium chloride solutions proved to have fewer deleterious effects on both durable and non-durable concretes. Three molar

sodium chloride brines were nearly non-destructive under wet/dry conditions at both the higher and lower drying temperatures, and under freeze/thaw with freezing at -70°C (Plts Xb - Xd). A slight brownish discoloration of the paste occurred when the concrete blocks were continuously soaked in 3M NaCl for 222 days. Sodium chloride at a lower concentration, 0.75M, caused moderate crumbling and a slight brownish cement paste discoloration during freeze/thaw cycling with freezing at 0°C . A few micro-cracks developed at the contact between dolomite aggregate and cement paste (Plts XIVe-f). The greater deterioration at 0°C freezing compared to -70°C was unexpected, and probably results from large ice crystals which slowly grew at the higher temperature compared to the small, rapidly grown crystals that formed at -70°C .

No new reaction rims could be observed (Plts XIVc-d). Electron microprobe traverses (Fig 31) were essentially identical to those of untreated concretes. On SEM/EDAX maps, a few localized concentrations of magnesium and oxygen indicate the presence of brucite (Fig 32).

DISCUSSION

GENERAL OBSERVATIONS

The experimental results are summarized in Table IV. General observations include:

(1) Essentially no deterioration was evident in concrete treated with distilled water, regardless of whether freeze/thaw, wet/dry, or continuous soaking was used (Plt IX).

(2) Sodium chloride solutions produced much less deterioration than calcium or magnesium chlorides. The most damage to concretes was produced by 0.75M NaCl under 0°C freeze/thaw conditions, in which moderate crumbling and brown paste discoloration occurred.

(3) Magnesium chloride and calcium chloride wet/dry and continuous immersion treatments produce much more severe deterioration than with sodium chloride solutions.

This was true regardless of solution concentration and whether the blocks were cut from durable or non-durable concretes (Plts VIIIa - Xd).

(4) Concrete deterioration in magnesium and in calcium solutions was more severe under wet/dry than in continuous immersion conditions (Plts IXb - Xd). Furthermore, wet/dry deterioration was more pronounced when samples were dried at 90°C rather than at 60°C.

(5) Calcium solutions produced deterioration which was characterized by crack development and brownish discoloration of the cement paste. Magnesium solutions typically caused deterioration by severe crumbling and dark brownish Portland cement paste discoloration. There was no distinct difference in deterioration of non-durable concretes compared with durable ones (Plts VIIIa - Xa).

(6) Reaction rims visually similar to those developed under highway conditions were induced in non-durable concretes by experiments utilizing calcium chloride. However, the new aggregate rims had compositions different from those described in Part I. The new dolomite aggregate rims did not exhibit an increase in CaO with corresponding decrease in MgO in the outermost part of the dolomite rims. These new rims typically showed an increase in MgO suggesting that the interior, more porous dolomite aggregate was slightly dedolomitized, but the less porous outer rim areas underwent less dedolomitization. No new rims formed in durable concretes under identical conditions.

(7) Magnesium acetate and magnesium nitrate were found to produce similar deterioration of concrete as magnesium chloride.

SIGNIFICANCE OF EXPERIMENTAL RESULTS

These experiments suggest that magnesium or calcium chloride deicers may produce more damage to highway concrete than the widely used sodium chloride deicers.

Non-durable concretes which were characterized by reaction rims sequences developed under highway conditions were also more reactive to laboratory-induced reaction rim alteration than durable concrete. This was especially common with calcium chloride treatments.

Magnesium chloride solutions were highly damaging to both non-durable and durable concretes. Because of this damage, there is a high probability that the addition of magnesium from any source, either from deicing salts or from dedolomitization reactions involving coarse dolomite aggregate, will be deleterious.

PART III. GENERAL CONCLUSIONS AND RECOMMENDATIONS

GENERAL CONCLUSION

ULTIMATE CAUSE OF IOWA CONCRETE DETERIORATION

Electron microprobe analyses and EDAX elemental mapping of the two groups of Iowa highway concretes studied here: those with short service lives (non-durable) concretes and those with extended service lives (durable) concretes disclose subtle chemical differences in the margins of dolomite coarse aggregates used in the concretes. Non-durable concretes, those containing dolomite coarse aggregate from Garrison, Paralta, or Smith quarries, exhibit abundant chemical reaction rims at the margins of the aggregate and in the paste immediately adjacent to aggregates. These rims are due to dedolomitization of dolomite adjacent to the highly alkaline and calcium-rich portland cement environment. Experiments revealed that the non-durable concrete aggregates also were highly susceptible to laboratory-induced reaction rim formation, especially by cycling the concretes in concentrated calcium chloride solutions through either freeze/thaw or wet/dry conditions.

Durable concretes containing dolomite coarse aggregate from either the Sundheim or the Mar-Jo Hills quarries, in contrast, contain only a few coarse aggregate particles which exhibit reaction rims, and when present, the rims are less well-developed than those in non-durable concrete aggregate. In addition, durable concrete aggregates are resistant to laboratory-induced reaction rim formation by concentrated calcium chloride solutions.

Reaction rims caused by dedolomitization, and susceptibility to laboratory-induced chemical reactions between aggregate and experimental solutions indicate that aggregate from the Garrison, Paralta, and Smith quarries are chemically reactive. Widespread susceptibility to dedolomitization through the alkali-dolomite reaction is the ultimate cause of short service lives of concretes containing these dolomite aggregates.

These reactions can be summarized by the reaction between dolomite in the coarse aggregate and hydroxide ions derived from the portland cement to produce calcite, brucite, and carbonate ions:



with the carbonate reacting with portlandite from the cement to produce additional calcite and hydroxide ions:



Brucite, $\text{Mg}(\text{OH})_2$, and calcite, CaCO_3 , are the two crystalline phases produced by these two closely related reactions. Supporting an alkali-dolomite reaction in non-durable concretes is the observation that both these minerals are far more common in non-durable concretes than in durable ones.

Although detailed chemical micro-analyses document that widespread dedolomitization reactions have occurred in the non-durable concrete aggregates, there was no evidence of complete dedolomitization. Reaction rims never were completely dedolomitized with complete replacement of dolomite by calcite crystals. In all cases, the alkali-dolomite reaction produced calcium-enriched dolomite crystals in which comparatively few magnesium sites were replaced by calcium.

DIRECT CAUSES OF CONCRETE DETERIORATION

The alkali-dolomite reaction is the ultimate cause of concrete deterioration, but the reaction itself does not produce deterioration. Dedolomitization, or partial dedolomitization, produces environmental changes in the concrete which cause concrete damage. The most probable direct cause of rapid deterioration of these concretes is that partial dedolomitization results in slight volume expansions with resultant weakening of aggregate-paste bonding and micro-cracking. Brucite and calcite are the two solid phases

precipitated by the two closely related chemical reactions involved in alkali-induced dedolomitization. Electron microprobe analyses reveal numerous occurrences of very high localized concentrations of brucite and calcite in the cement adjacent to partially dedolomitized aggregate. Precipitation and growth of these two minerals very likely produced crystal growth pressures which were highly important in causing expansion. Although clay is not very abundant in the reactive aggregates, the access of water to clay minerals may be facilitated by partial dedolomitization. Wetting of small amounts of clay inclusions may also enhance expansion as proposed by Gillot (1978) and others.

ALKALI-DOLOMITE REACTIONS AND THE NATURE OF COARSE AGGREGATES

Several previous studies, for example those by Gillot (1978) and Hadley (1961) concluded that coarse-grained dolomitic limestones with abundant clay inclusions were most susceptible to alkali-dolomite reactions, hence the commonly applied term alkali-carbonate reaction, rather than alkali-dolomite reaction, as used here. The above rock description does not describe the reactive carbonate rocks observed in the present study. All aggregate interiors, from both non-durable and durable concretes, were composed of dolomite with very little accessory calcite, and there were essentially no consistent compositional differences between dolomite crystals in aggregates from non-durable concretes and durable concretes. None of the aggregates contained very large quantities of clay inclusions as shown by Si + Al + K concentrations.

The only consistent differences between durable and non-durable concretes observed in our study was in texture which is clearly manifested both in petrographic microscope and electron microscope observations. The non-durable concrete dolomite aggregates were porous without a strongly interlocking crystal fabric, and contained abundant small, euhedral to subhedral, dolomite crystals. Durable concrete dolomite aggregates were composed of coarser, tightly interlocked, dolomite crystals with few

ehedral or subhedral outlines, and the aggregate possessed low porosity as determined by SEM studies.

ROLE OF MAGNESIUM IN DETERIORATION

Experiments with chloride solutions revealed that magnesium chloride and calcium chloride solutions were exceptionally aggressive in promoting concrete deterioration. The exact chemical reactions involved in deterioration are undoubtedly complex, but very likely involve both replacement and dissolution reactions with concrete phases, and precipitation of new mineral phases in voids and cracks. Depending on the specific solutions used in experiments, common mineral precipitates include brucite, portlandite, calcite, halite, and various hydrated chloride mineral species. Precipitation of the minerals will very likely produce crystal growth pressures analogous to those proposed to occur in concrete undergoing alkali-carbonate reactions. Magnesium and calcium chloride minerals have many different hydration states, and expansion pressures may be produced by hydration changes during conditions of different relative temperature, water activity and humidity. Crystal growth and hydration state expansion pressures are the most likely direct causes of concrete expansion and resultant deterioration. These experiments inevitably lead to a conclusion that magnesium chloride or calcium chloride deicers may accelerate or initiate concrete deterioration under certain conditions of long-term use.

Sodium chloride proved to be the least aggressive in promoting concrete deterioration in laboratory experiments. The relatively benign character of sodium chloride solutions may be a result of a lack of several different hydrates of sodium chloride. Although $\text{NaCl} \cdot 2\text{H}_2\text{O}$ occurs at low temperature, this is the only hydrate known, so that fewer hydration changes are possible as a result of relatively minor changes in environmental conditions. $\text{NaCl} \cdot 2\text{H}_2\text{O}$ also has a much smaller molar volume than magnesium or calcium chloride hydrates, so lesser growth pressures would be expected from hydration of NaCl.

ROLE OF ROCK SALT DEICERS IN ACCELERATING DETERIORATION

Personnel of the Iowa DOT have noted that the non-durable concretes studied here are much more deteriorated on primary highways than on secondary roads. They have speculated that differing degrees of damage result from greater deicing rock salt use on the primary highways. Although our experiments disclosed that sodium chloride is relatively benign in terms of concrete deterioration, we did observe some deterioration under freeze/thaw cycling using relatively dilute 0.75M NaCl solutions and 0°C freezing (Table IV). These conditions are commonly encountered on Iowa highways during winters.

Concretes containing reactive dolomite aggregate, which has undergone alkali-dolomite reactions and resulting expansion and micro-cracking, may be more susceptible to rock salt deterioration under actual winter highway conditions. Enhanced susceptibility to rock salt deicer damage may develop during dedolomitization because salt solutions may have easier access into those concretes in comparison to concretes with less reactive aggregate. The presence of sodium chloride brines at aggregate-paste boundaries may be especially damaging if bonding at the boundary has already been weakened by dedolomitization and micro-crack formation. Repeated freezing and thawing conditions will cause enhanced deterioration on roads where rock salt is used abundantly. In addition, magnesium released by alkali-dolomite reactions may react with chloride from rock salt deicers to form magnesium chloride hydrates. Hydration state changes will also induce expansion pressures and deterioration.

RECOMMENDATIONS

Upon consideration of the results of this investigation, several recommendations are made. The first is that dolomite aggregate source rocks should be screened for average crystal size as well as porosity. Those with small euhedral and subhedral dolomite crystals and with relatively high porosity should be eliminated for concrete use. Screening can be

accomplished by SEM and petrographic microscope studies. The present research proves that these methods can easily distinguish poorly-performing aggregate [Smith and Garrison quarries (basal Coralville Member of the Devonian Cedar Valley Formation) and the Paralta quarry (Otis Member of the Devonian Wapsipinicon Formation)] from suitable materials [Sundheim quarry (Silurian Hopkinton Formation) and Mar-Jo Hills quarry (Stewartville Member of the Ordovician Galena Formation)].

A second recommendation is that further experiments should be instituted to determine whether Iowa dolomites can be classified into reactive and non-reactive groups on the basis of reactivity to concentrated calcium chloride brine treatments. Our research concluded that reactive and poorly-performing dolomite rock is more susceptible to chemical reaction rim formation as a result of immersion in calcium chloride brines in conjunction with freeze/thaw and wet/dry cycling than are non-reactive dolomites.

A final recommendation is that magnesium chloride and calcium magnesium acetate (CMA) should be used for highway deicers only after further long-term testing to determine if they accelerate highway concrete deterioration. Our observations, together with those of many other workers, strongly suggest that magnesium has a major role in concrete deterioration, either by promoting expansion of the concrete because of brucite crystal growth or by less obvious chemical reactions with the cement.

ACKNOWLEDGMENTS

This project was funded primarily by the Iowa Department of Transportation, Project No. HR-355. This support is gratefully acknowledged. We particularly want to thank Messers. Vernon Marks, Jim Myers, and Wendell Dubberke, as well as Dr. Wallace Rippie for their advice, suggestions, and support of this project. Without their help the project would not have been possible. We thank Drs. Jerry Amenson and Scott Schlorholtz, of the ISU Materials Research Laboratory, for their assistance with SEM

analyses. Appreciation is also extended to Dr. Alfred Kracher for help with the electron microprobe studies, and to Mr. Scott Thieben for assistance with x-ray diffraction analyses. Discussions with Dr. Robert Dawson, Ames Research Laboratory, concerning various aspects of our studies are also gratefully appreciated. Partial financial support was also provided to Guo-Liang Gan through the Iowa State Mining and Mineral Resources Research Institute program.

APPENDIX

REPRESENTATIVE ELECTRON MICROPROBE ANALYSES OF CARBONATE AGGREGATE IN IOWA CONCRETE

Additional data on compositions of aggregate from the Iowa concretes studied in the project is presented in an appendix which is not included in the current report because its detailed nature will probably interest only a few readers specializing the Iowa dolomite compositions. It is available under separate cover from Iowa Department of Transportation.

The aggregate of all concretes studied here consisted almost entirely of dolomite, and Table II presents dolomite averages from the Appendix. Over 20,000 electron microprobe data were obtained in this study, primarily from automated scans, or traverses, across aggregate grains and adjacent cement paste. Representative traverses are shown in the Figures and discussed in the text. The Appendix presents representative and selected analyses of carbonate aggregate only.

REFERENCES

- Bisque R. E., 1959, Silicification of argillaceous carbonate rocks. Ph.D. dissertation, Iowa State University, 64 pp.
- Bisque R. E. and Lemish J., 1958, Chemical characteristics of some carbonate aggregates as related to durability of concrete. Highway Research Board Bull., [196] (Air Voids in Concrete and Characteristics of Aggregates), 29-45.
- Carles-Gibergues A., Ollivier J. P., Fournier B., Berube M. A., 1989, A new approach to the study of alkali - aggregate reaction mechanisms. In: Alkali - Aggregate Reaction (Proc. 8th International Conf., eds. Okada K., Nishibayashi S., Kawamura M.), Elsevier Applied Science, New York, 161-166.
- Deng M. and Tang M. Sh., 1993, Mechanism of dedolomitization and expansion of dolomitic rocks. Cement and Concrete Research, 23 [6] 1397-1408.
- Donovan, J. J., Rivers, M. L., and Armstrong, J. T., 1992, PRSUPR: Automation and analysis software for wavelength dispersive electron-beam microanalysis of a PC: American Mineralogist, 77, 444-445.
- Dubberke W., 1983, Factors relating to aggregate durability in Portland Cement Concrete. Interim report for Project HR-2022, Iowa Department of Transportation.
- Dubberke W. and Marks V. J., 1985, The effects of deicing salt on aggregate durability. Transportation Research Record, [1031] (Geotechnical Engineering Research), 27-34.
- Dubberke W. and Marks V. J., 1987, The instability of ferroan dolomite aggregate in concrete (presented at the 66th Annual Meeting of the Transportation Research Board, Washington, D.C.). Final Report for Iowa Highway Research Board Research Project HR-266. 18pp.
- Gillott J. E., 1964, Mechanism and kinetic of expansion in alkali - carbonate rock reaction. Canadian J. Earth Sci., 1 121-145.

- Gillott J. E., 1975, Alkali - aggregate reactions in concrete. *Engineering Geol.*, 9 [4] 303-326.
- Gillott J. E., 1978, Effect of deicing agents and sulphate solution on concrete aggregate. *Q. J. Engng. Geol.*, 11 177-192.
- Gillott J. E. and Swenson E. G., 1969, Mechanism of the alkali - carbonate rock reaction. *Q. J. Engng. Geol.*, 2 [1] 7-23.
- Girard R. J., Myers W., Manchester G. D., Trimm W. L., 1982, D-cracking: Pavement design and construction variables. *Transportation Research Record*, [853] (Concrete Analysis and Deterioration), 1-9.
- Hadley D. W., 1961, Alkali reactivity of carbonate rocks - expansion and dedolomitization. *Highway Research Board*, 40 (Proc. 40th Annual Meeting, Washington D. C.), 463-474.
- Hadley D. W., 1964, Alkali reactivity of dolomitic carbonate rocks. *Highway Research Record*, [45] (Symp. Alkali - Carbonate Rock Reactions), 1-19.
- Lemish J. and Moore W. J., 1964, Carbonate aggregate reactions: Recent studies and an approach to the problem. *Highway Research Record*, [45] (Symp. Alkali - Carbonate Rock Reactions), 57-71.
- Lemish J., Rush F. E., Hiltrop C. L., 1958, Relationship of physical properties of some Iowa carbonate aggregates to durability of concrete. *Highway Research Board Bull.*, [196] (Air Voids in Concrete and Characteristics of Aggregates), 1-16.
- Marks V. J. and Dubberke W., 1982, Durability of concrete and the Iowa Pore Index test. *Transportation Research Record*, [853] (Concrete Analysis and Deterioration), 25-30.
- Mather B., 1974, Developments in specification and control. *Highway Research Record*, [525] (Cement - Aggregate Reactions), 38-42.
- Myers J. and Dubberke W., 1980, Iowa Pore Index Test. Interim Report, Iowa Department of Transportation.

- Oberste-Padtberg R., 1985, Degradation of cements by magnesium brine: A microscopic study. In: Proceedings of the 7th International Conference on Cement Microscopy, Texas, 24-36.
- Pitt J. M., Carnazzo R. A., Vu J., 1989, Control of concrete deterioration due to trace compounds in deicers. Phase II Report for Iowa DOT Project HR-299, ERI Project 3071 and ISU-ERI-Ames-89419. 45pp.
- Poole A. B., 1981, Alkali - carbonate reactions in concrete. In: Alkali - Aggregate Reaction in Concrete (Proc. 5th International Conf.), National Building Research Institute, Council for Scientific and Industrial Research, Pretoria, South Africa, Publication S252/1981, 327-334.
- Poole A. B. and Sotiropoulos P., 1978, The interaction of alkalis with dolomite and quartz in experimental concrete systems. In: Effects of Alkalies in Cement and Concrete (Proc. 4th International Conf.), Publication No. CE-MAT-1-78, Purdue University, Indiana, 163-179.
- Poole A. B. and Sotiropoulos P., 1980, Reactions between dolomitic aggregate and alkali pore fluids in concrete. *Q. J. Eng. Geol. London*, 13 281-287.
- Sayward J. M., 1984, Salt action on concrete (Special report CRREL-SR-84-25), Cold Regions Research and Engineering Lab., Hanover, NH, 76 pp.
- Sherwood W. C. and Newlon H. H., 1964, Studies on the mechanisms of alkali - carbonate reaction. Part I - Chemical reactions. *Highway Research Record*, [45] (Symp. Alkali - Carbonate Rock Reactions), 41-56.
- Swenson E. G. and Gillott J. E., 1964, Alkali - carbonate rock reaction. *Highway Research Record*, [45] (Symp. Alkali - Carbonate Rock Reactions), 21-45.
- Swenson E. G. and Gillott J. E., 1967, Alkali reactivity of dolomitic limestone aggregate. *Mag. Concrete Res.*, 19 [59] 95-104.

- Tang M. Sh., Liu Zh., Han S. F., 1986, Mechanism of alkali - carbonate reaction. In: Concrete Alkali - Aggregate Reaction (Proc. 7th International Conf., ed. Grattan-Bellew P. E.), Noyes Publications, New Jersey, 275-279.
- Tang M. Sh., Lu Y. N., Han S. F., 1989, Kinetics of alkali - carbonate reaction. In: Alkali - Aggregate Reaction (Proc. 8th International Conf., eds. Okada K., Nishibayashi S., Kawamura M.), Elsevier Applied Science, New York, 147-152.
- Tang M. Sh., Liu Zh., Lu Y. N., Han S. F., 1991, Alkali - carbonate reaction and pH value. *Il Cemento*, 88 [3] 141-150.
- Winkler E. M. and Singer P. C., 1972, Crystallization pressure of salts in stone and concrete. *Bull. Geol. Soc. Am.*, 83 [11] 3509-3514.

PLATES

PLATE AND FIGURE ABBREVIATIONS

In the Plates and Figures, the following abbreviations will be used:

ce	= cement.	C	= light-colored dolomite rim.
dol	= dolomite aggregate.	D	= light-colored paste rim adjacent to aggregate boundary.
A	= dolomite aggregate interior.	E.	= cement farther from aggregate boundary, which is less affected by aggregate-paste chemical reactions than the D zone.
B	= dark dolomite rim.		

In Plates and Figures treating with experimental deterioration of concretes, zones with the subscript 'e' refers to the same zones after experimental treatments. Ae = aggregate interior after experimental concrete deterioration; Be = dark dolomite rim after experiments; Ce = thin light-colored dolomite rim after experiments; De = light-colored cement reaction rim or zone after experiments; and Ee = cement farther from aggregate-paste boundary after experiments.

PLATE I.

Plt I. Core samples of Iowa highway concrete. The concrete contains aggregates from the following quarries (a) Smith, (b) Paralta, (c) Garrison, (d) Ames gravel pit, (e) Sundheim, (f) Mar-Jo Hills. Service records are Smith: 12 yrs., Paralta: 8 yrs., Garrison: 12 yrs, Sundheim: > 40 yrs., and Mar-Jo Hills: > 40 yrs. Arrows indicate that non-durable concretes (those with short service lives) with aggregate from Smith, Paralta, Garrison, and Ames pit quarries show more pronounced reaction rims and micro-cracks than durable (long service lives) Sundheim and Mar-Jo Hills concretes. Bars = 2 cm.

PLATE I

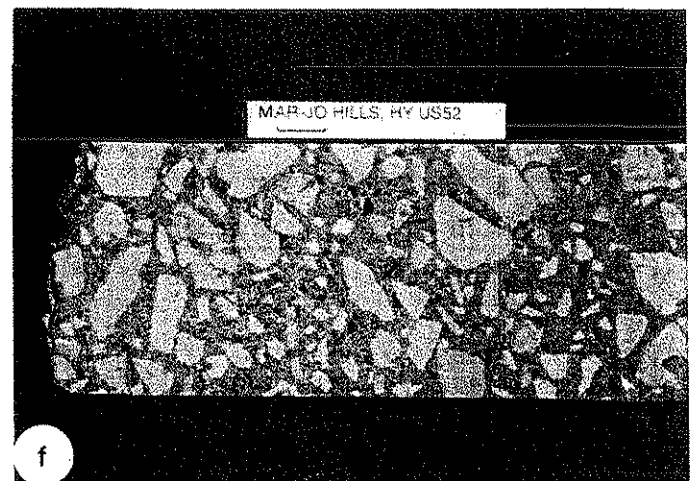
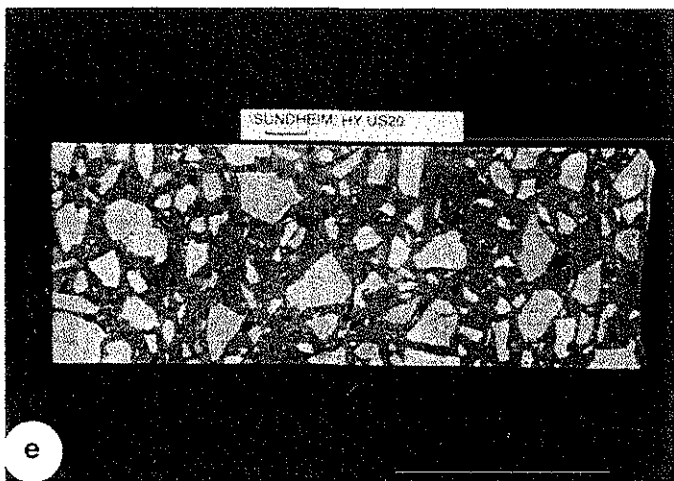
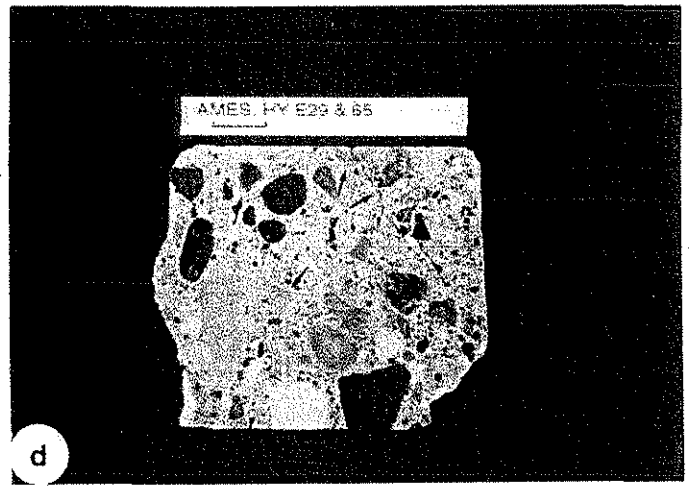
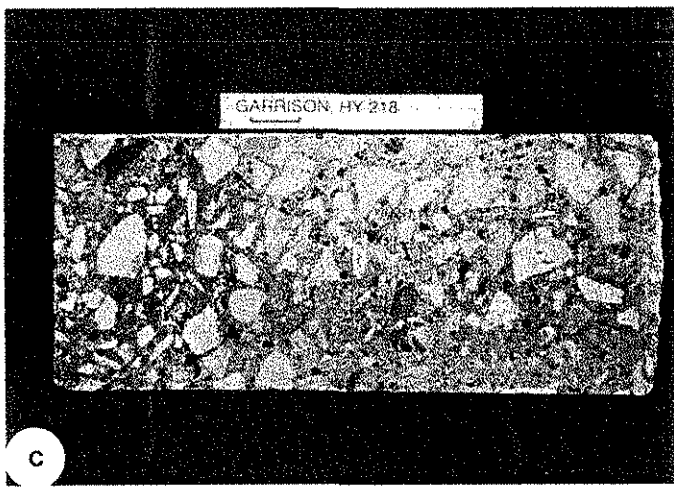
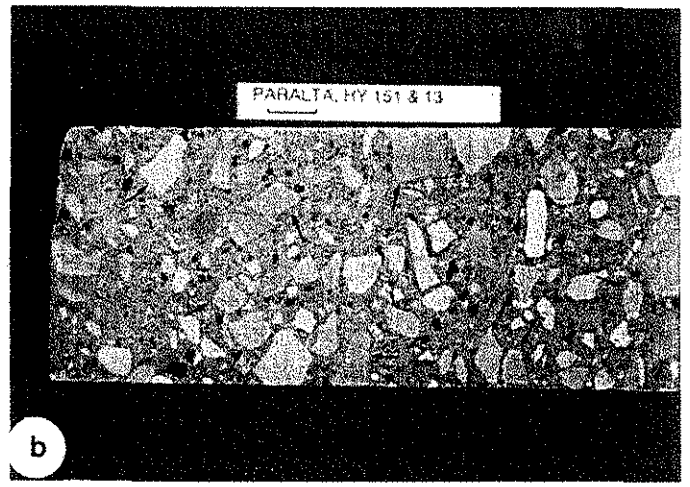
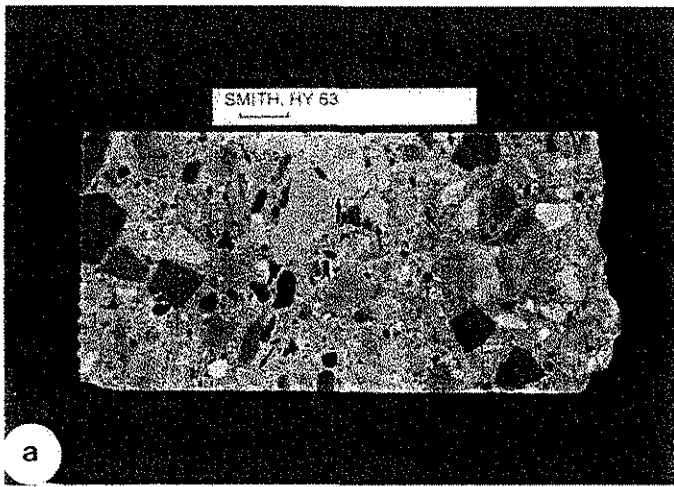


PLATE II.

Plt II. SEM micrographs of non-durable and durable concretes. Each concrete contains aggregate from the following quarries. Magnifications of the four photographs are approximately equal.

- a. Smith quarry aggregate (non-durable)
- b. Paralta quarry aggregate (non-durable)
- c. Mar-Jo Hills aggregate (durable)
- c. Sundheim quarry aggregate (durable)

The Smith and Paralta quarries dolomite aggregates, which produce concretes with short service lives, are more finer-grained than the Mar-Jo Hills and Sundheim quarries dolomite which produce highly durable concretes.

- e. Paralta quarry aggregate (non-durable)
- f. Sundheim quarry aggregate (durable)

These SEM micrographs show sections through aggregate interiors. Magnification of the Paralta dolomite (e) is 3x than of the Sundheim dolomite (f). The Paralta quarry dolomite is very finely crystalline, with abundant euhedral and subhedral dolomite crystals, is highly porous, and contains small unidentified minerals, possible clays in the voids. The Sundheim quarry dolomite, in contrast, consists of tightly intergrown dolomite crystals which exhibit almost no crystal faces, and has almost no voids between the crystals.

PLATE II

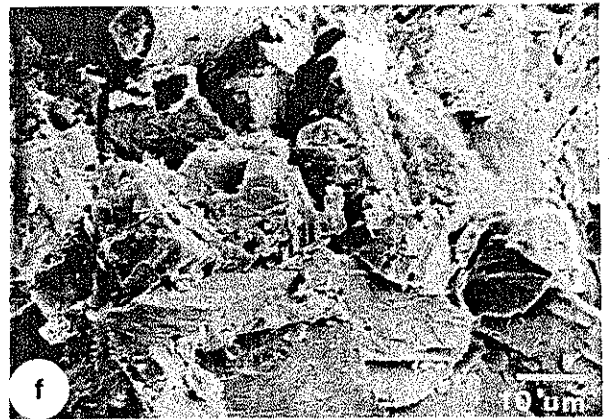
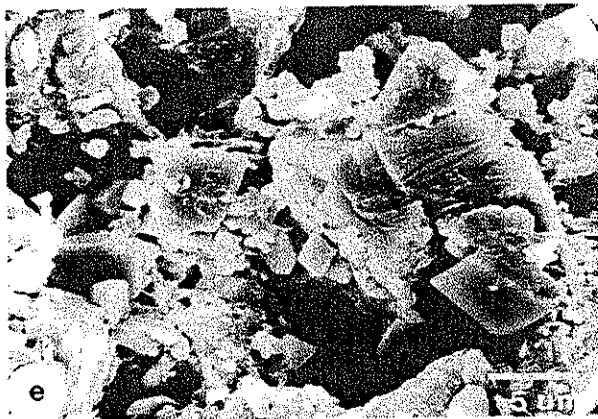
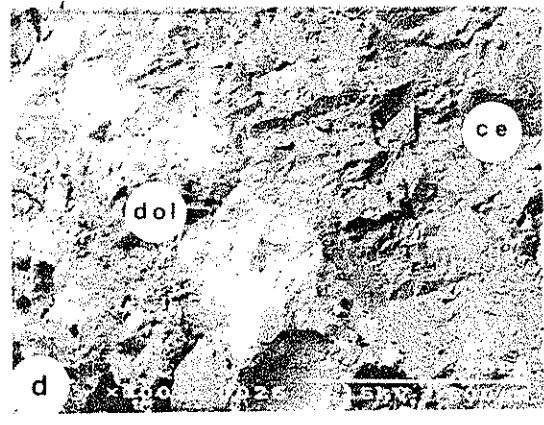
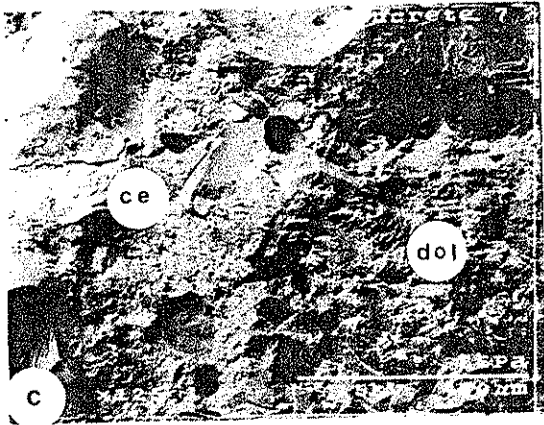
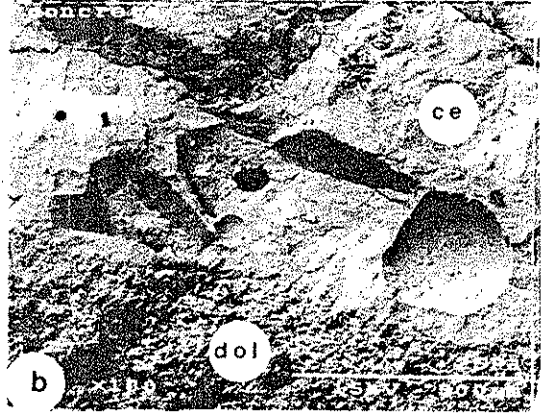
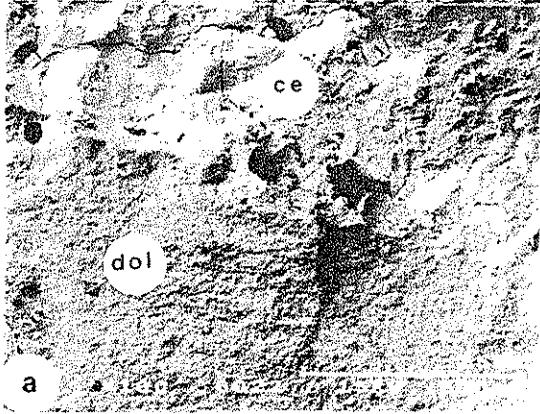


PLATE III.

Plt III. SEM and light micrographs of concretes.

- a. SEM micrograph of a section through durable Sundheim quarry concrete. Many small spherical to subspherical grains with concentric lamination (shown by arrows) are present in the paste. The concentric structure is difficult to see because of low magnification. EDAX data indicates that the major components of these grains are Ca + Si in ratios that suggest they are calcium silicate hydrates. Bar = 250 μm .
- b. SEM micrograph of a section through non-durable Paralta quarry concrete. Many small spherical to subspherical grains (arrows) with abundant micro-cracks are present in the paste. These grains are probably calcium silicate hydrates.
- c. Light micrographs of the aggregate-paste interface in non-durable Smith quarry concrete, in plane-polarized light. Bar = 250 μm
- d. Light micrograph of same area as (c), between cross-polarizers. Bar = 250 μm
- e. SEM micrograph of dolomite aggregate-paste interface in non-durable Smith quarry concrete, same area as shown in Plate IIIc,d.
- f. SEM micrograph of aggregate-paste interface in non-durable Smith quarry concrete, same area as shown in Plates IVa,b.

Boundaries between the different zones are gradational except for that between zones C and D. Compared to zone A, zone B is more porous, and zone C is less porous. In SEM view, Zone D is brighter (whiter) than zone E. Most interstitial voids in zone C are filled with white Ca-rich minerals which decrease in abundance from aggregate-paste interface toward the unaltered paste, Zone E. More micro-cracks are visible in zone E than in zone D, and some air voids in E are partially filled with secondary materials. Figs 1,2 are electron microprobe traverses and EDAX elemental maps of the area shown in IIIe, whereas Figs 3,4 are of area shown in IIIf.

PLATE III

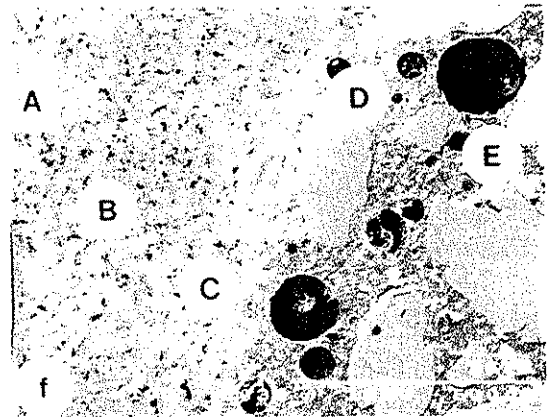
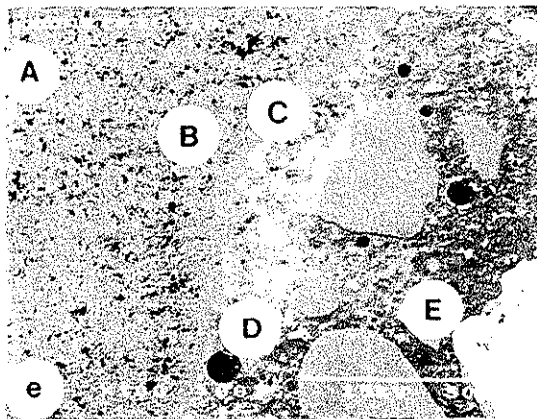
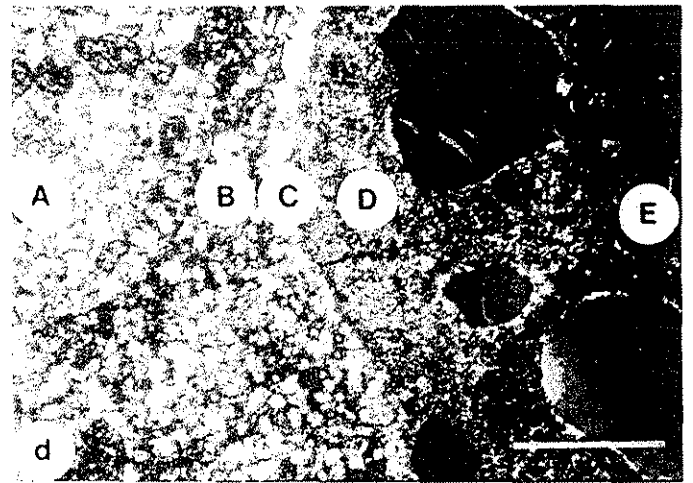
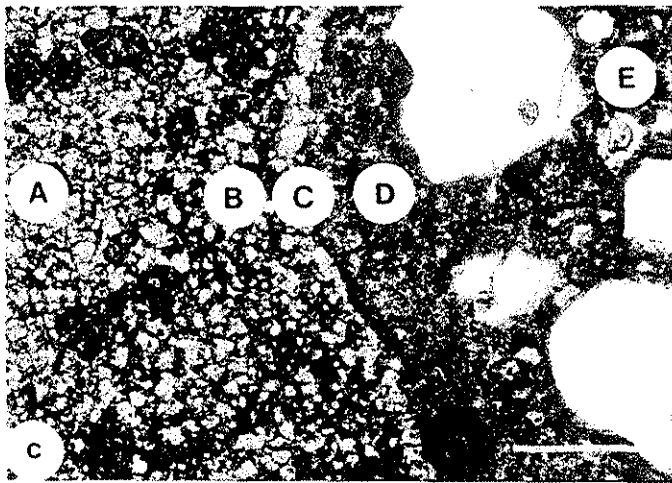
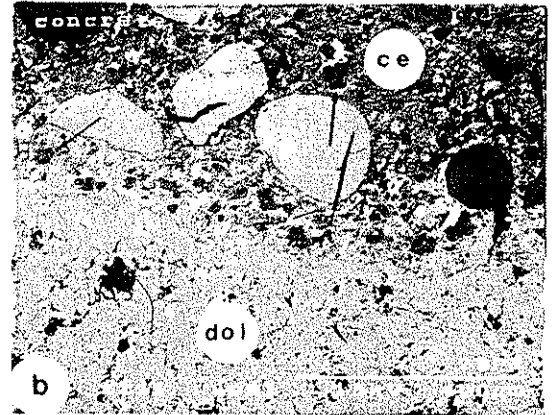
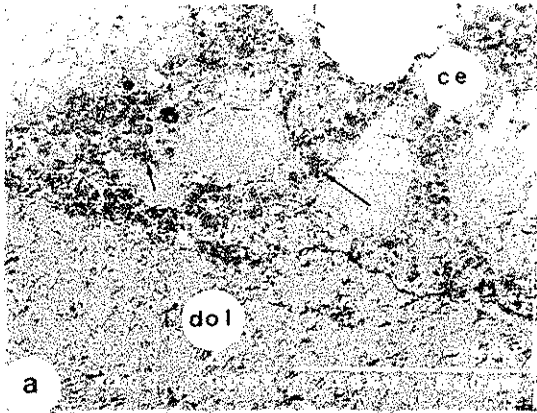


PLATE IV.

Plt IV. Light and SEM micrographs of Smith quarry concrete and Paralta quarry concrete.

a. Light micrograph of dolomite-paste interface in non-durable Smith quarry concrete, in plane-polarized light. Bar = 250 μm .

b. Light micrograph between crossed-polarizers, same area as IVa. Bar = 250 μm .

Boundaries between different zones are gradational except that between the dark and light-colored dolomite rims (B and C). Zone B containing smaller and fewer visible dolomite crystals than zone A. Fig 3 shows electron microprobe traverses and Fig 4 shows EDAX elemental maps of area shown in the above photographs.

c. Plane-polarized light micrographs showing dolomite aggregate-paste interface in non-durable Paralta quarry concrete. Bar = 250 μm .

d. Light micrograph between crossed-polars of same area as IVb. Note gradational boundaries between the various zones. The light-colored dolomite rim, (Zone C) is missing. Bar = 250 μm .

e. SEM micrograph of similar area shown in IVc,d.

f. Enlarged SEM view of left side of IVe.

Note the variable width of the light-colored cement paste rim, zone D, the high porosity of the inner region of the dark dolomite rim, zone B, and the reduced porosity of the outer part of zone B. Interstitial voids have been filled with secondary minerals. Between the more porous inner part and less porous outer part of the dark dolomite rim, B, there is a crack which is parallel to the aggregate edge. The crack is filled minerals that appear white and gray in SEM views. There are many micro-cracked grains in the cement paste, as indicated by arrows. Refer to Fig 5 for EDAX maps of area.

PLATE IV

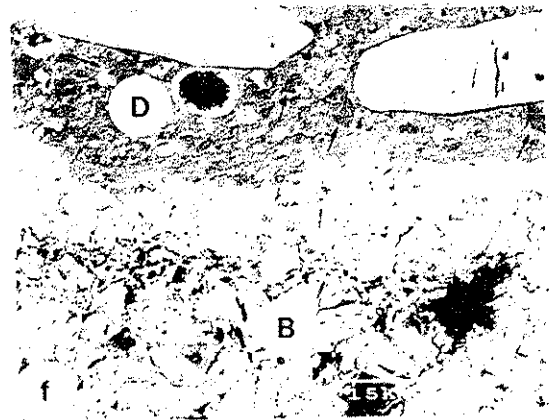
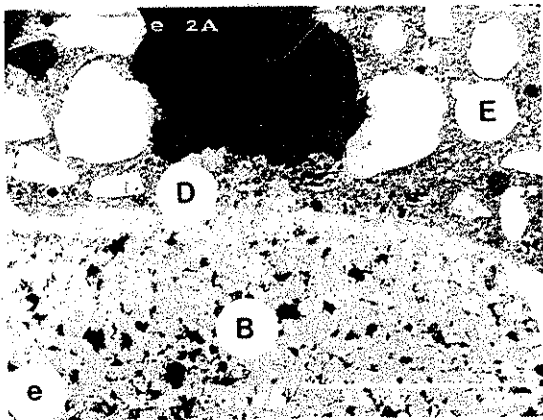
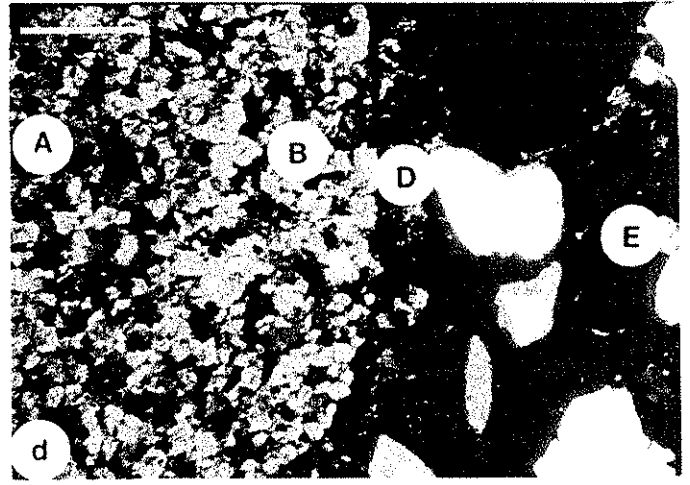
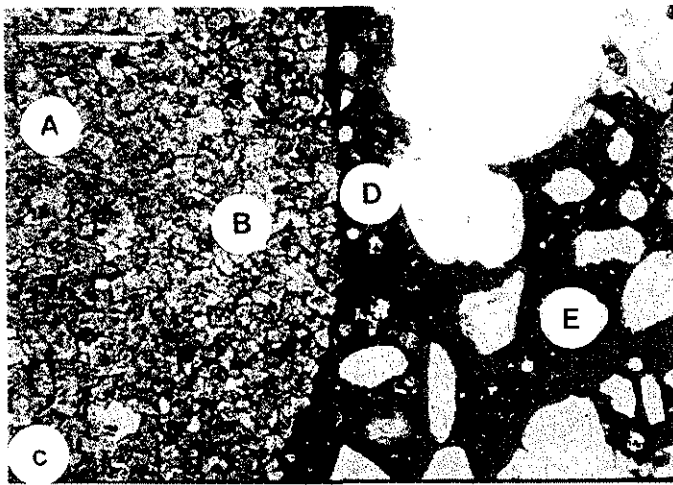
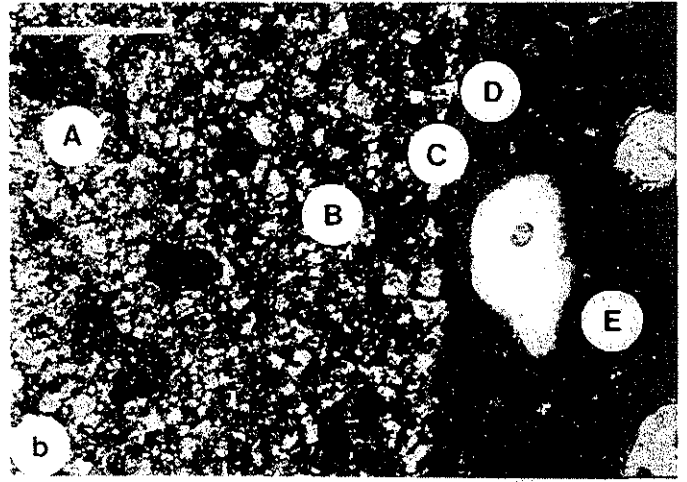
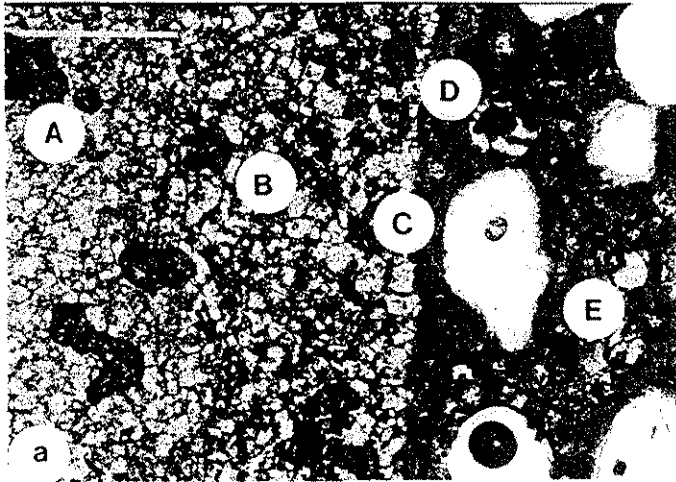


PLATE V.

Plt V. Light and SEM micrographs of Paralta concrete and Smith quarry concrete.

a. Light-micrographs of non-durable Paralta quarry concrete, plane-polarized light.

Bar = 250 μm .

b. Light-micrographs between crossed-polarizers, same area as Va. Bar = 250 μm .

The boundary between the dark dolomite rim, zone B, and unaltered dolomite, A, is difficult to define from the photographs. The light dolomite rim (zone C) is absent.

Bar = 250 μm . Refer to Fig 6 for microprobe traverse of area shown in Va,b.

c, d. SEM micrographs of aggregate-paste interface of non-durable Smith quarry concrete.

The dark dolomite rim, zone B, is very porous and voids are filled with new minerals.

The light-colored dolomite rim, zone C, is absent. Refer to Figs 8-9 for EDAX element maps of the area showed in Va,b.

e. Light micrographs of non-durable Smith quarry concrete, plane-polarized light.

Bar = 250 μm .

f. Light micrograph with crossed-polarized of same area as Ve, crossed-polarizers.

Bar = 500 μm .

No reaction rims are evident. Note the fine grain size of the dolomite aggregate characteristics of non-durable concretes compared to the large grains of aggregate from durable concretes (Plt VIa, b)

PLATE V

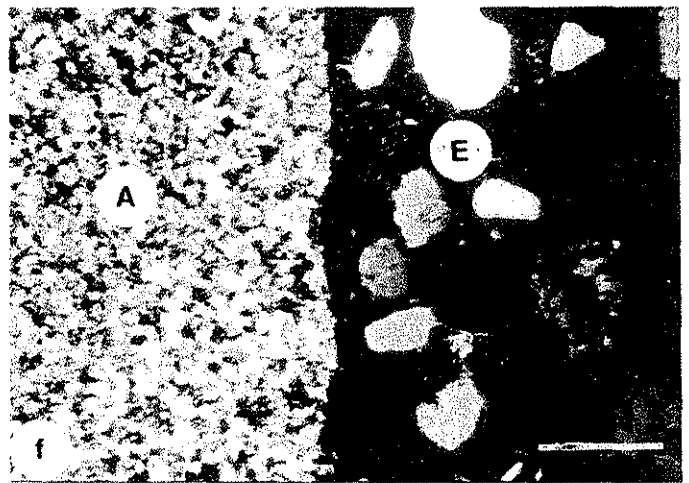
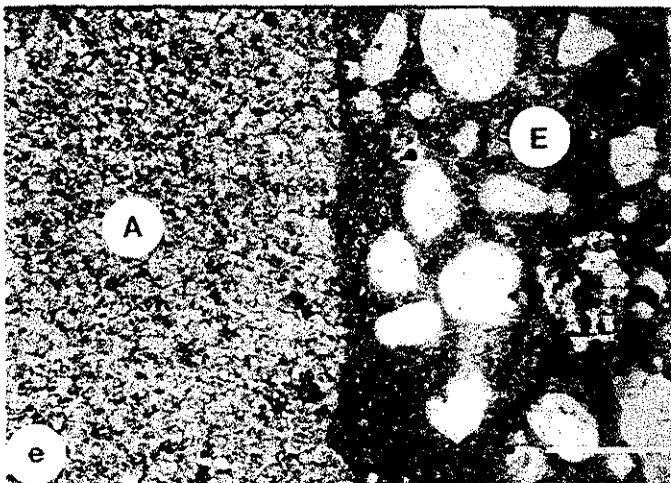
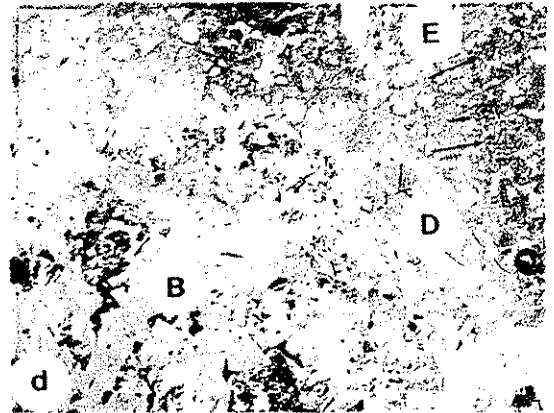
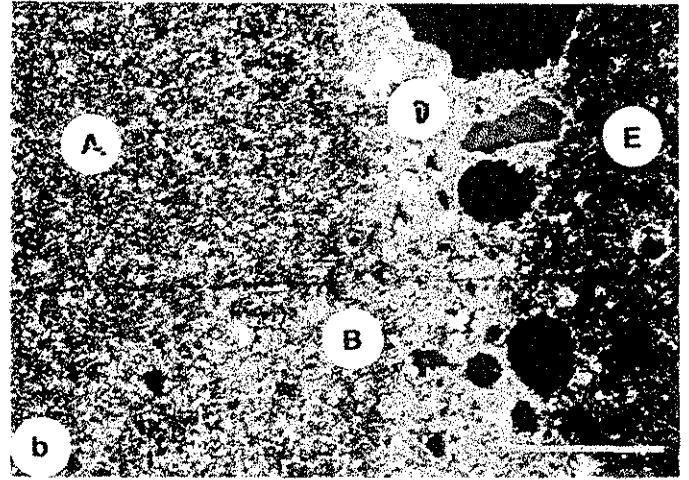
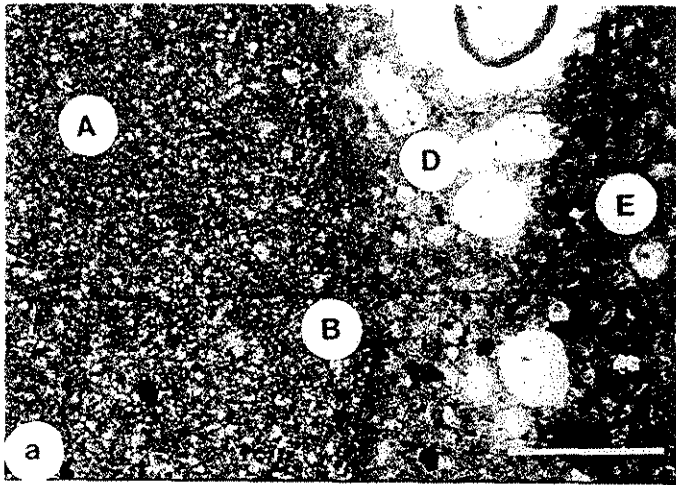


PLATE VI.

Plt VI. Light and SEM micrographs of Mar-Jo Hills and Sundheim aggregate concretes.

- a. Mar-Jo Hills, plane-polarized light b. Mar-Jo Hills, crossed-polarizers.
c. Sundheim, plane-polarized-light d. Sundheim, crossed-polarizers.

No reaction rims are observable in dolomite or paste in these durable concretes containing aggregate from either the Mar-Jo Hills or Sundheim quarries. Fig 10 gives microprobe traverse for Mar-Jo Hills sample shown in VIa,b, and Fig 11 for Sundheim sample. In Plt VIa and VIb bar = 250 μm , In Plt VIc and VI d bar = 500 μm .

- e. SEM micrographs of durable Sundheim quarry concrete traversed by electron microprobe in Fig 11 and shown in EDAX element maps, Fig 12.
f. SEM micrograph, enlargement of nodular section in center previous micrograph, Plt VIe. No reaction rim is visible in aggregate or cement paste, and only a very few micro-cracks are visible in the paste. Fig 12 gives corresponding EDAX mapping.

PLATE VI

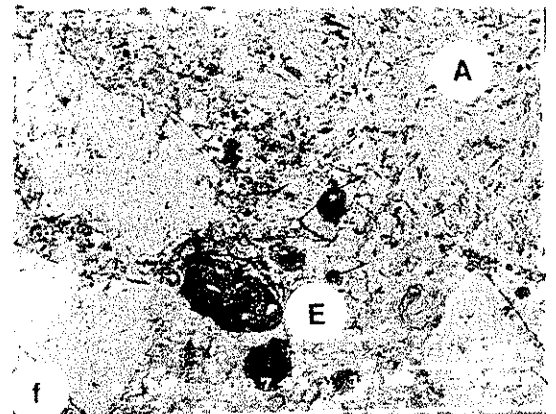
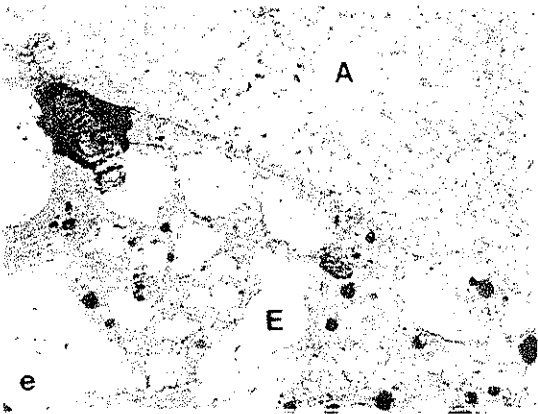
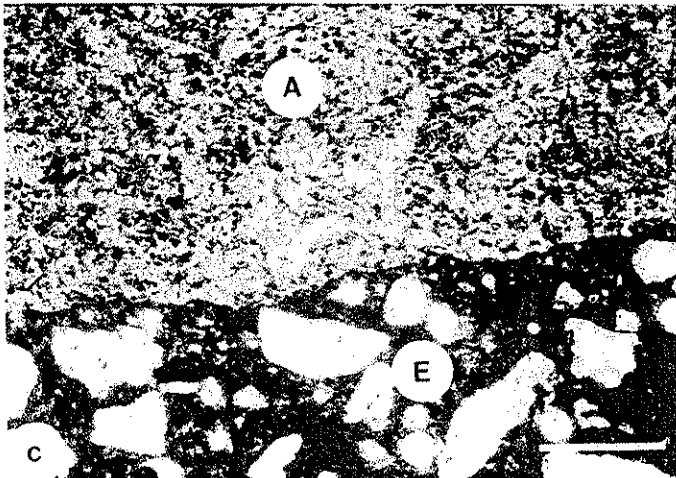
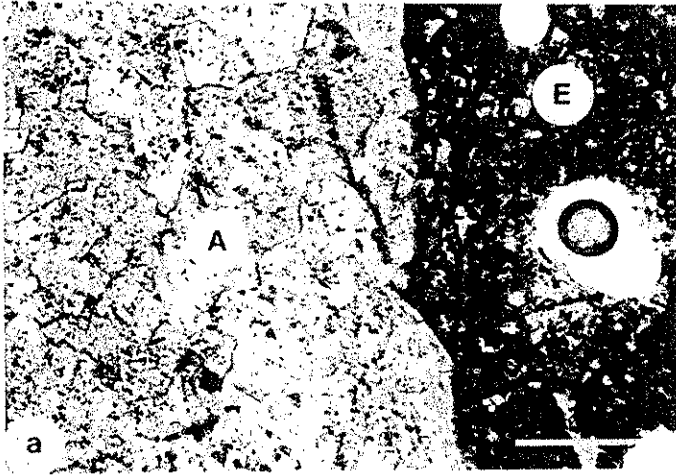


PLATE VII.

Plt VII. Light and SEM micrographs of durable Mar-Jo Hills and Sundheim and non-durable Smith quarry concretes.

a. Light micrograph of Mar-Jo Hills quarry concrete, plane-polarized light. Bar = 500 μm .

b. Same area as VIIa, between crossed-polarizers. Bar = 500 μm .

The boundaries between zone A, the unaltered dolomite interior, and zone B, the dark dolomite rim are gradational, as is the boundary between zone D, the light-colored cement paste rim and E, the unaltered paste. Fig 14 gives the corresponding electron microprobe traverse.

c. Light micrograph of durable Sundheim quarry concrete, plane-polarized light.

Bar = 500 μm .

d. Same area as VIIb, between crossed-polarizers. Bar = 500 μm .

Boundaries between zones are gradational as shown in the previous micrographs of the Mar-Jo Hills concrete. Fig 15 gives the corresponding electron microprobe traverse.

e. SEM micrograph of interior part of Mar-Jo Hills dolomite aggregate particle. The dolomite is well-crystallized and characterized by relatively low porosity. Refer to Fig 16 for corresponding EDAX element maps.

f. SEM micrograph of Smith quarry concrete, showing aggregate-paste boundary, and high porosity. Fig 17 gives corresponding EDAX maps.

PLATE VII

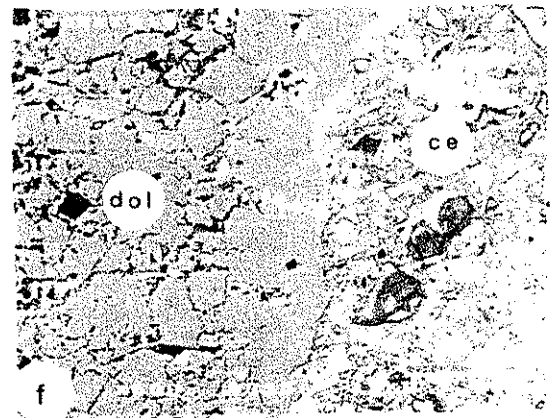
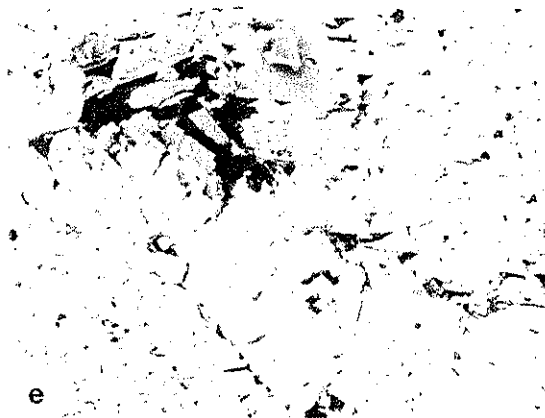
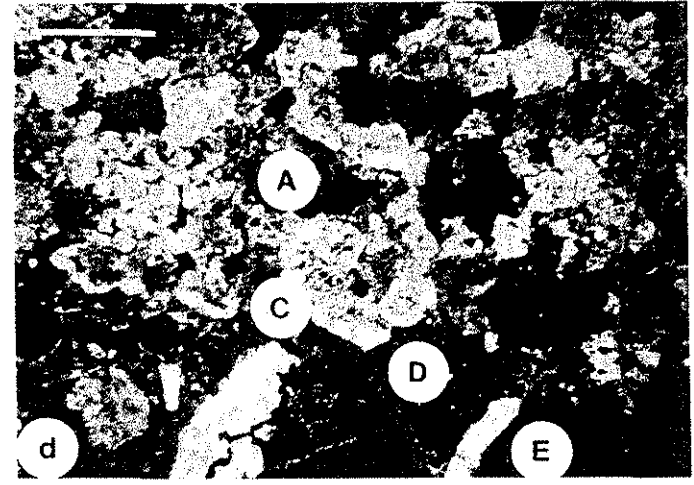
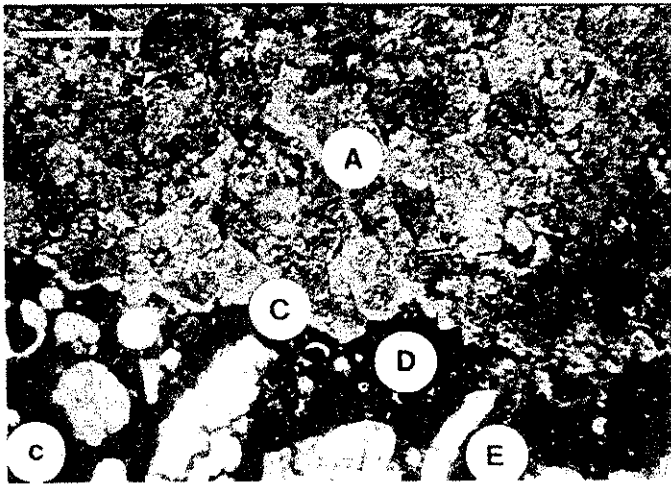
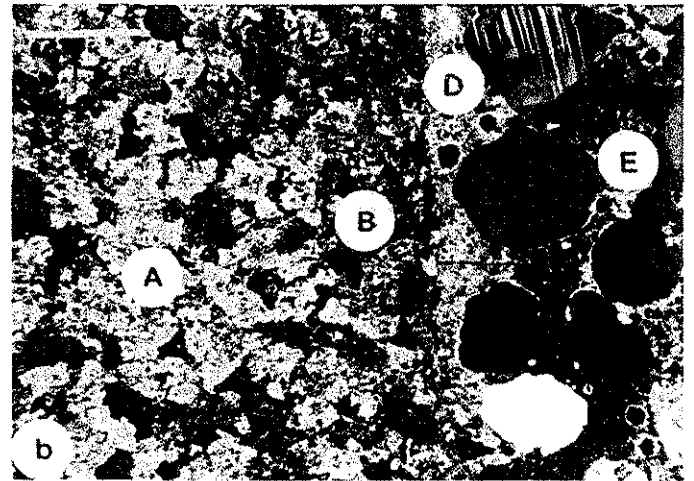
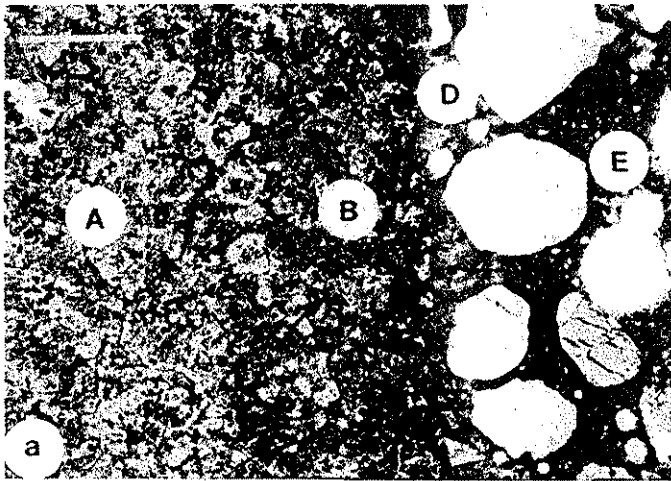


PLATE VIII.

Plt VIII. Experimentally-produced deterioration of Iowa highway concrete. The concretes contain aggregates from (a) Smith, (b) Paralta, (c) Garrison, (d) Ames gravel pit, (e) Sundheim, and (f) Mar-Jo Hills quarries.

All of the concretes exhibited marked cracks (arrows) and browning paste discoloration from CaWD cycles. All concretes exhibited severe crumbling and decomposition, and dark brown paste discoloration wet/dry cycling in magnesium whereas concretes showed little deterioration from Na wet/dry cycling. No = no treatment, CaWD, MgWD, and NaWD = wet/dry cycling with 3M $\text{CaCl}_2 \cdot 2\text{H}_2\text{O}$, $\text{MgCl}_2 \cdot 6\text{H}_2\text{O}$, and NaCl solutions, 60°C immersion and 90°C drying. Bar scale in cm and mm.

PLATE VIII

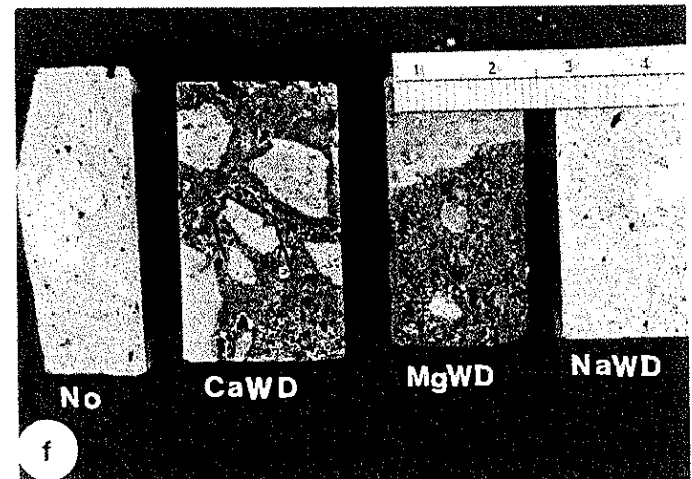
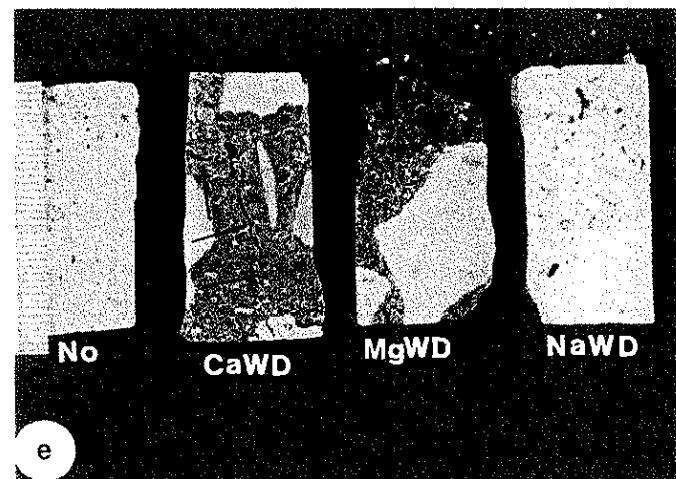
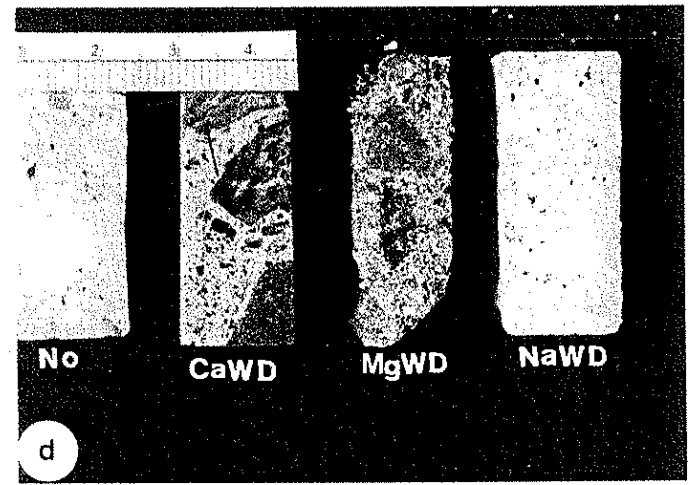
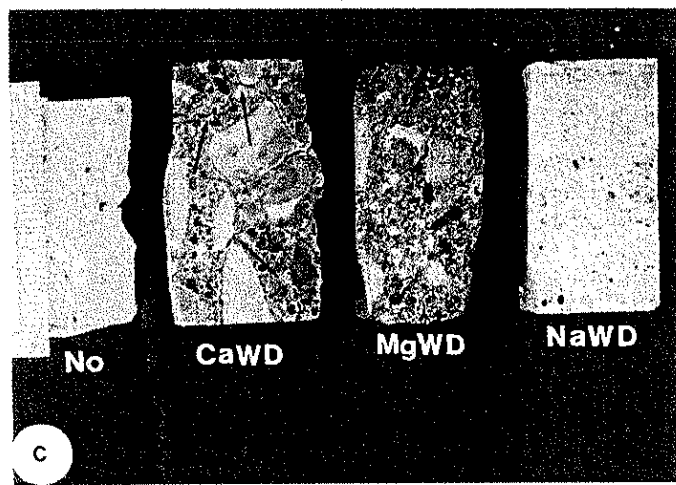
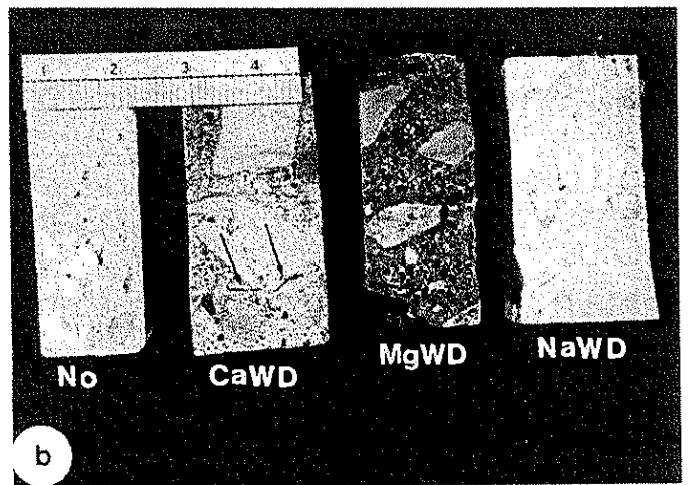
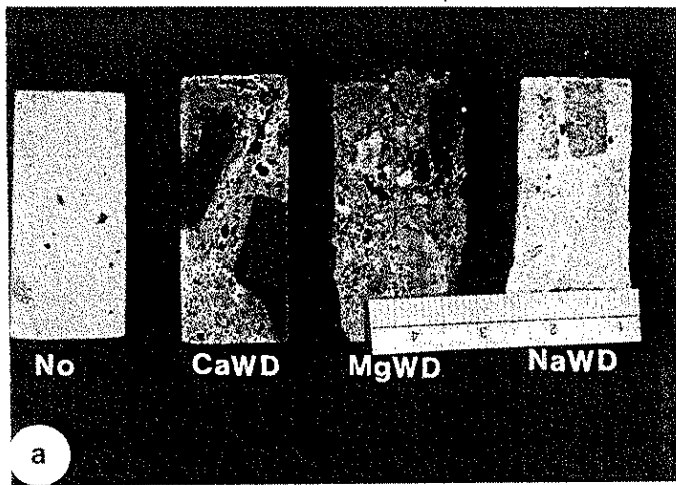


PLATE IX.

Plt IX. Experimentally-produced deterioration of concrete containing Smith, Garrison, Sundheim, and Mar-Jo Hills dolomite coarse aggregate.

- | | |
|-------------|-----------------|
| a. Smith | d. Mar-Jo Hills |
| b. Garrison | e. Smith |
| c. Sundheim | f. Garrison |

Essentially no deterioration was observed from wet/dry cycles in water or NaCl solutions. All concretes exhibited a slight brown discoloration of cement paste in $\text{CaCl}_2 \cdot 2\text{H}_2\text{O}$ with freeze/thaw cycling, and all exhibited severe crack development and dark brown paste discoloration after Ca wet/dry cycling. Severe decomposition and dark paste discoloration was evident from cycling between wet/dry and freeze/thaw conditions in $\text{MgCl}_2 \cdot 6\text{H}_2\text{O}$ solutions. H_2O WD = wet/dry cycling at $60^\circ\text{C}/90^\circ\text{C}$ in distilled water; NaWD = same but with 3M NaCl solution; CaFT = freeze/thaw, with freezing at -70°C , thawing at 25°C , and solution immersion at 60°C , 3M $\text{CaCl}_2 \cdot 2\text{H}_2\text{O}$; No = no treatment; MgWD and MgFT refers to identical experimental conditions but with 3M $\text{MgCl}_2 \cdot 6\text{H}_2\text{O}$.

PLATE IX

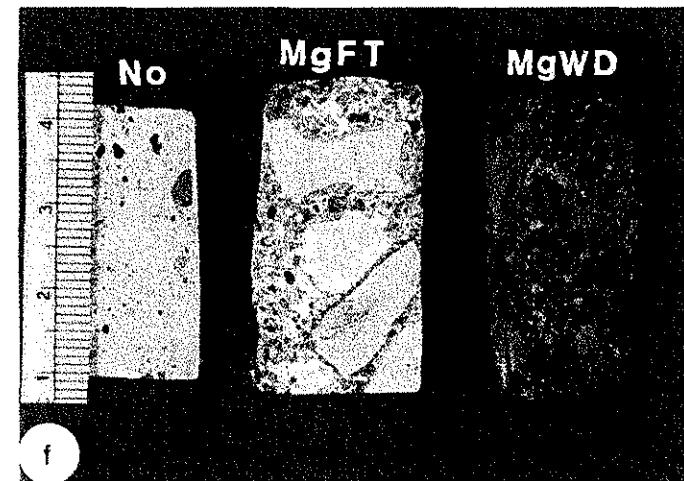
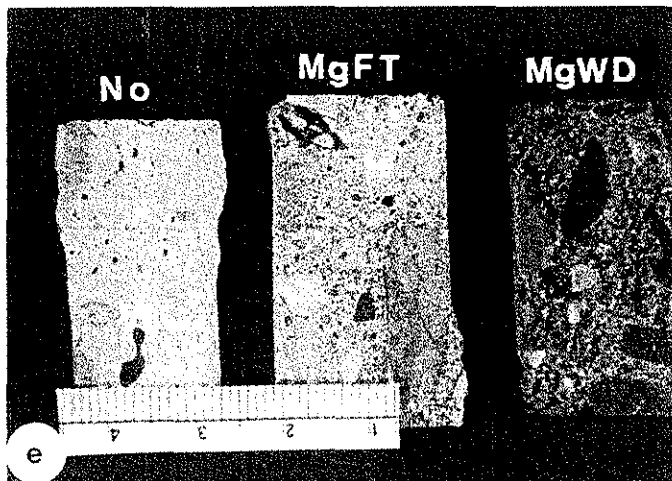
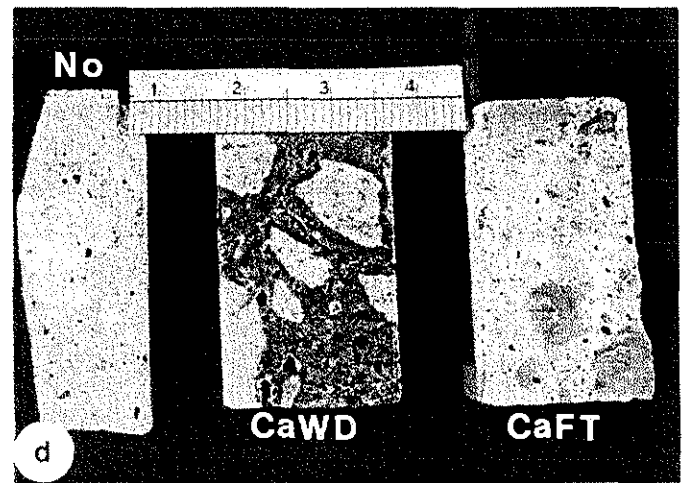
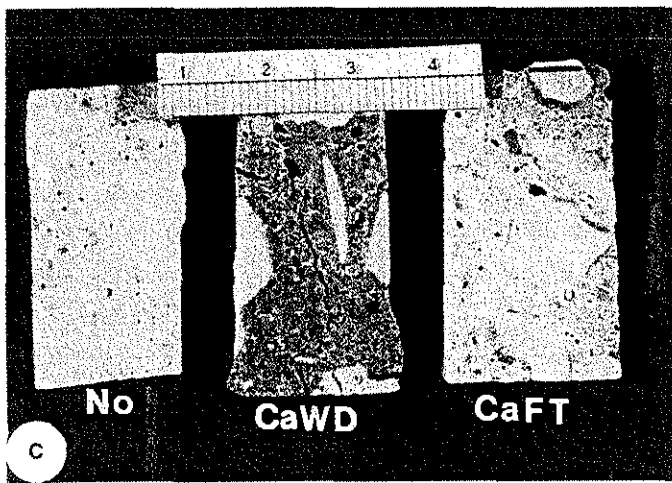
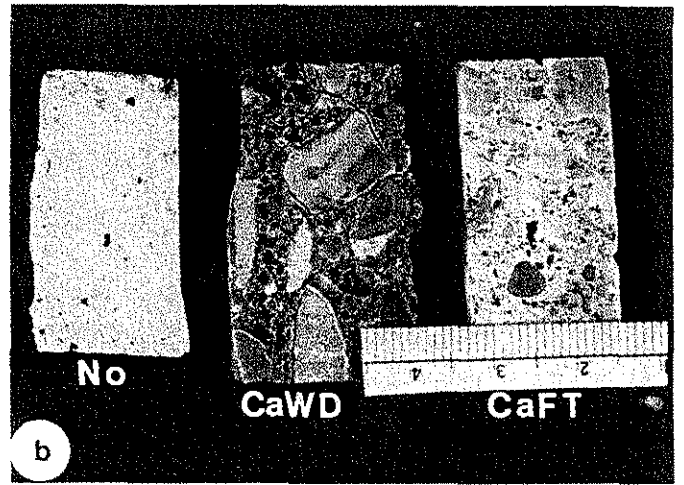
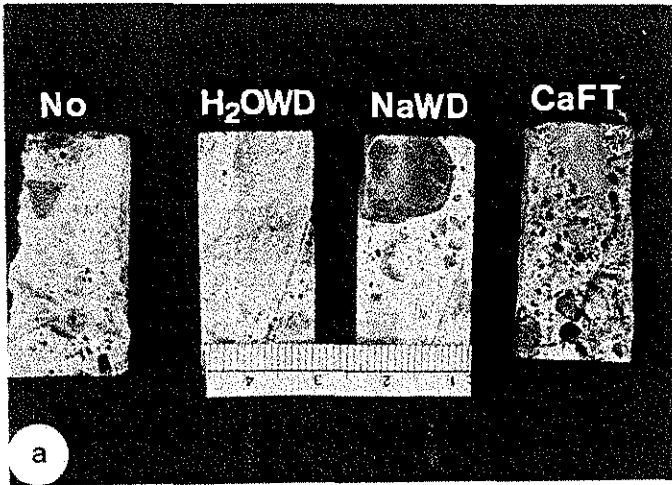


PLATE X.

Plt X. Experimental deterioration of concretes and micrographs of treated materials.

a. Mar-Jo Hills

b. Mar-Jo Hills

c. Paralta

d. Ames gravel pit

Both non-durable concretes and durable ones show severe decomposition and dark brown paste discoloration from wet/dry conditions utilizing $MgCl_2 \cdot 6H_2O$. Almost no decomposition occurred during wet/dry and freeze thaw conditions using NaCl solutions.

e. SEM micrograph of Garrison quarry concrete from wet/dry cycling in Ca solutions.

Large cracks are evident in cement paste and at the aggregate-paste interface. Air-voids and cracks are partially or completely filled with late-formed minerals. See Fig 18 for EDAX maps of the area shown in photo.

f. Experimental deterioration of concretes. Light micrograph of aggregate/paste interface developed in non-durable concretes with Paralta aggregate by wet/dry cycling in Ca solutions, crossed-polarizers.

Boundaries between zones Ae and Be, and between zones De and Ed, are gradational. Dark and light dolomite reaction rims, zones Be and Ce, are continuous along the aggregate edge where dolomite was directly in contact with Ca solution (lower left) and along the margins of aggregate in contact with the paste.

Refer to Plt. IIIc-d for similar rim development in untreated concrete.

PLATE X

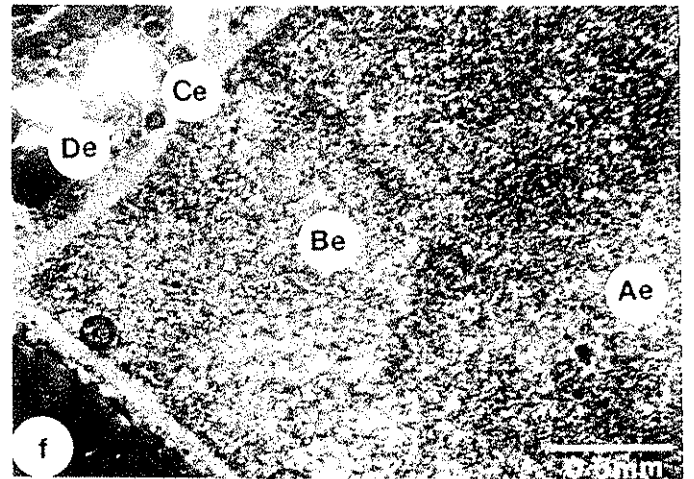
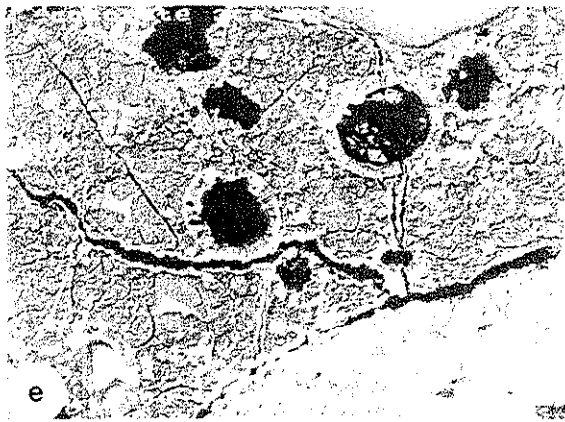
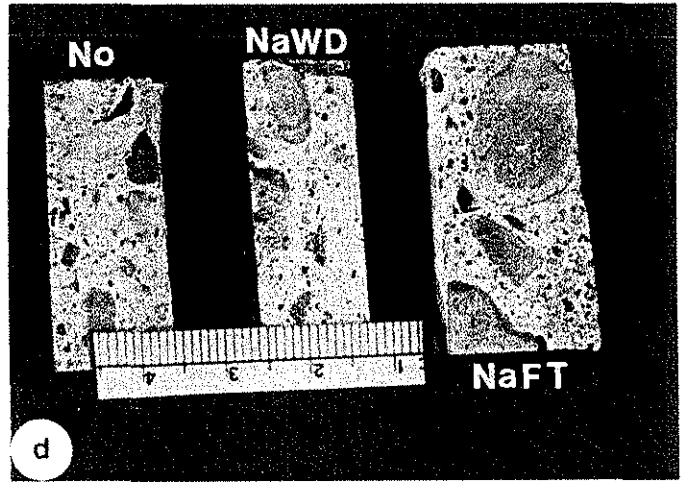
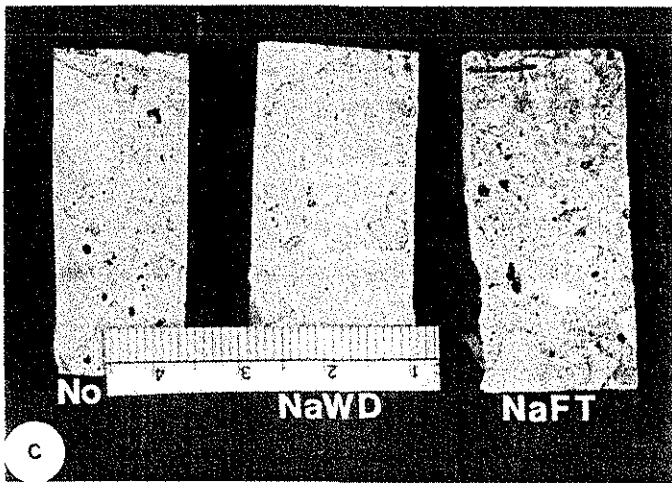
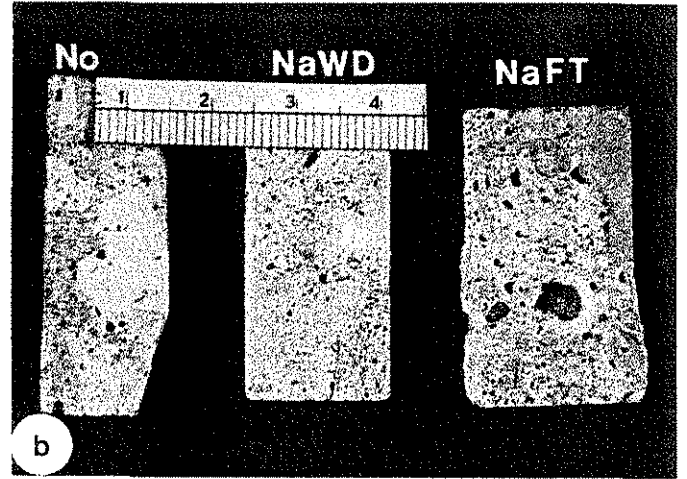
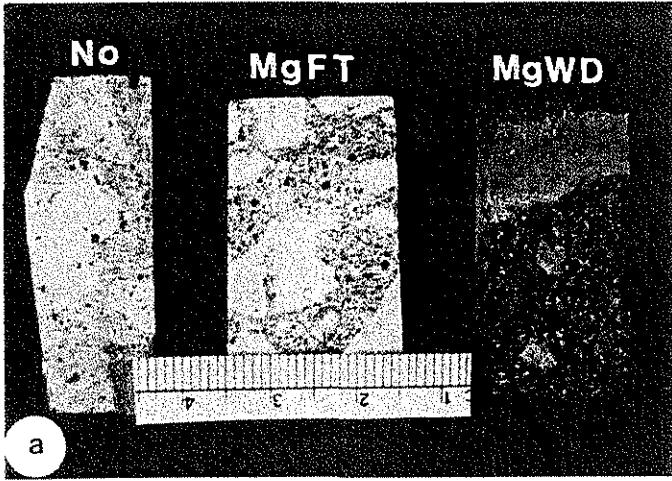


PLATE XI.

Plt XI. Experimental deterioration of concretes. Light and SEM micrographs of concretes containing Paralta and Smith aggregate.

- a. Light micrograph of aggregate-paste boundary after wet/dry cycling in Ca solutions, Paralta aggregate concrete, plane-polarized light.
- b. Same area as XIa, crossed-polarizers. Dark and light-colored dolomite rims, zones Be and Ce, are visible at the aggregate-paste boundary and along the crack within the aggregate interior. A light-colored paste reaction rim, zone De, is also visible.
- c. SEM micrograph of concrete after wet/dry cycling in Ca solution, Paralta aggregate concrete. Plt XIc shows almost same area as in Plt XIa,b
- d. SEM micrograph, enlargement of central area of previous view (Plt XIc), but rotated by 90° . Both zones Be and Ce contain abundant void-filling minerals, and the porosity of the light-colored dolomite rim is less than of the dark dolomite rim. Boundaries between rims are gradational except for that between the dark and light-colored dolomite rims. Fig 21 shows EDAX maps corresponding to Plt XI d.
- e. Light micrograph of concrete after freeze/thaw in Ca solution, Paralta aggregate concrete, crossed-polarizers. The aggregate-paste interface of this experimentally-treated non-durable concrete is notably different from that of the non-treated concrete shown in Plt IVc,d. Parts of aggregate rim appear lighter colored. Fig 22b are corresponding electron microprobe traverses of the area.
- f. Light micrograph of concrete after wet/dry cycles in Ca solution, Smith quarry aggregate, crossed-polarizers. The aggregate-paste interface resembles that in untreated concretes shown in Plts IIIc-d and IVa,b. It differs from that formed by Ca wet/dry cycling in having a thinner dark Ce rim than that shown in XIa,b. Fig 23 gives corresponding electron microprobe traverse.

PLATE XI

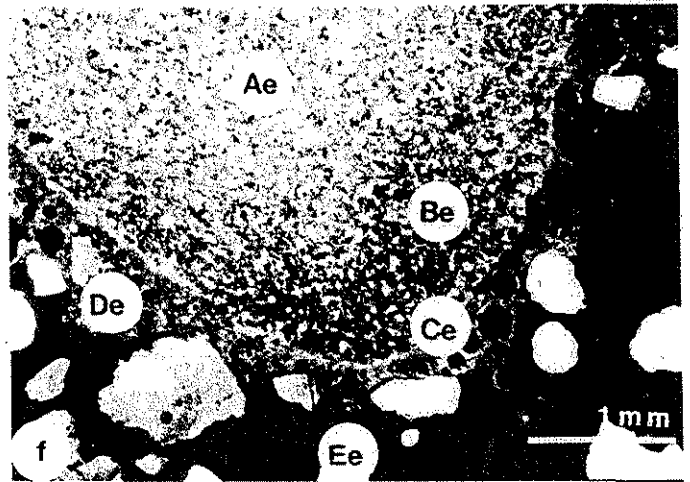
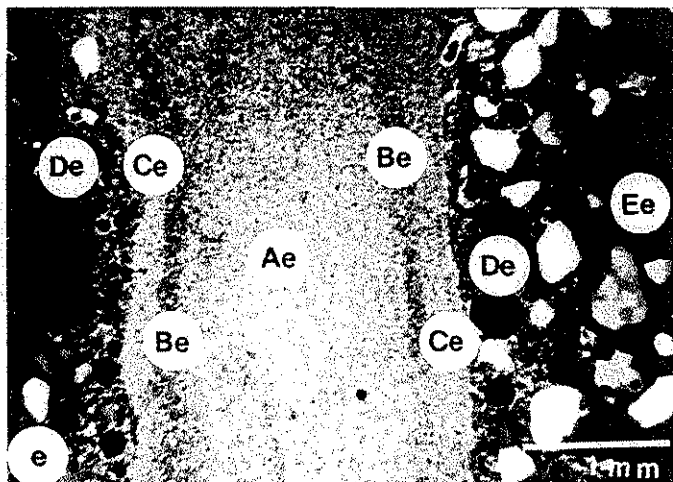
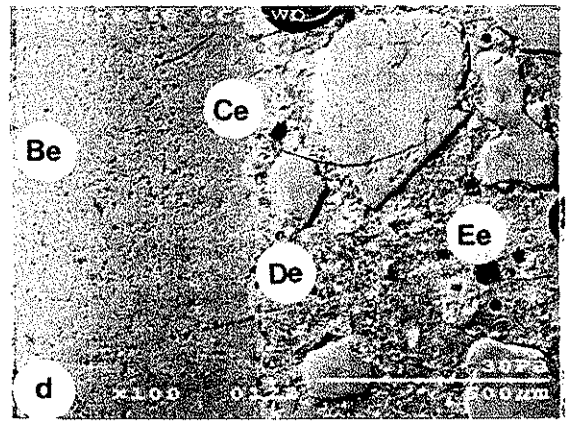
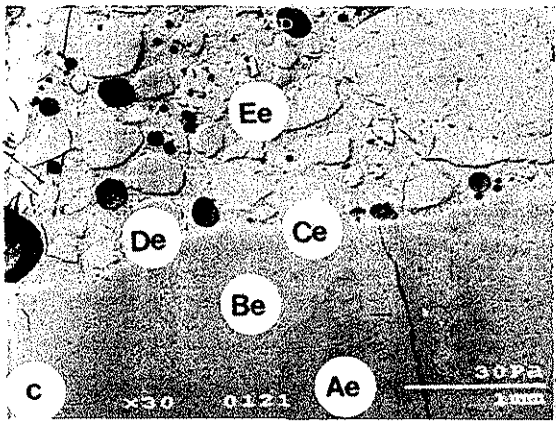
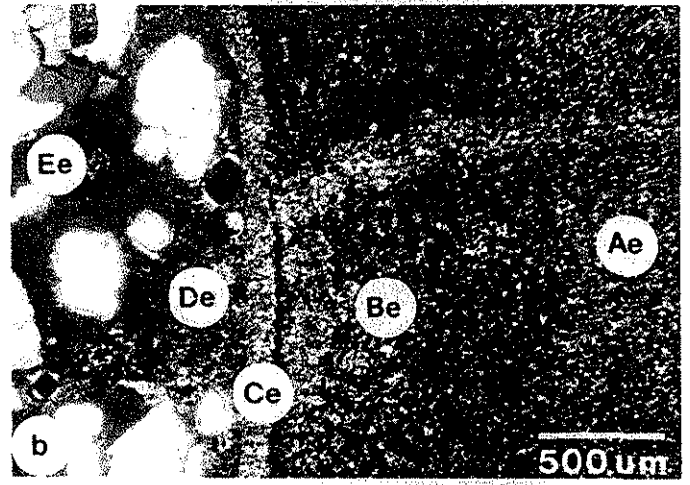
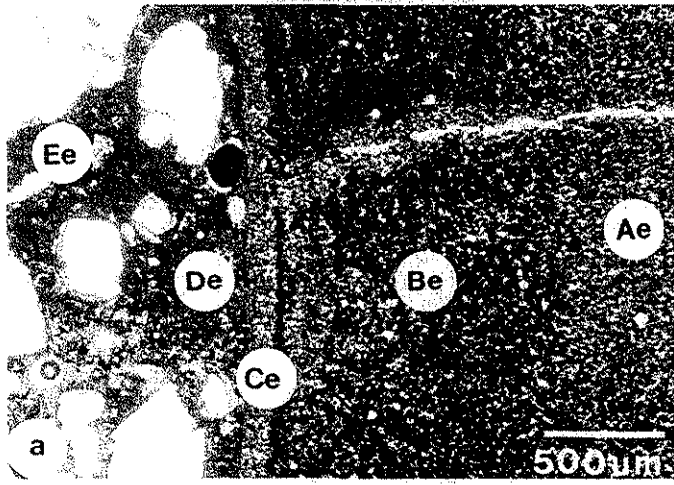


PLATE XII

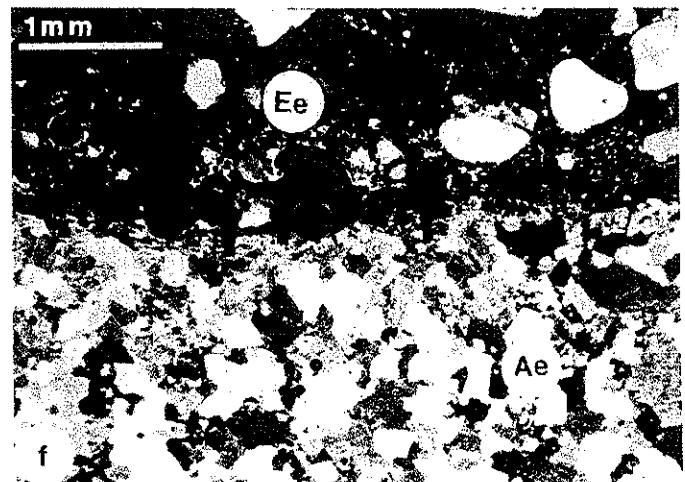
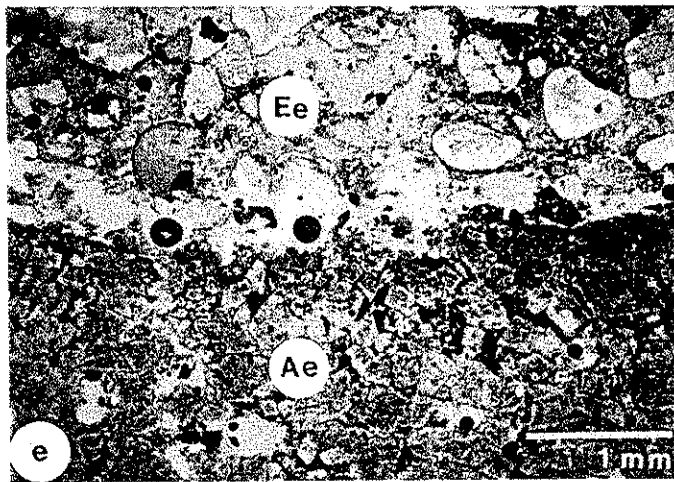
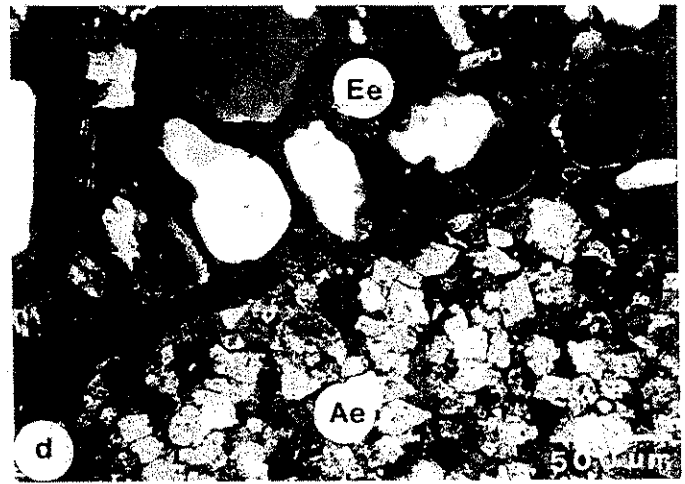
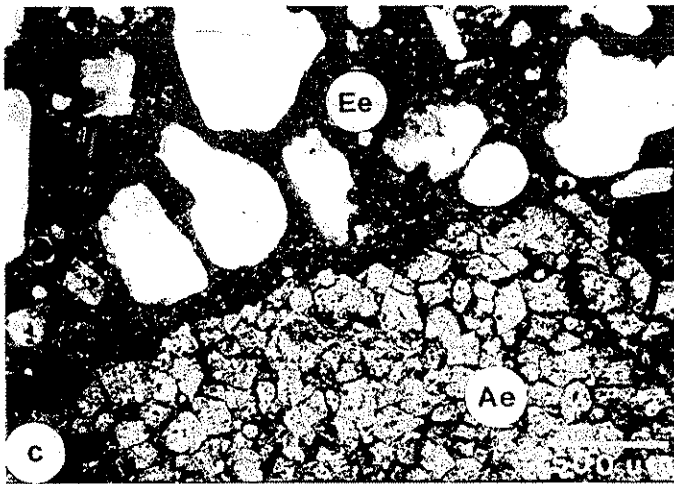
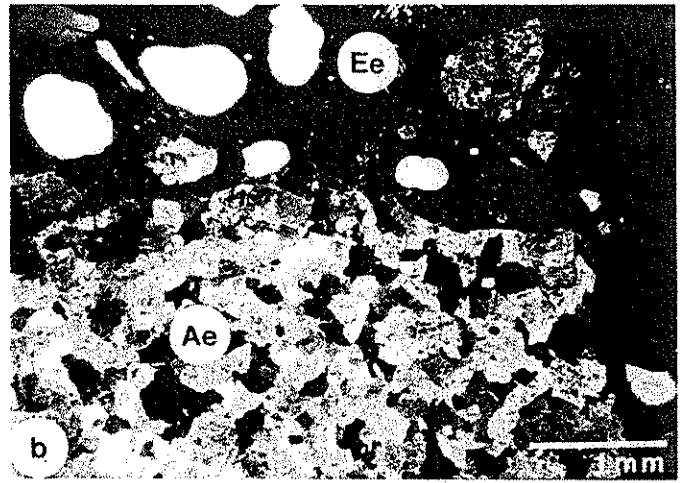
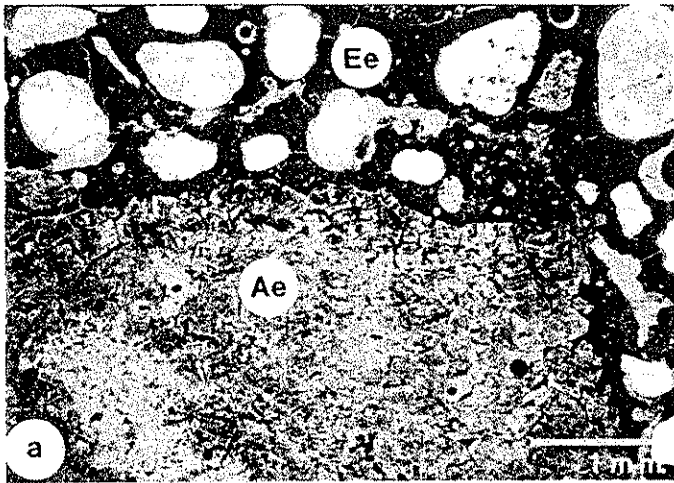


PLATE XIII.

Plt XIII. Experimental deterioration of concretes. SEM and light micrographs of Mar-Jo Hills and Garrison aggregate concretes.

- a. SEM micrograph of aggregate-paste boundary of Mar-Jo Hills concrete after wet/dry cycling in Mg solution.
- b. SEM micrograph, enlargement of central area of previous view, Plt. XIIIa.
Micro-cracks in dolomite aggregate are filled with abundant material which appears white, light and dark gray in SEM views. Cement paste shows severe cracking, decomposition, and abundant void fills of material similar in character to that in dolomite cracks. Figs 26 shows electron microprobe traverse of the area, and Figs 27,28 give EDAX maps.
- c. Light-micrographs of wet/dry Mg-solution cycled Garrison quarry concrete, plane-polarized light.
- d. Same area as previous photo, Plt. XIIIc, cross-polarized light.
Zone Ee, dark paste region after experiments, exhibits extreme decomposition.
Fig 29a,b gives corresponding electron microprobe traverses, and Fig 30 gives EDAX element mapping.
- e. SEM micrographs of wet/dry Mg-solution cycled Garrison quarry concrete.
- f. SEM micrograph, lower magnification view of area.
The dark dolomite rim is very porous, whereas the light-colored dolomite rim has reduced porosity. Interstitial voids in dolomite aggregate are filled with abundant minerals. The light-colored cement rim shows little cracking, whereas the outer cement (which appears darker on the SEM photo) exhibits severe cracking.

PLATE XIII

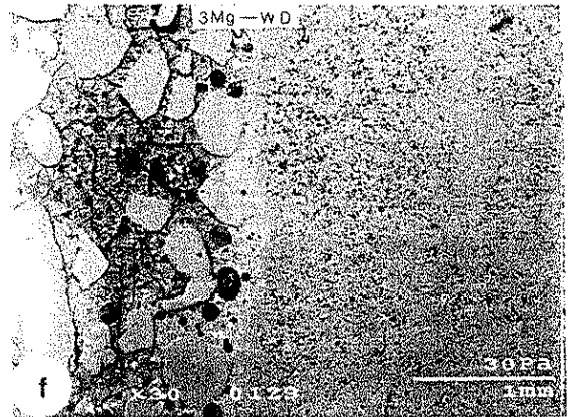
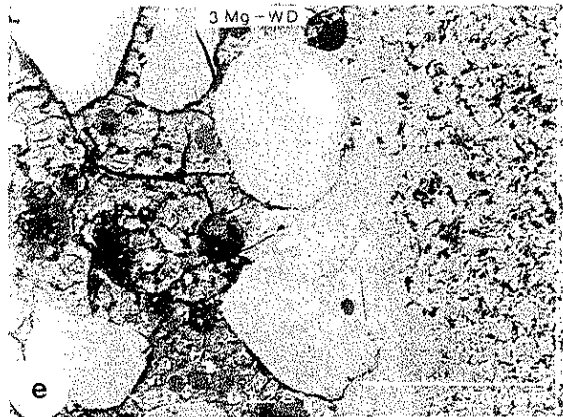
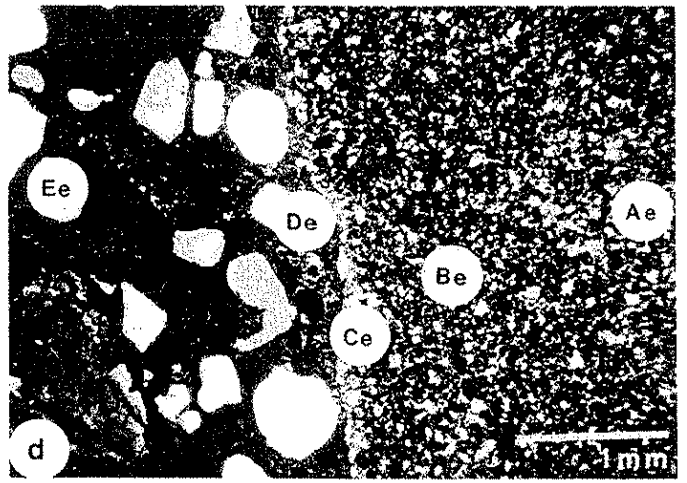
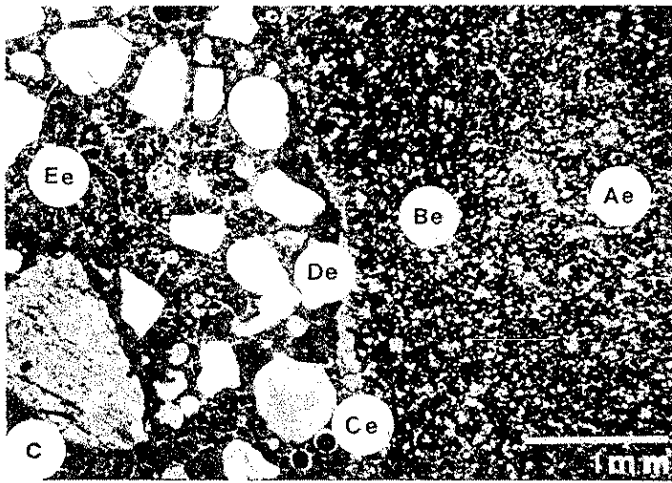
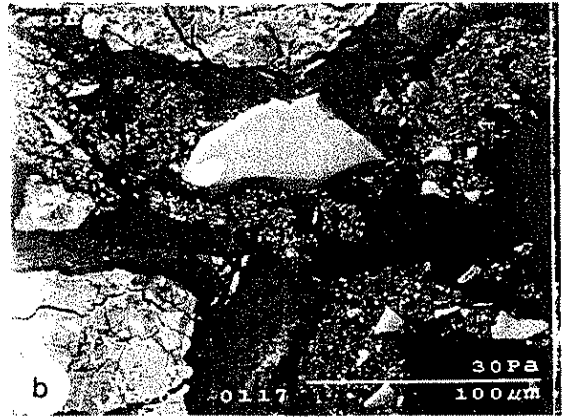
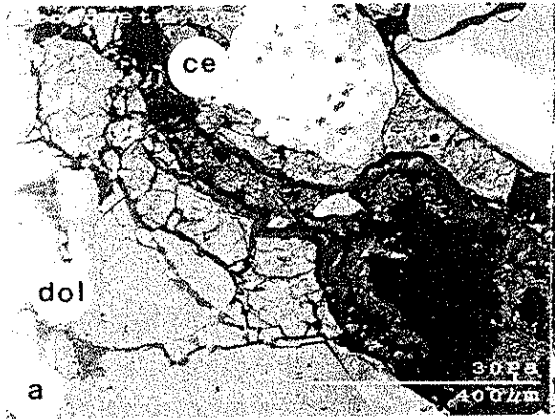


PLATE XII.

Plt XII. Experimental deterioration of concretes. Light micrographs of aggregate-paste interfaces, durable Mar-Jo Hills aggregate concrete.

- a. Wet/dry cycling in Ca solution, plane-polarized light
- b. Same area, between crossed-polarizers.
- c. Freeze/dry cycling in Ca solution, plane-polarized light.
- d. Same area, between crossed-polarizers.
- e. Wet/dry cycling in Mg solution, plane-polarized light.
Note dissolution of aggregate/paste boundary.
- f. Same area, between crossed-polarizers.

No reaction rims are visible after the different experimental treatments. Cement paste shows cracks after both freeze/thaw and wet/dry Ca solution treatments. Severe paste decomposition and in some locations is completely dissolved from wet/dry cycling in Mg solutions. Fig 26, 30 are electron microprobe traverses of this area.

PLATE XIV.

Plt XIV. Experimental decomposition of concretes. Light and SEM micrographs of concrete containing Paralta aggregate.

a. Light micrograph of wet/dry Mg solution cycled Paralta concrete, plane-polarized light.

b. Same area as previous photograph, Plt IVa, between crossed-polarizers.

The interface between aggregate and paste resembles that found in untreated concretes containing the same aggregate. Zone Ee, the cement paste, shows considerable decomposition as a result of the treatments.

c. Light micrograph of wet/dry Na solution cycling of Paralta concrete, plane-polarized light.

d. Same area as previous photograph, Plt IVb, between crossed-polarizers.

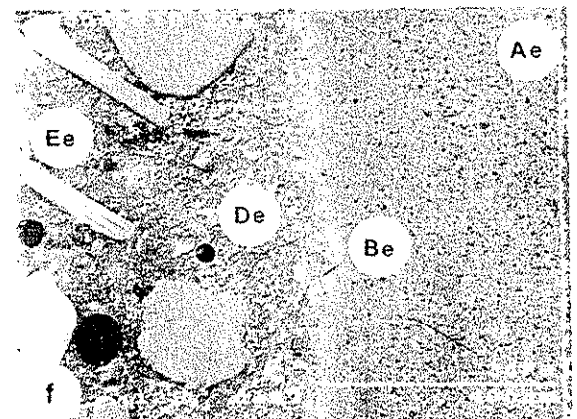
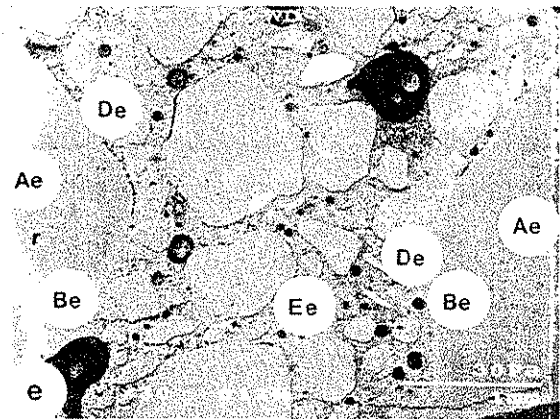
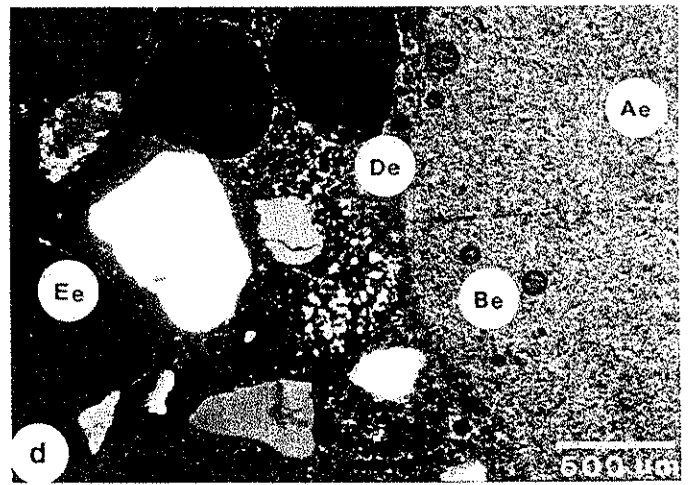
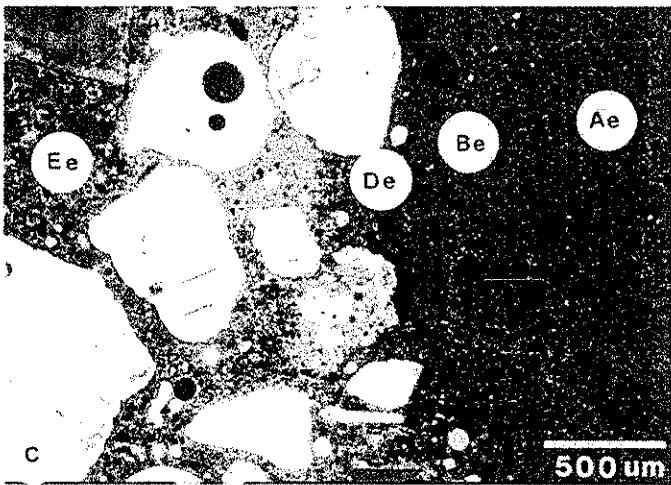
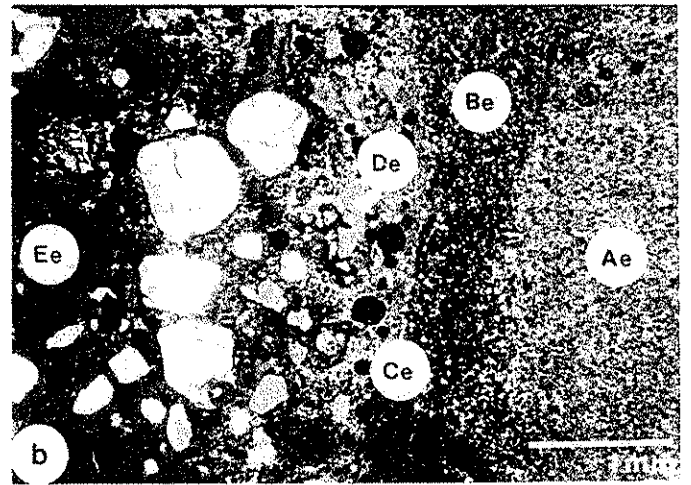
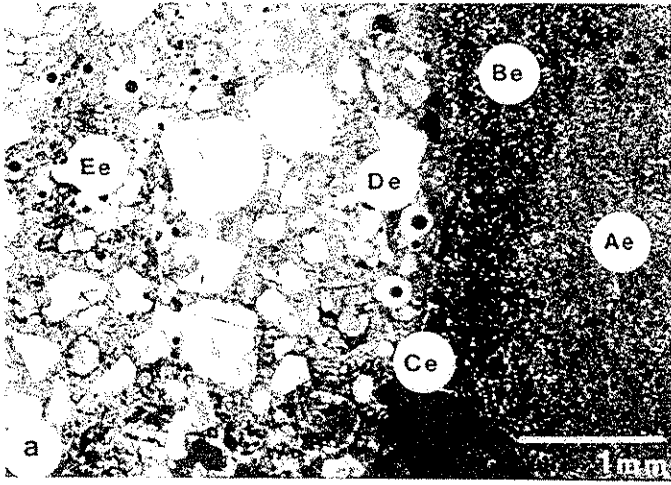
Very few effects of experimental treatments are visible. A few cracks developed in the cement paste and at the contact between the dark dolomite rim and the paste adjacent to the aggregate, at the contact between zones Be and De.

e. SEM micrograph of wet/dry Na solution cycled Paralta concrete.

f. SEM micrograph, enlargement of the lower right part of the previous photograph. Plt IVe.

Zone Be, the dark dolomite rim, is less porous than zone Ae, dolomite aggregate interior. Dry salt deposits are visible in cement voids. See Fig 31 for corresponding electron microprobe traverse, and Fig 32 for EDAX maps.

PLATE XIV



FIGURES

Figure 1.

Fig 1. Electron microprobe traverse across non-durable concrete containing Smith quarry aggregate.

a. CaO, MgO, and SiO₂ traverse.

b. Al₂O₃ and FeO traverse.

c. K₂O and Na₂O traverse.

The traverses show chemical variations across the dolomite aggregate-cement paste interface. This traverse shows an increase in CaO with a corresponding, but slighter than expected, decrease in MgO at the outermost region of zone C. The very irregular profile of the unaltered cement paste is typical. The sharp enrichment in SiO₂, FeO, and K₂O at about 200 μm distance probably is due to an illite clay inclusion. Plts IIIc-e shows corresponding light and SEM micrographs. Fig 2 gives a corresponding EDAX maps of area traversed by electron microprobe.

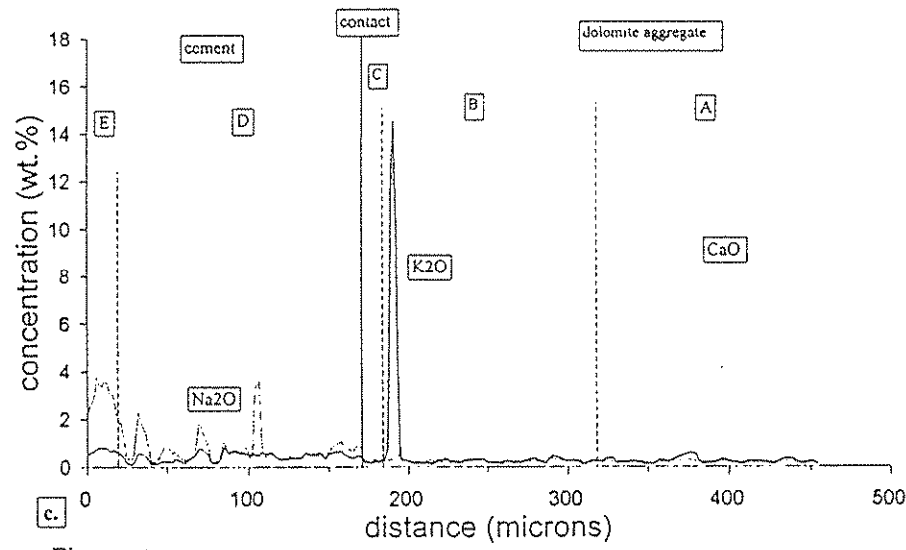
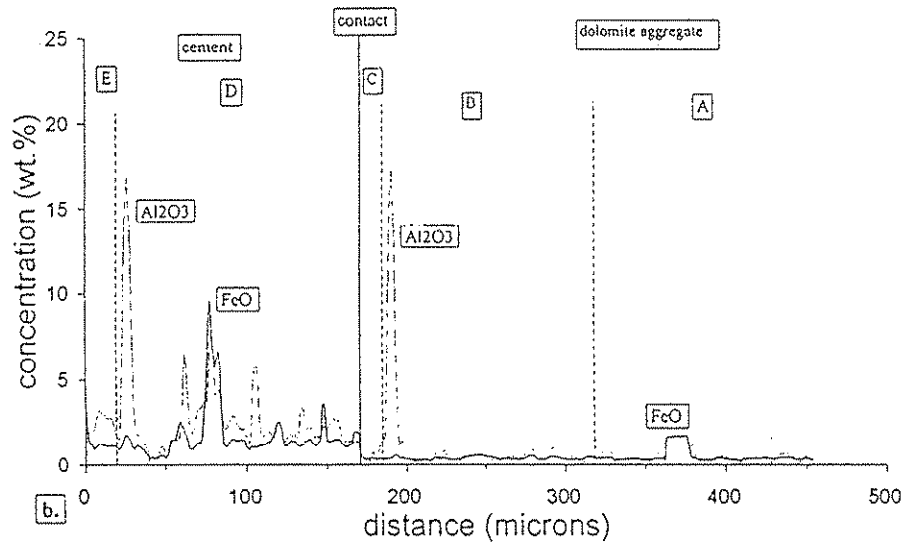
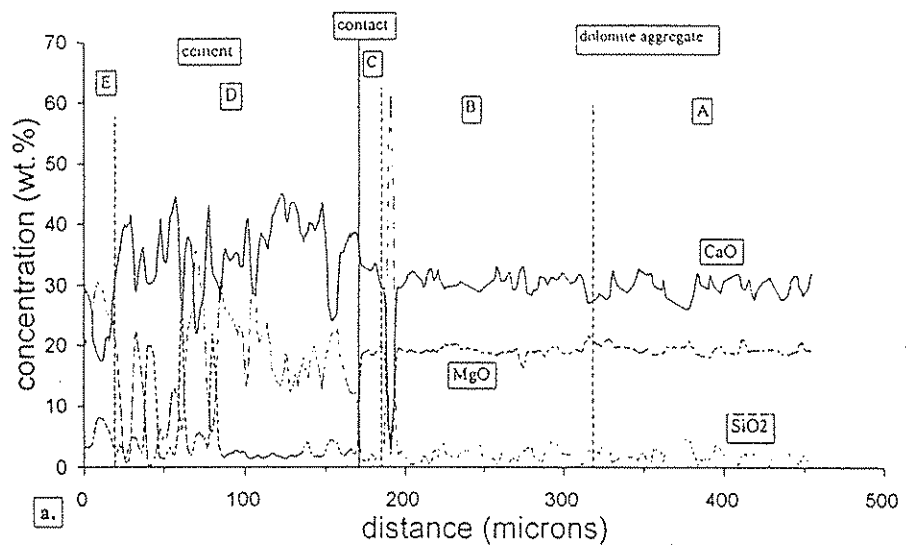


Figure 1

Figure 2.

Fig 2. EDAX element maps of Smith quarry concrete.

Although not very clear, the high Ca region of D, Fig 1, is visible and is indicated by arrow. Mg and O concentrations probably indicate brucite crystals. Plt IIIc,d show corresponding light micrographs.

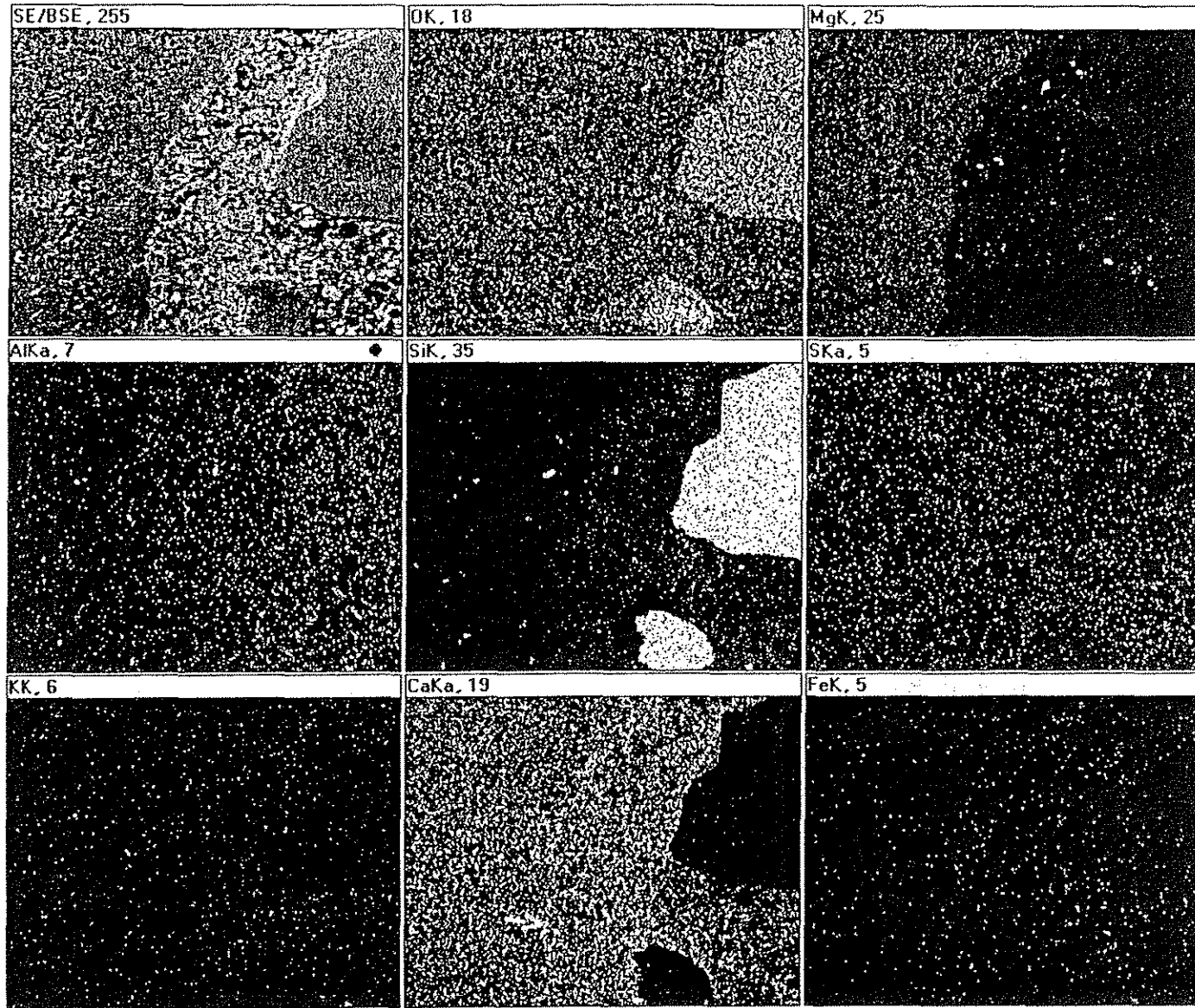


Figure 2

Figure 3.

Fig 3. Electron microprobe traverse across non-durable concrete containing Smith quarry aggregate.

a. CaO and MgO traverse.

b. Al₂O₃ and FeO traverse.

c. K₂O and Na₂O traverse.

CaO significantly increases in the light-colored dolomite rim, C, with a correspondingly large decrease in MgO in the rim. Zone C is also characterized by elevated Al₂O₃, K₂O, and Na₂O. Plts IIIf, IVa,b provide light and SEM micrographs of traversed area. Fig 4 gives EDAX element maps of area.

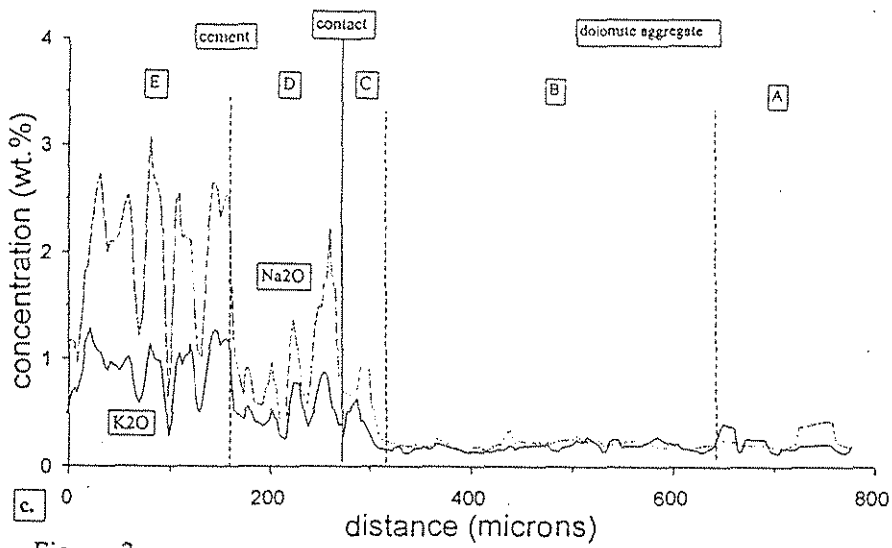
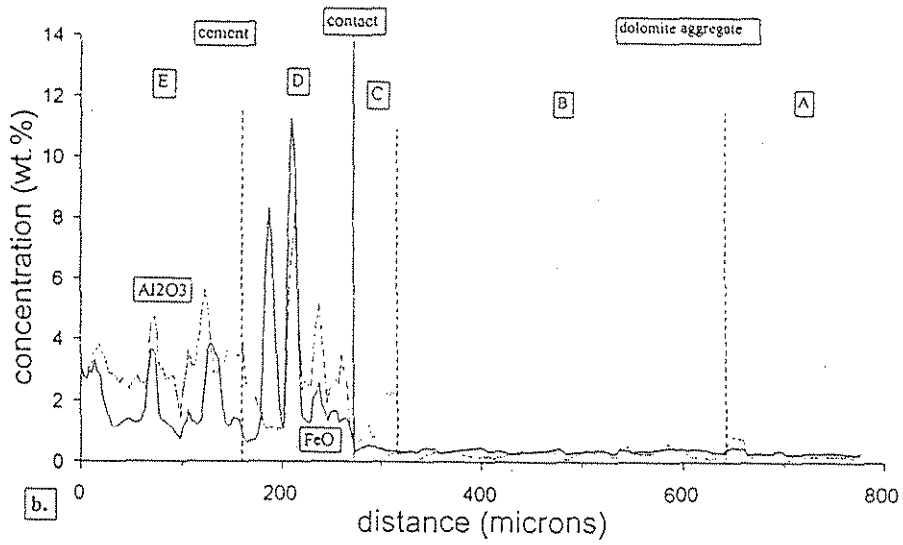
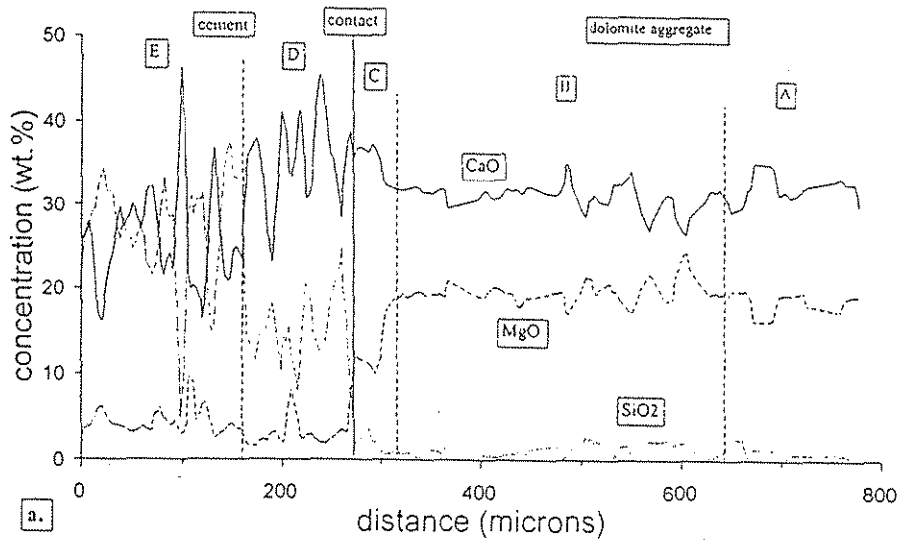


Figure 3

Figure 4

Fig 4. EDAX element maps of Smith quarry concrete.

Arrow indicates enrichment in CaO that is especially evident in D, the light-colored paste rim

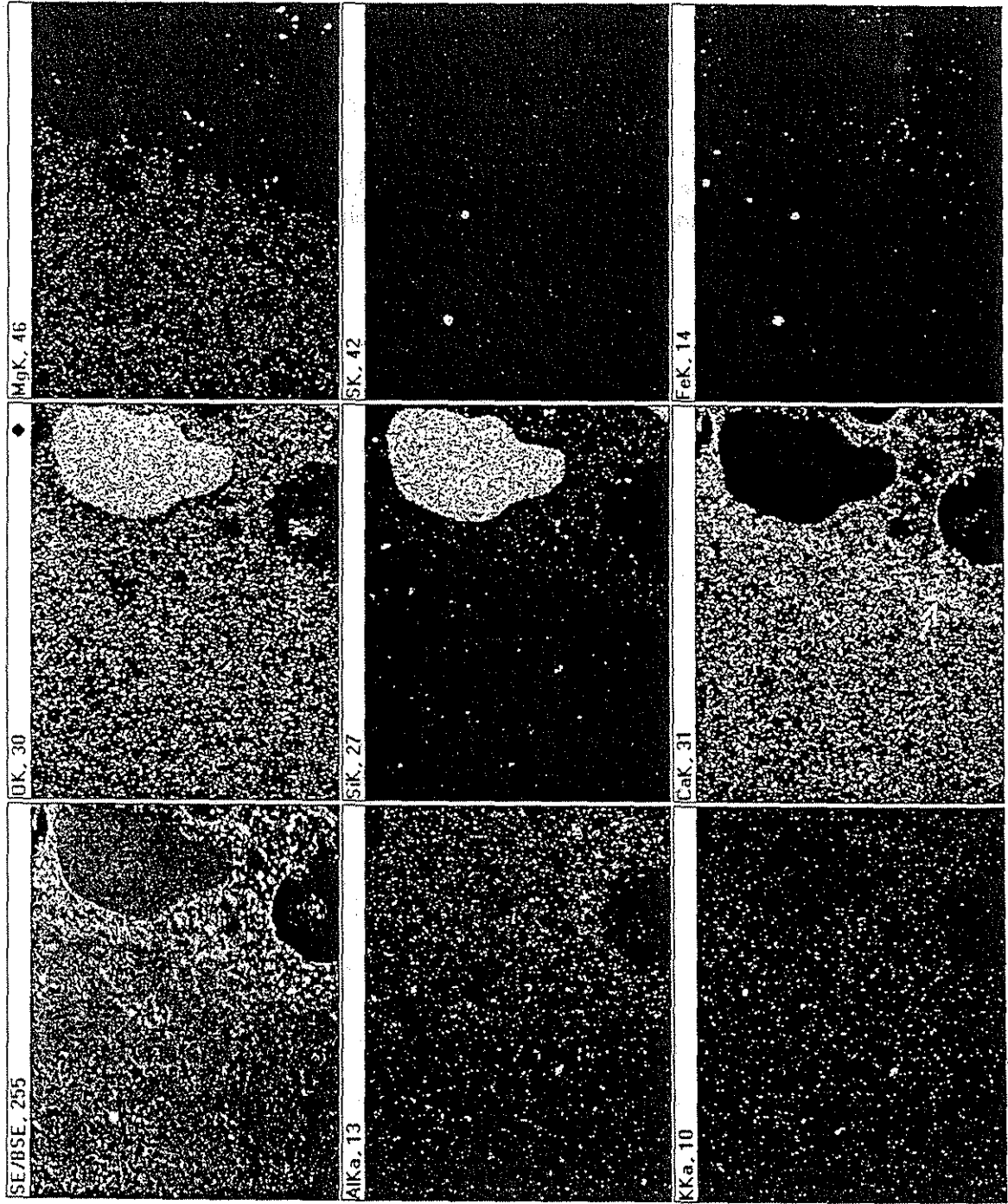


Figure 4

Figure 5

Fig 5. EDAX element maps of Paralta quarry concrete.

There is a significant concentration of MgO and CaCO₃ in the dolomite aggregate parallel to the aggregate-paste boundary. Small clay and pyrite inclusions probably are responsible for elevated Al, O, Fe, and S in localized concentrations. Plts IVe,f and IVa,b show corresponding SEM and light micrographs.

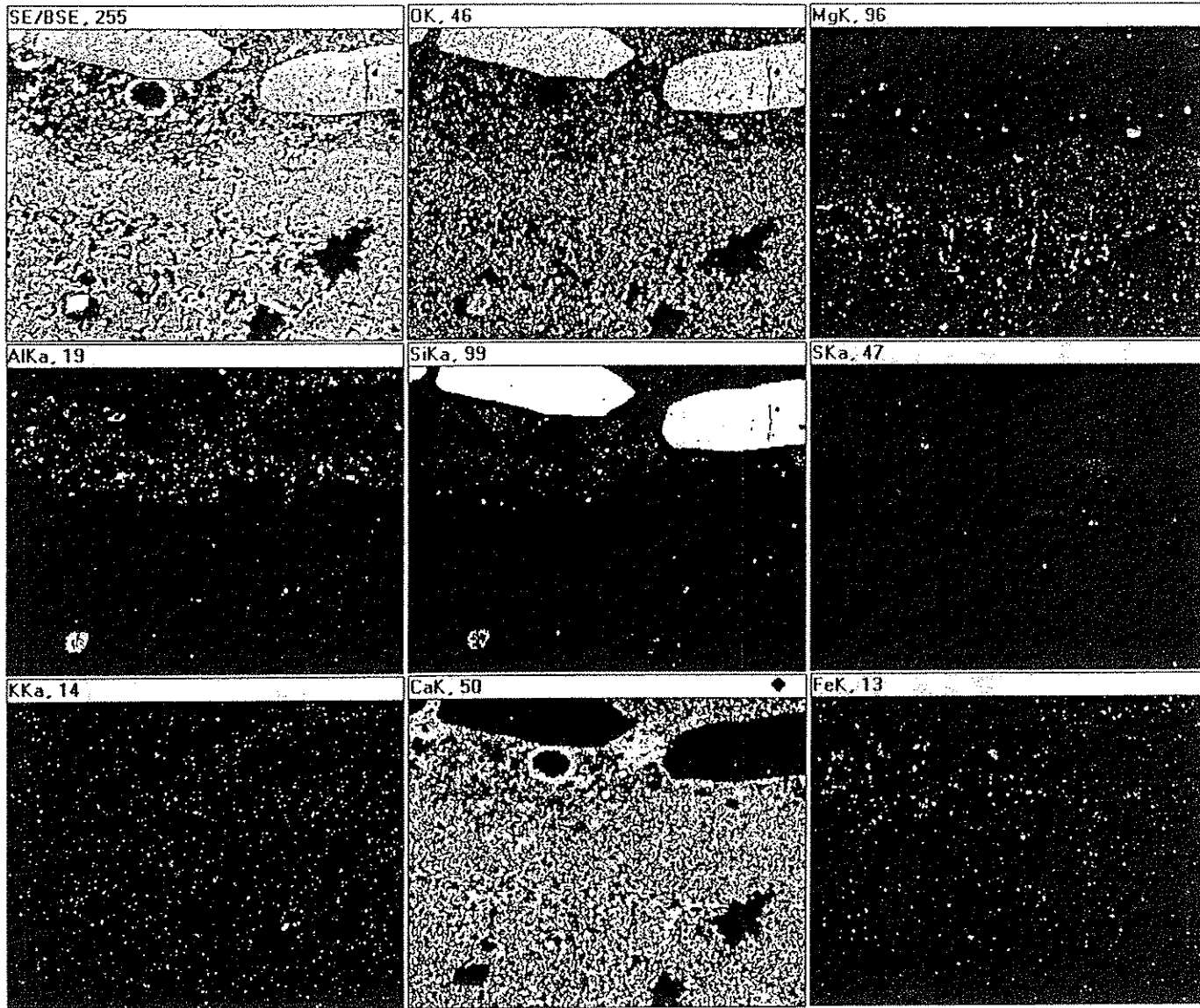


Figure 5

Figure 6

Fig 6. Electron microprobe traverse across non-durable concrete containing Paralta quarry aggregate.

a. CaO and MgO traverse.

b. Al₂O₃ and FeO traverse.

c. K₂O and Na₂O traverse.

This sample lacks the light-colored dolomite rim, and zone B, the dark dolomite rim, is directly in contact with the paste. CaO is elevated and MgO is significantly reduced in the outer region of B. Zone D, the light-colored paste rim is extremely enriched in Ca from calcite precipitation, probably derived from the alkali-dolomite reaction. Light micrographs of corresponding area are shown in Plt Va,b.

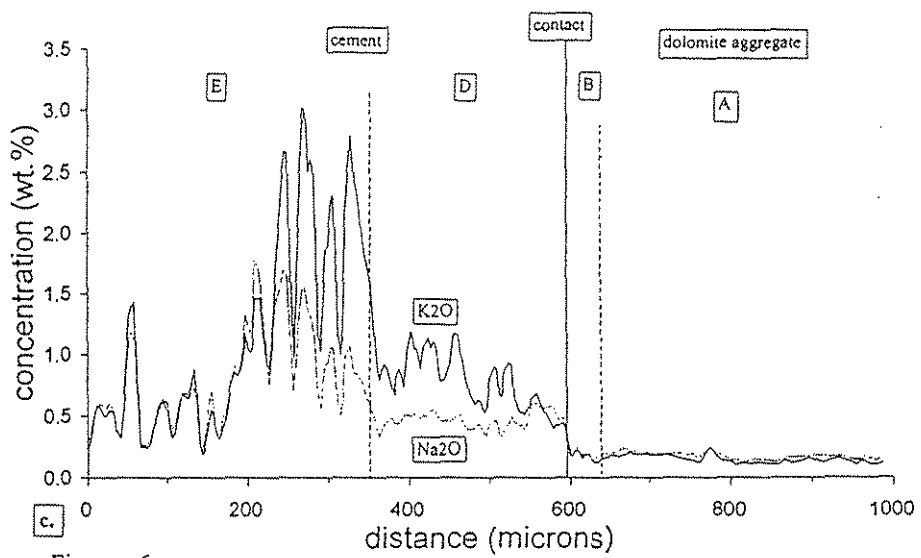
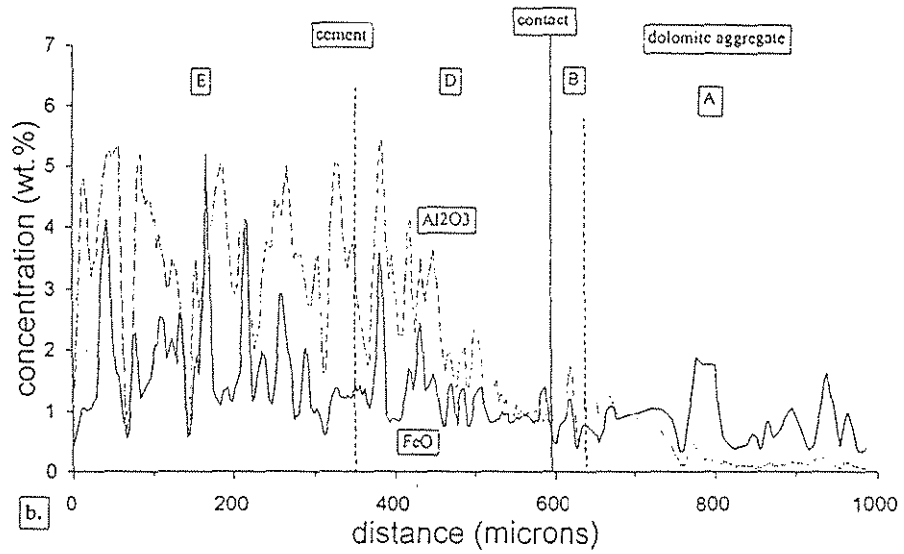
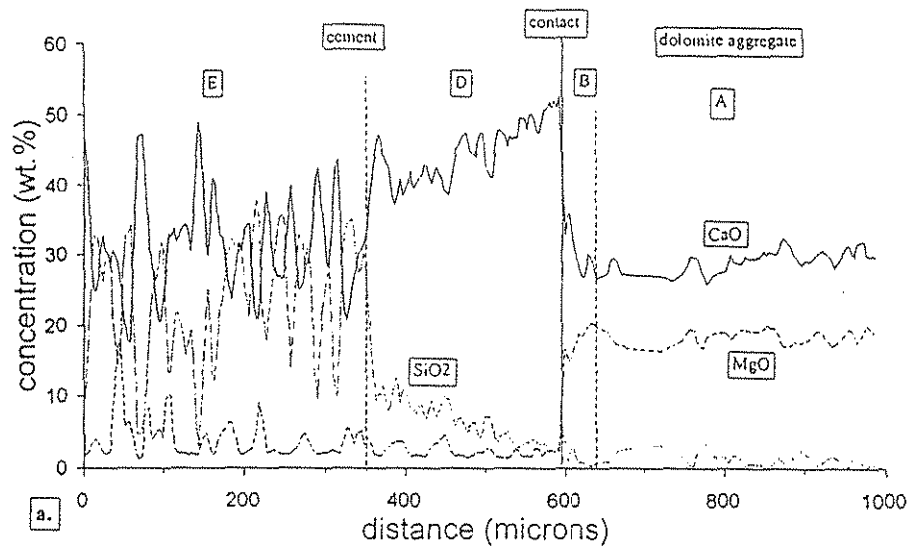


Figure 6

Figure 7

Fig 7. Electron microprobe traverse through non-durable Smith quarry concrete.

a. CaO and MgO traverse.

b. Al₂O₃ and FeO traverse.

c. K₂O and Na₂O traverse.

This sample shows a small enrichment in CaO in the outer part of the dark dolomite rim, B, but there is no detectable MgO decrease in the rim. The inner, light-colored paste rim is also strongly enriched in Ca.

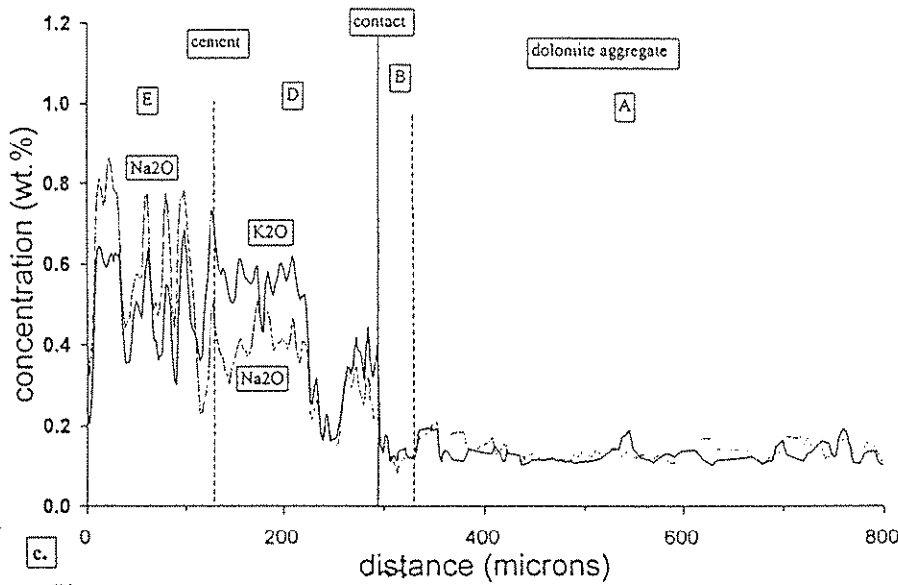
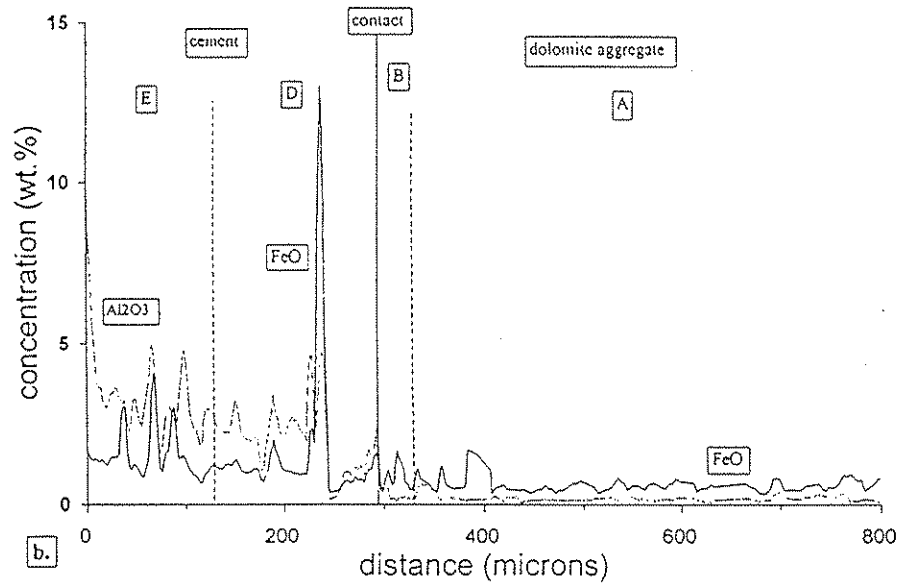
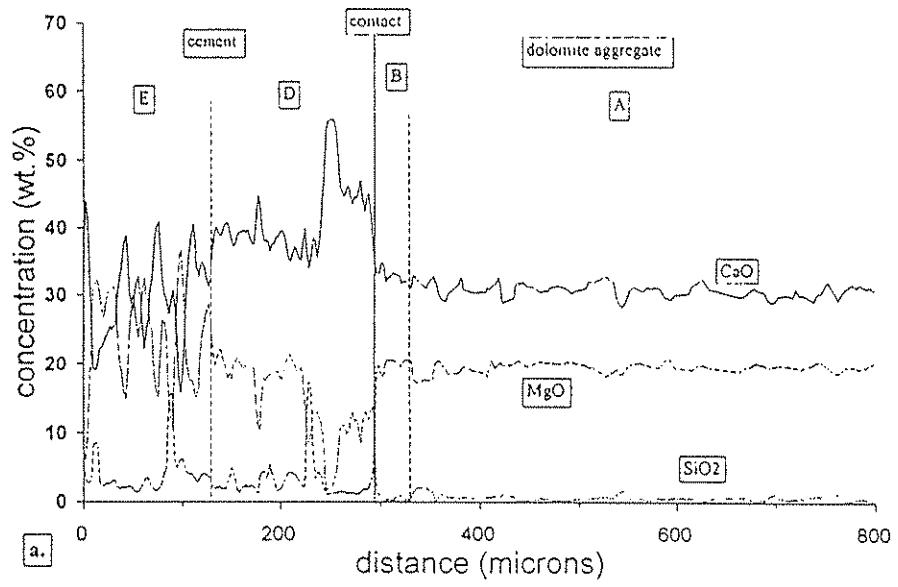


Figure 7

Figure 8.

Fig 8. EDAX element maps of non-durable Smith quarry concrete.

Abundant Ca enrichment occurs in voids within the porous dolomite aggregate. Area is shown in SEM photos Plt Vc,d.

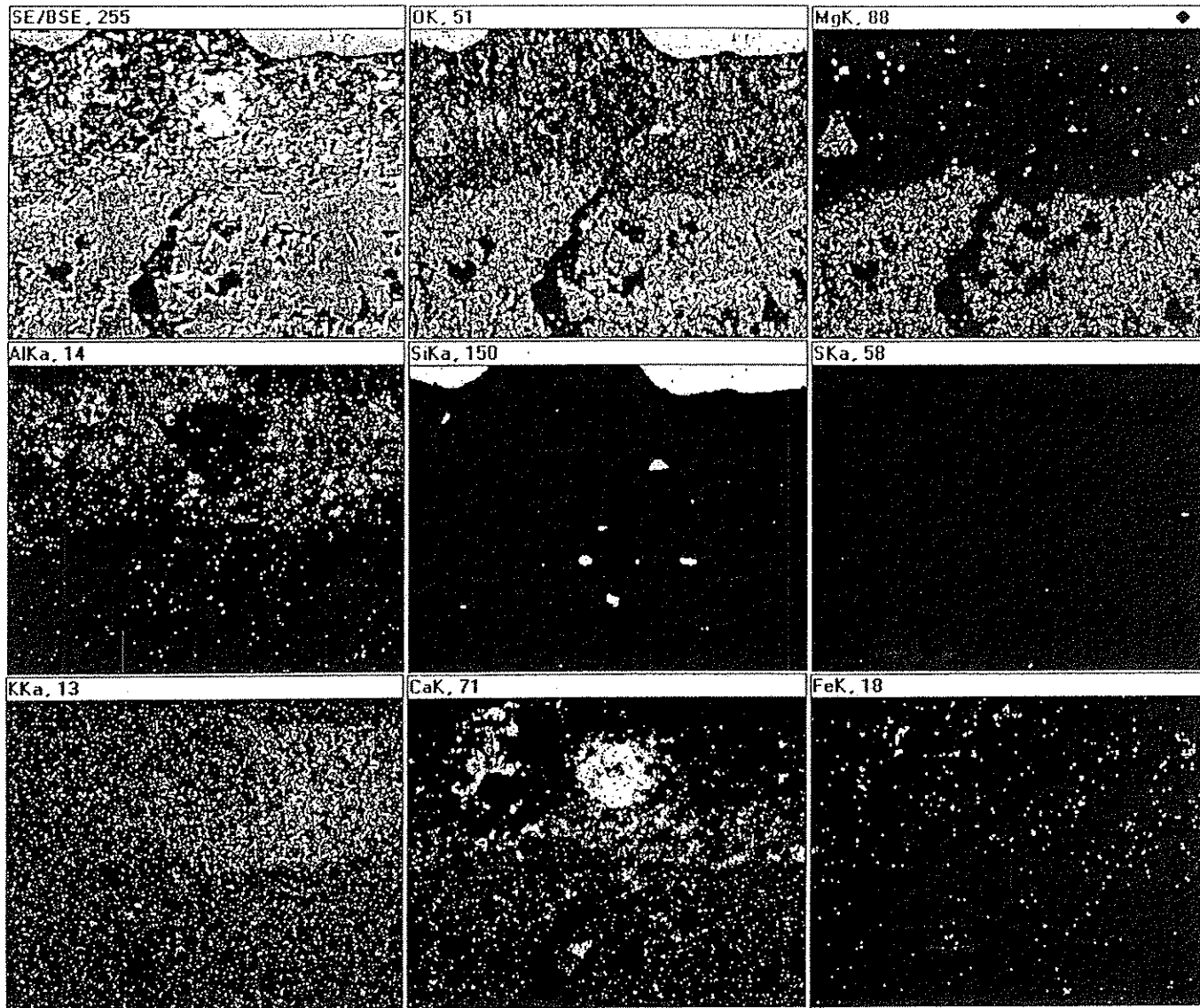
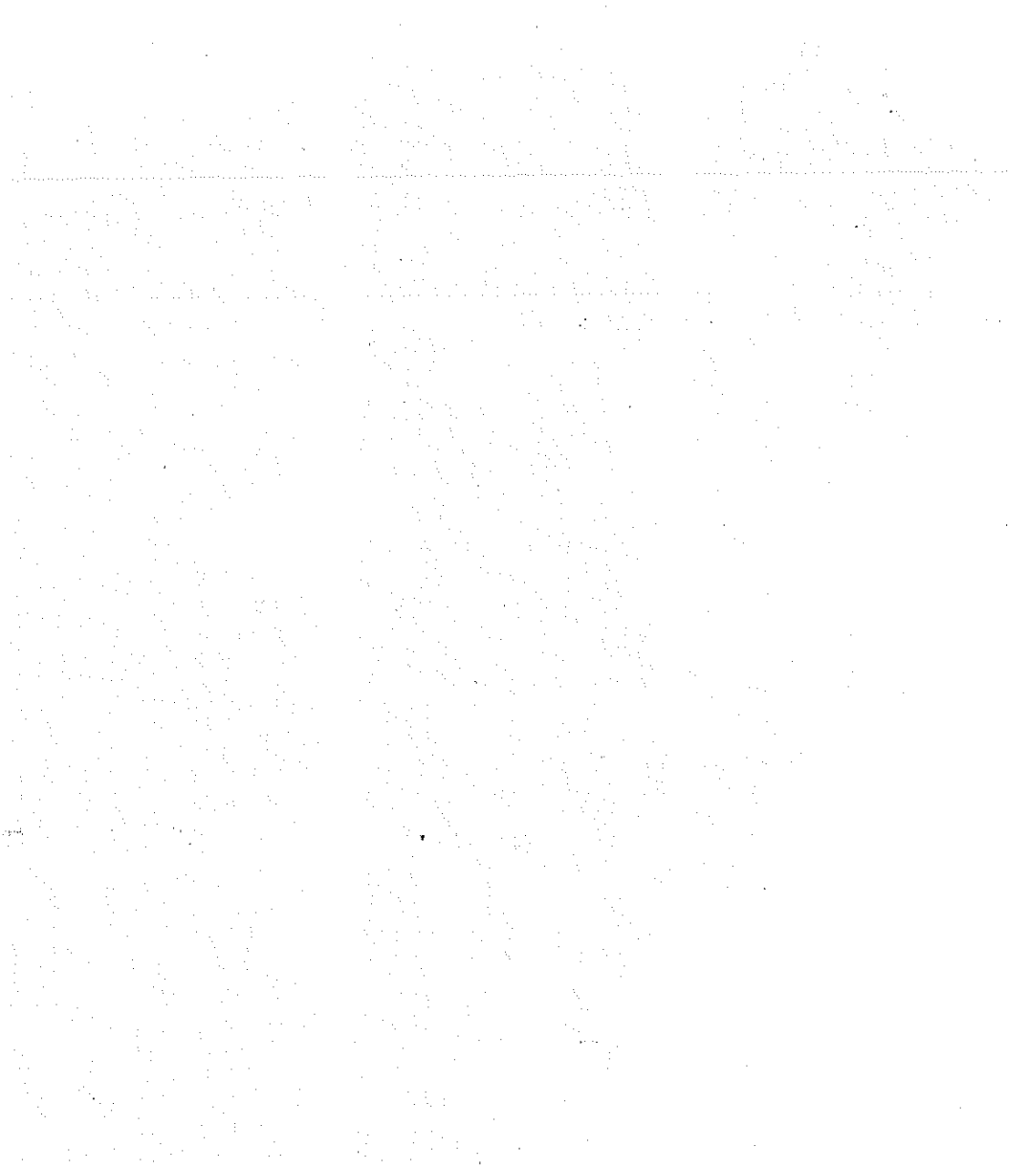


Figure 8

Figure 9.

Fig 9. EDAX element maps of non-durable Smith quarry aggregate, second sample.



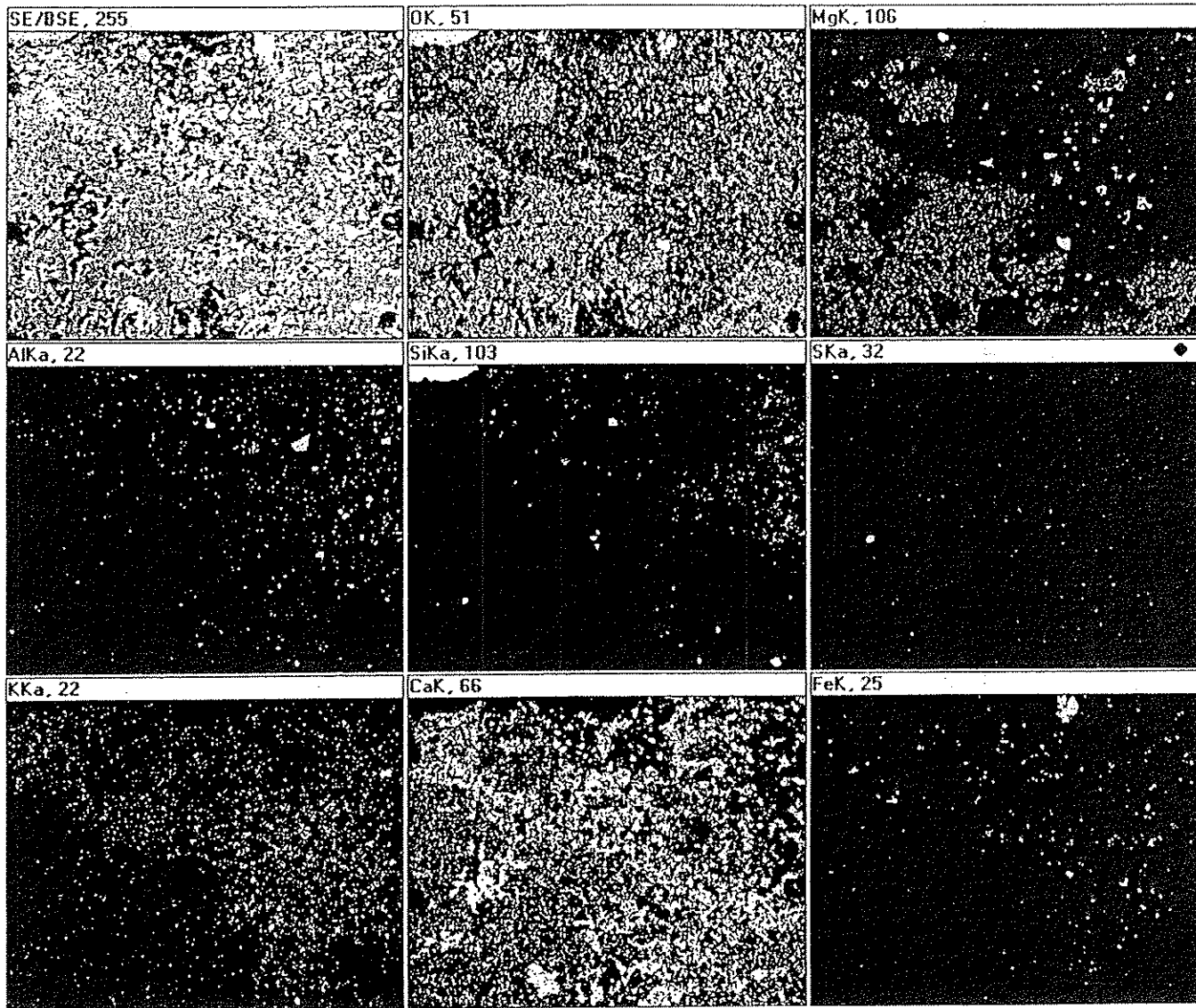


Figure 9

Figure 10.

Fig 10. Electron microprobe traverse across durable concrete containing Mar-Jo Hills quarry aggregate.

a. CaO and MgO traverse.

b. Al₂O₃ and FeO traverse.

c. K₂O and Na₂O traverse.

No reaction rims are visible in the dolomite aggregate or cement paste. Plt VIa,b shows corresponding light micrograph of area traversed.

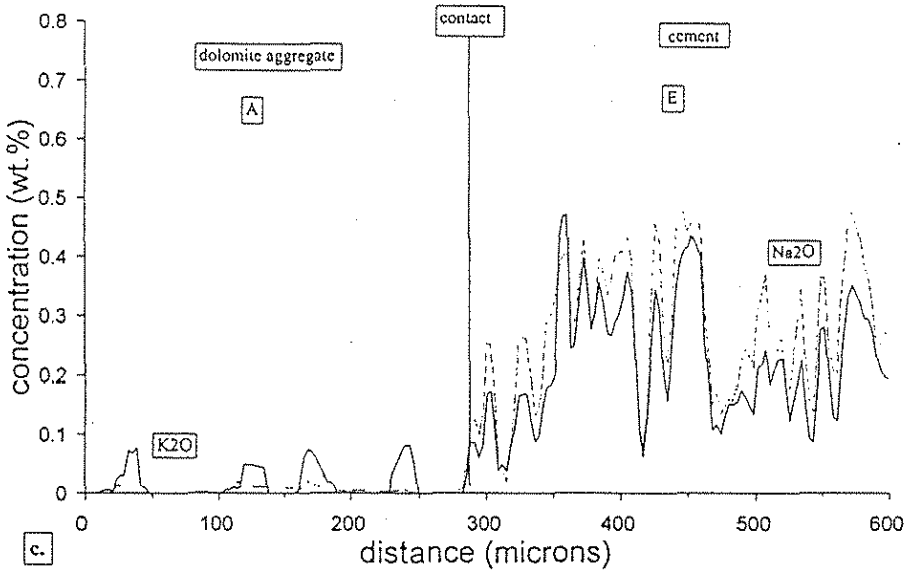
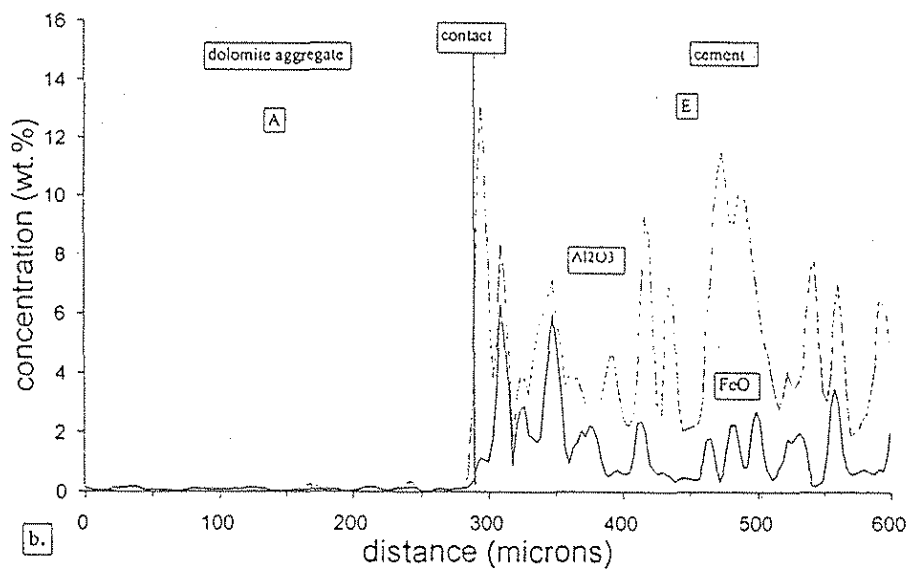
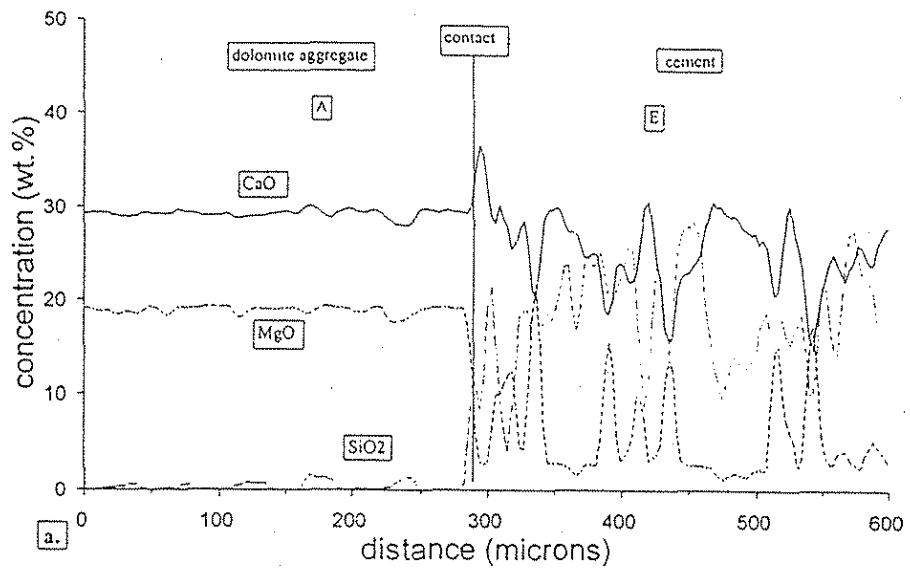


Figure 10

Figure 11.

Fig 11. Electron microprobe traverse through durable concrete containing Sundheim quarry aggregate.

a. CaO and MgO traverse.

b. Al₂O₃ and FeO traverse.

c. K₂O and Na₂O traverse.

As with concrete containing Mar-Jo Hills aggregate (Fig 10), no reaction rims are visible in the dolomite aggregate or cement paste. The sharp enrichment in SiO₂, Al₂O₃, and K₂O at the 1000 μm site probably indicates illite. Fig VIc-e shows corresponding light and SEM micrographs of traversed area.

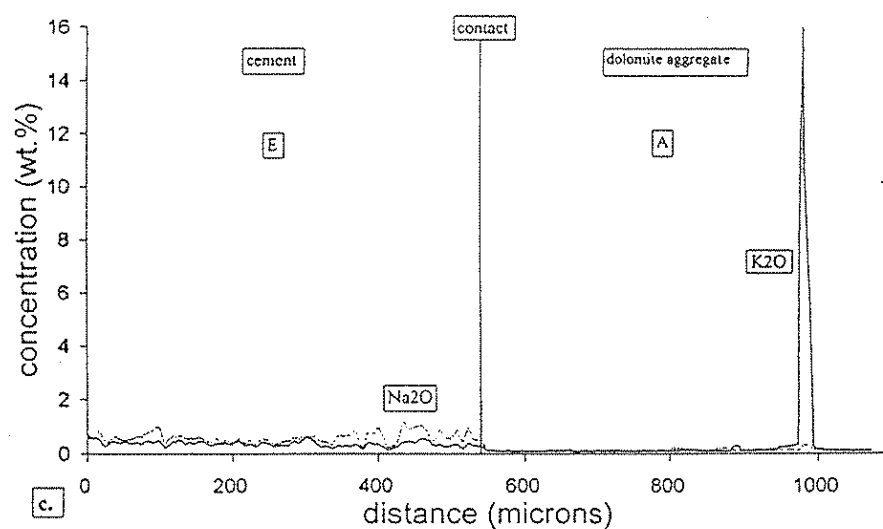
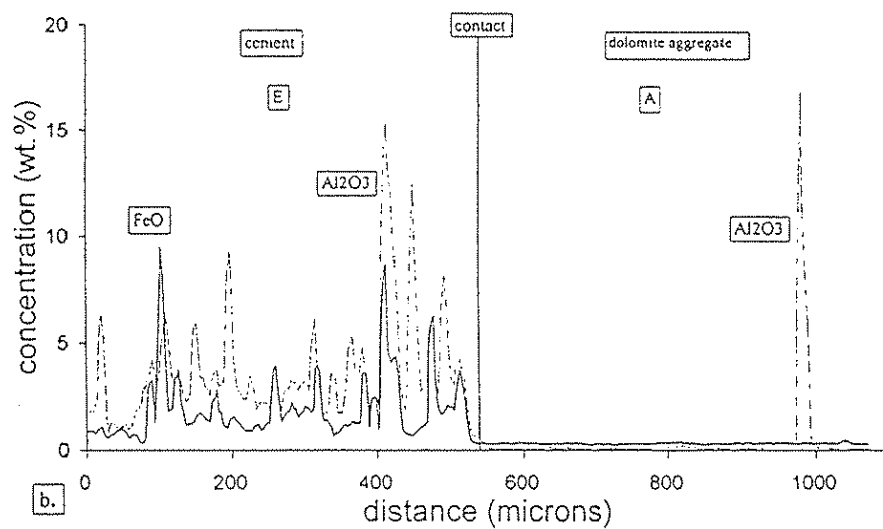
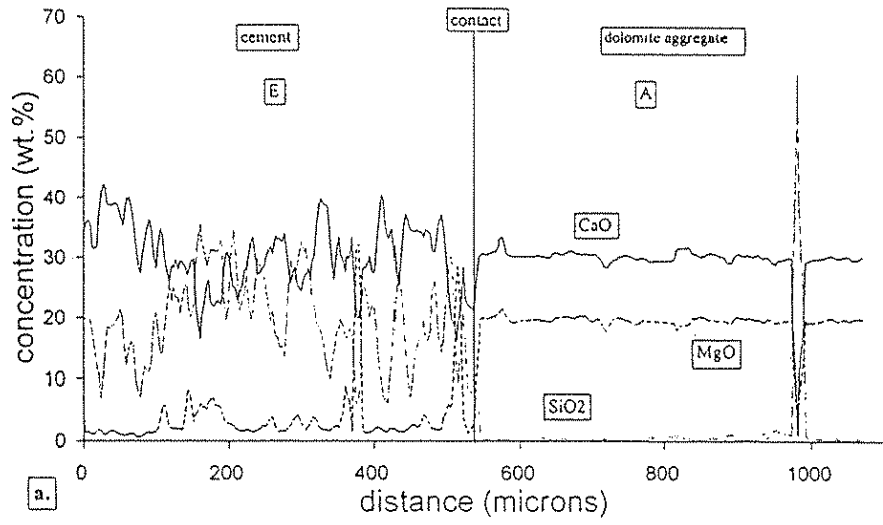


Figure 11

Figure 12.

Fig 12. EDAX element maps of durable concrete containing Sundheim aggregate. Both the dolomite aggregate and the cement paste are much more uniform in composition than the corresponding phases in non-durable concretes. Small Si-rich dots in dolomite indicate quartz inclusions, and Mg-rich dots indicate brucite. Plt VIe shows an SEM view and Plt VIc,d shows corresponding light micrographs of area of maps.

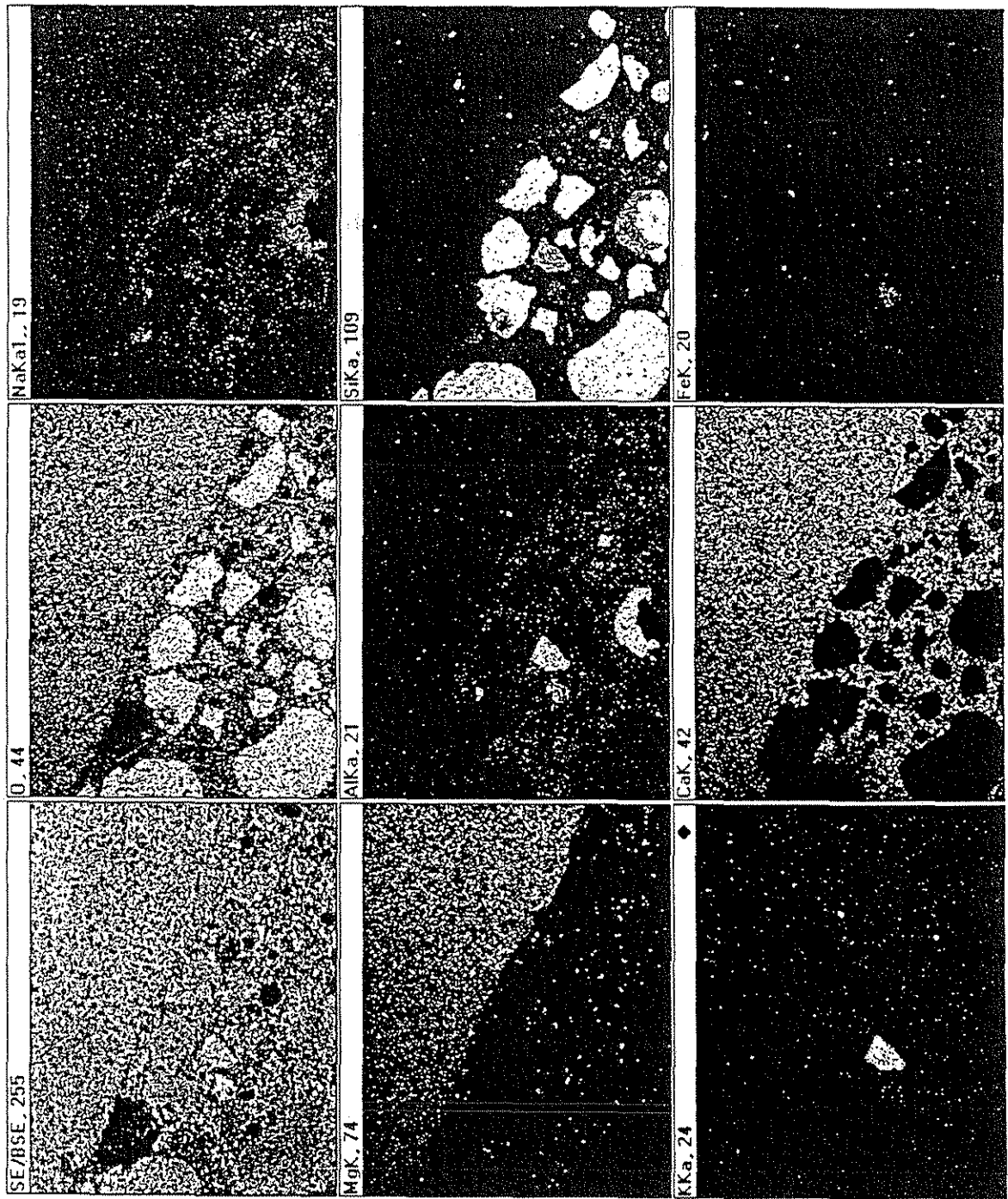


Figure 12

Figure 13.

Fig 13. Electron microprobe traverse across durable concrete containing Sundheim quarry aggregate.

a. CaO and MgO traverse.

b. Al₂O₃ and FeO traverse.

c. K₂O and Na₂O traverse.

No reaction rims are visible, and the aggregate shows almost constant composition throughout most of its extent.

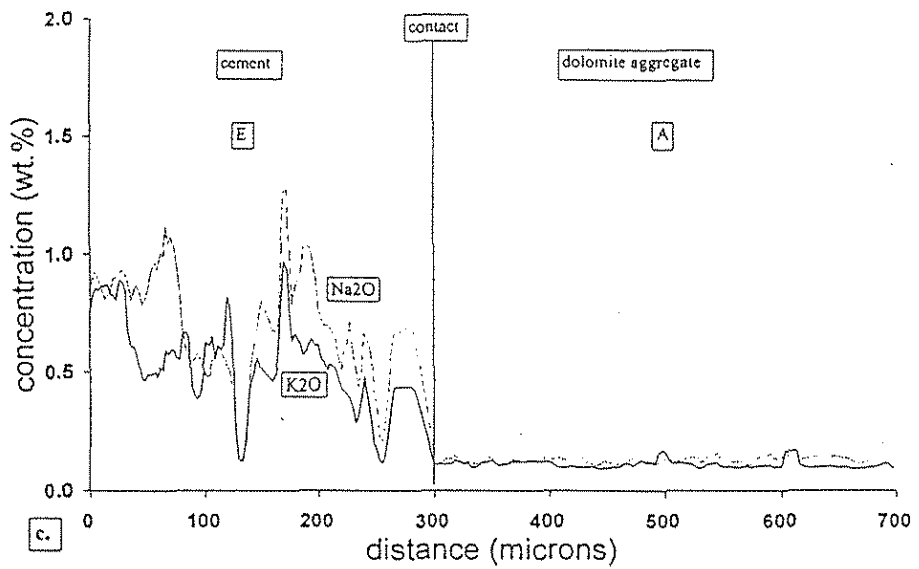
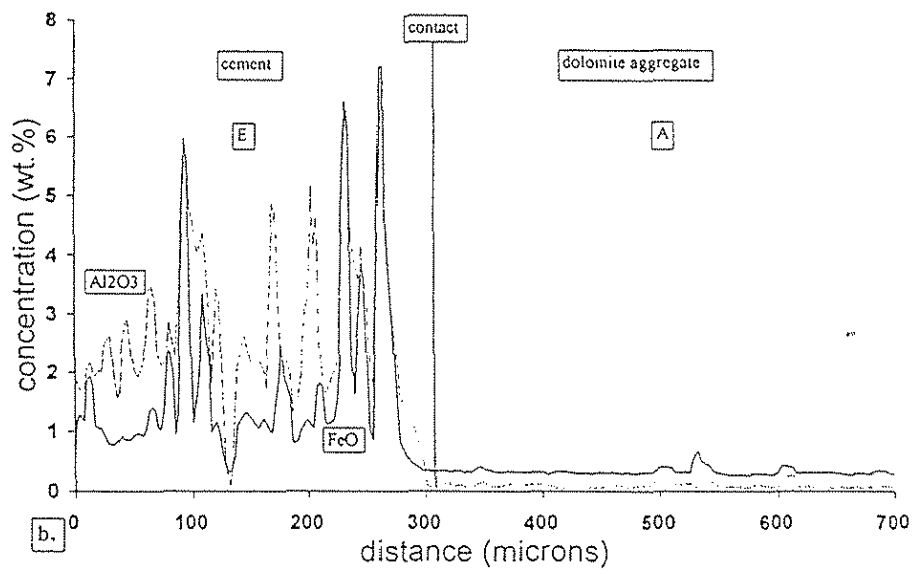
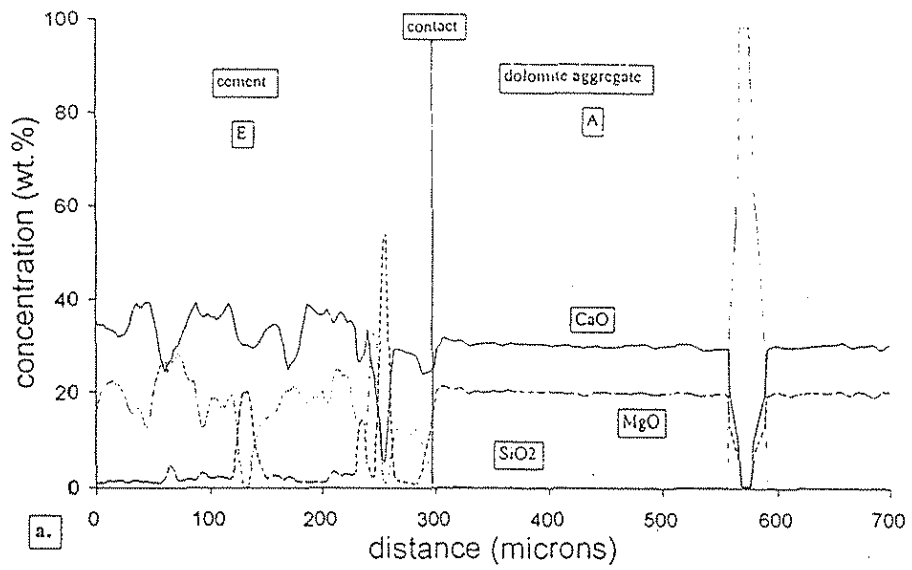


Figure 13

Figure 14.

Fig 14. Electron microprobe traverse across durable concrete containing Mar-Jo Hills quarry aggregate.

a. CaO and MgO traverse.

b. Al₂O₃ and FeO traverse.

c. K₂O and Na₂O traverse.

This sample has a very thick dark dolomite rim, zone B, which exhibits sharp and very irregular local increases in CaO with corresponding decreases in MgO. These sharp irregularities are in marked contrast to the dolomite interior which shows typical nearly constant CaO and MgO concentrations. Presumably these changes in aggregate rim B indicate localized dedolomitization and subsequent precipitation of calcite. There is also slight enrichment in K₂O and Na₂O in the boundary between D and E. Plt VIIa,b shows light micrographs of corresponding area.

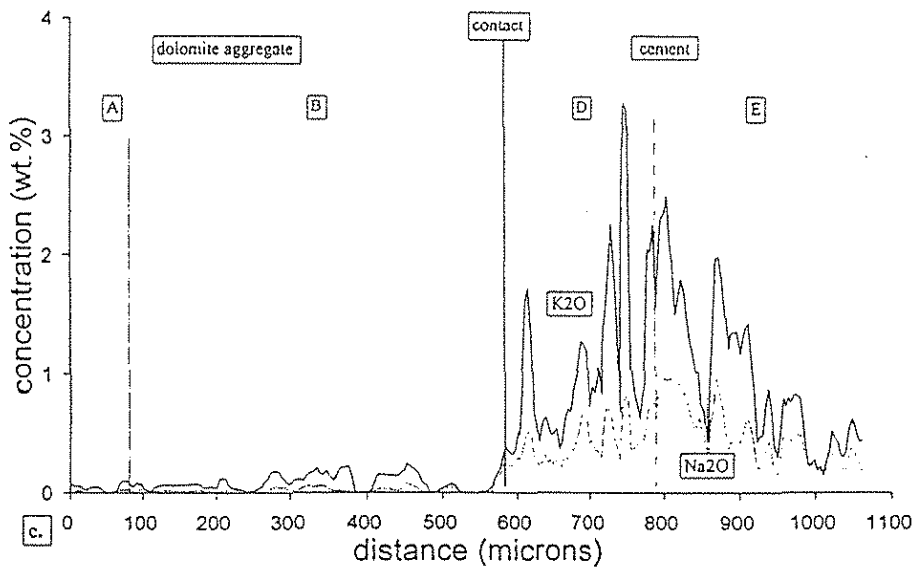
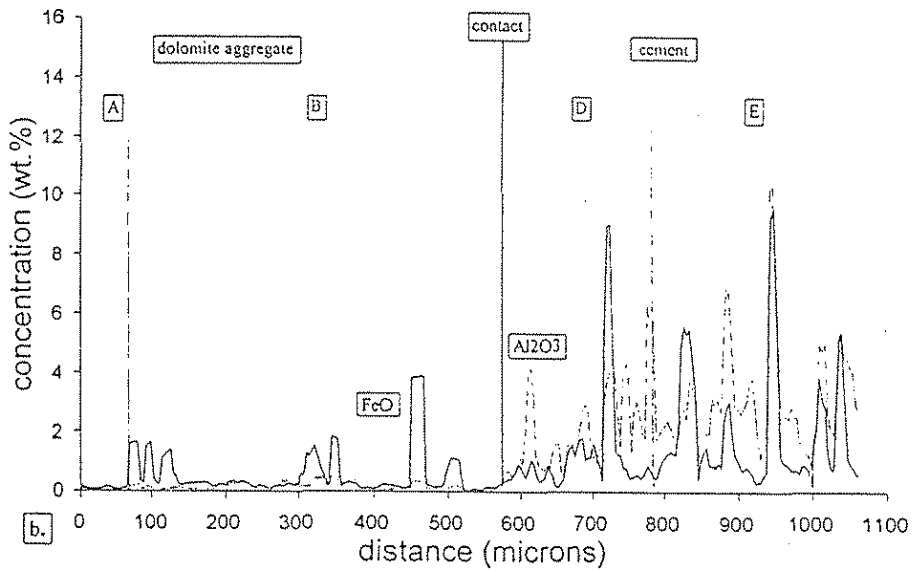
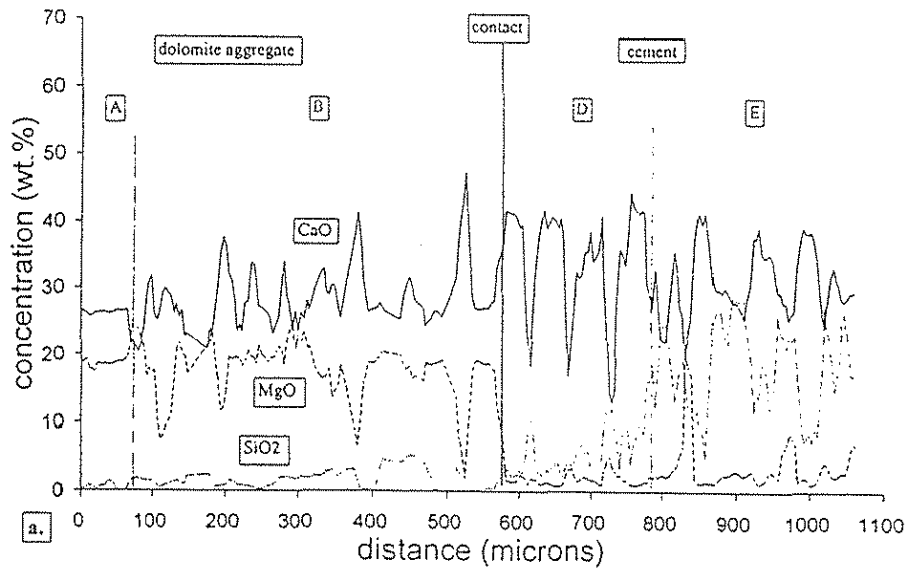


Figure 14

Figure 15.

Fig 15. Electron microprobe traverse across durable concrete containing Sundheim quarry aggregate.

a. CaO and MgO traverse.

b. Al₂O₃ and FeO traverse.

c. K₂O and Na₂O traverse.

The dolomite interior has a very uniform composition, with a very thin light-colored dolomite rim, C. In C rim has an elevated CaO and reduced MgO characteristic of dedolomitization. Corresponding views of area are shown in Plt VIIc,d.

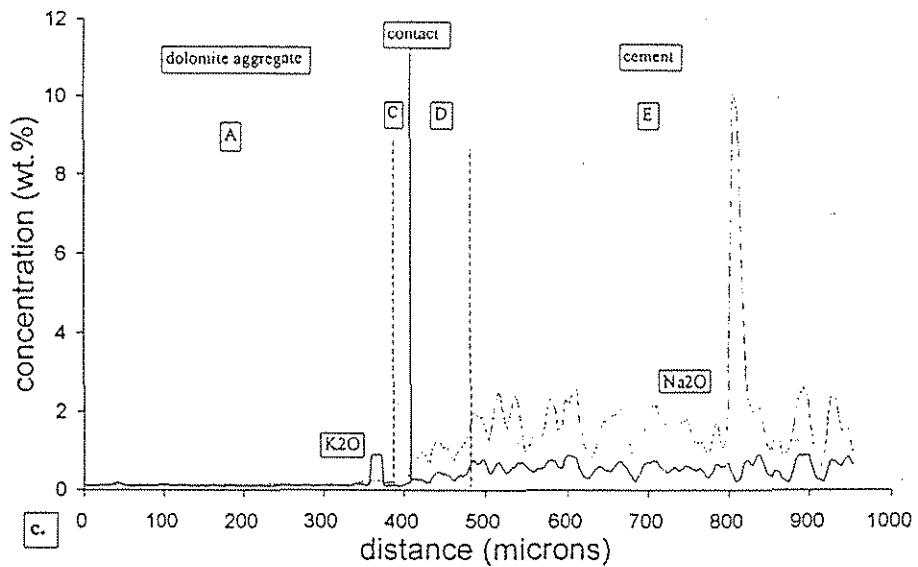
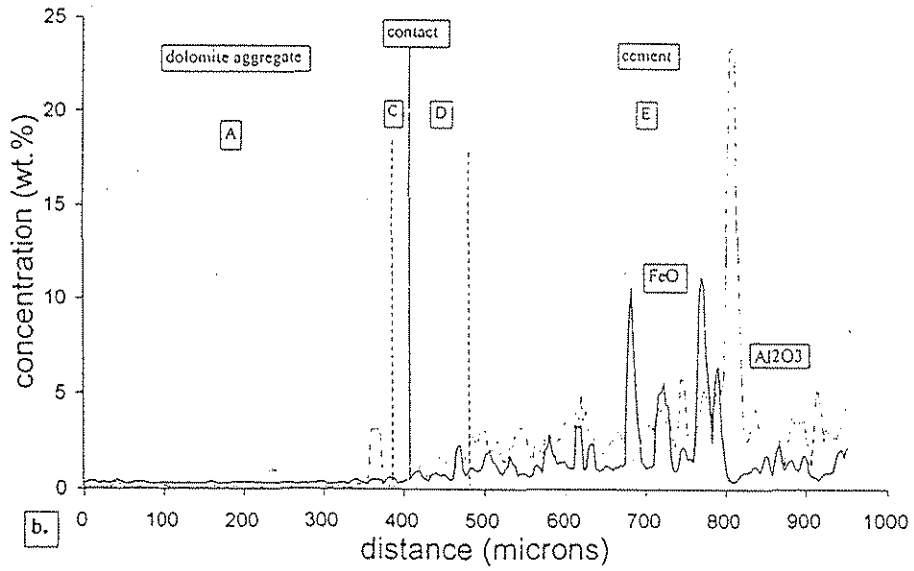
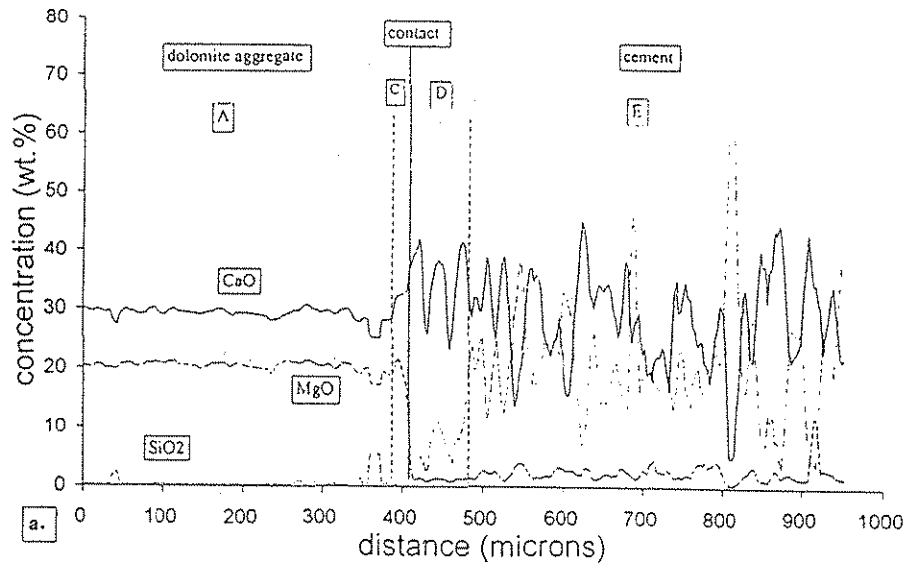


Figure 15

Figure 16.

Fig 16. EDAX element maps for concrete containing Mar-Jo Hills quarry aggregate.
SEM photograph of area is shown in Plt VIIe.

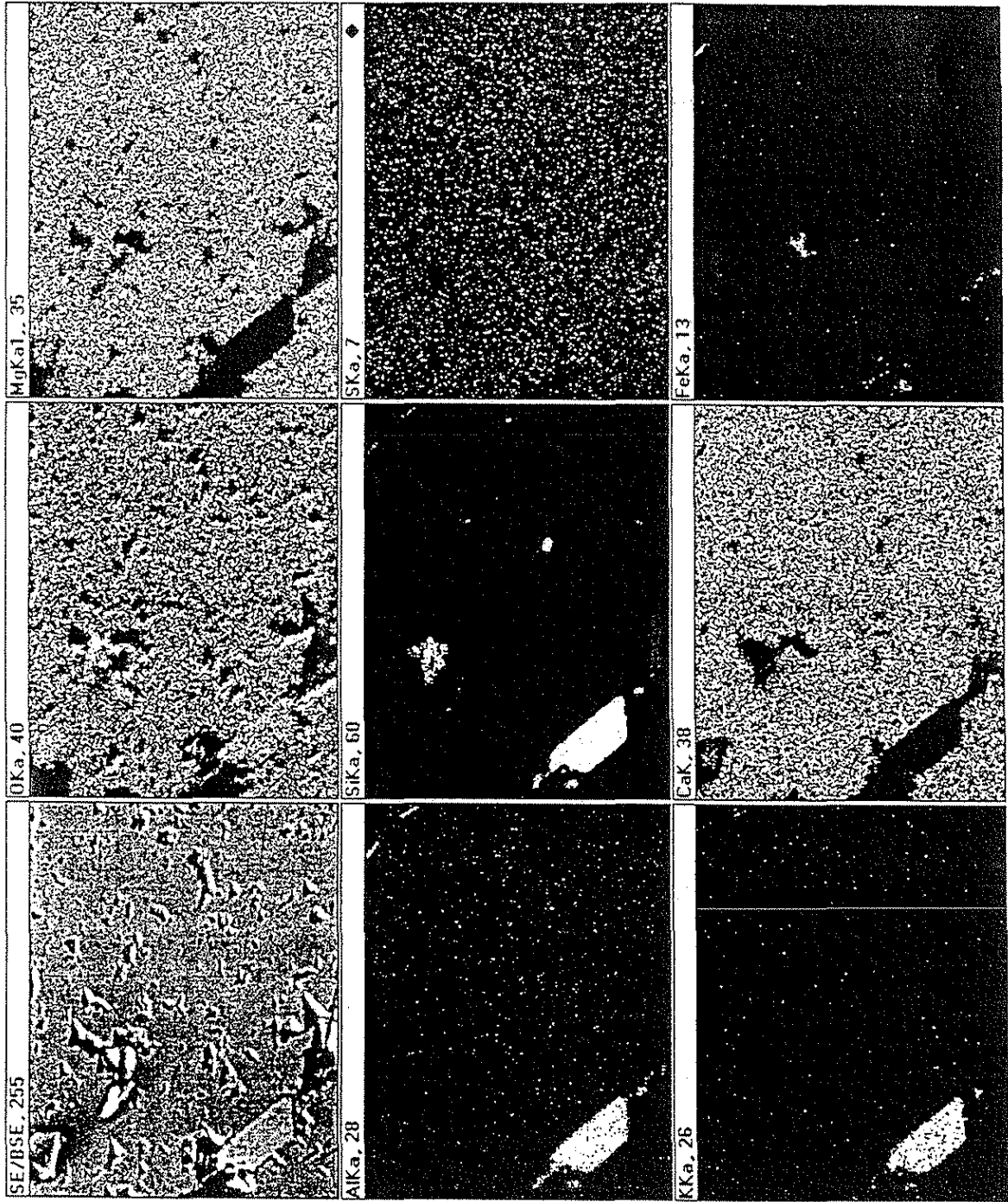


Figure 16

Figure 17.

Fig 17. EDAX element maps for concrete containing Smith quarry aggregate.
SEM photograph of area is shown in Plt VIIf.



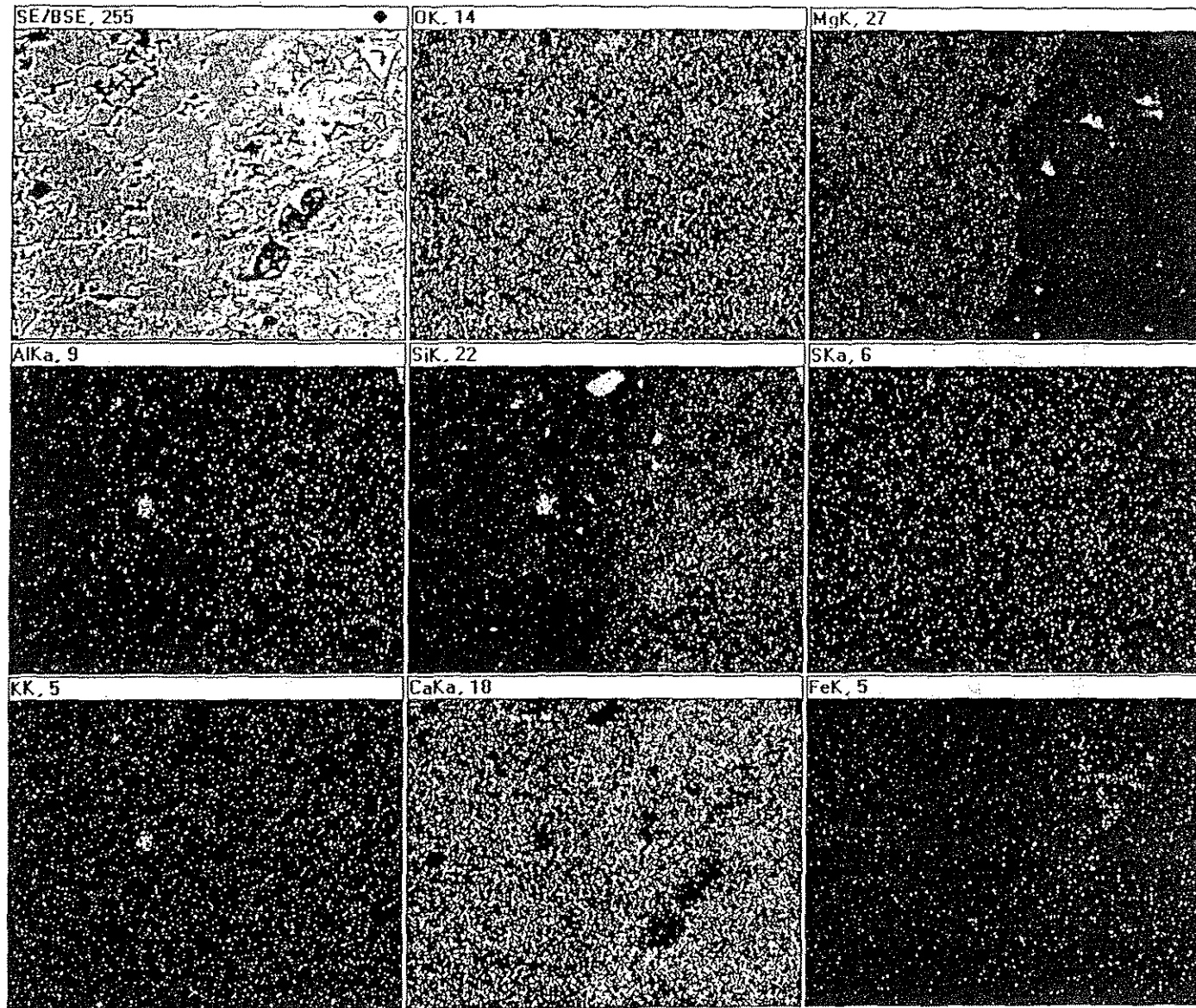


Figure 17

Figure 18.

Fig 18. Experimental decomposition of concrete. EDAX element maps of concrete containing Garrison quarry aggregate after wet/dry cycling in Ca solution. Abundant Ca-chloride and Al + O crystals line void 2 and upper part of void 1. Ca + S + O (gypsum?) fills lower part of void 1. Brucite and probable calcite occurs in the paste. Crack-filling minerals are calcite, and also an Al + O mineral (arrows). Plt Xe shows equivalent SEM photograph.

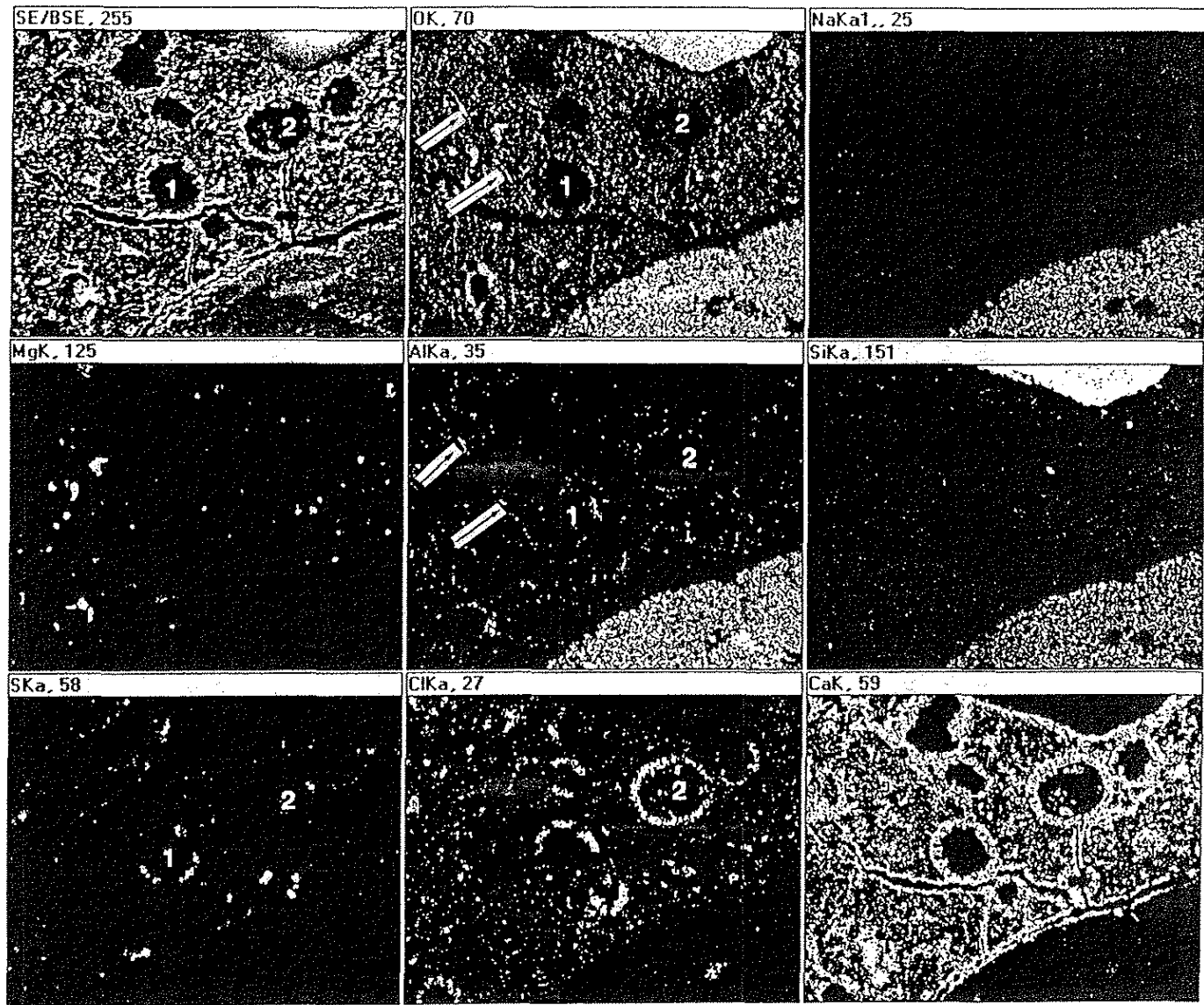


Figure 18

Figure 19.

Fig 19. Experimental decomposition of concrete. Electron microprobe traverse across concrete containing Paralta quarry aggregate after wet/dry cycling in Ca solution.

a. CaO and MgO traverse.

b. Al₂O₃ and FeO traverse.

c. K₂O and Na₂O traverse.

A slight but significant increase in MgO occurs in the light-colored dolomite rim, Ce, with essentially no corresponding CaO change. As expected, CaO/SiO₂ ratio in the paste is much higher after Ca treatment than the ratio in untreated concretes. See Plts XIa,b, XIc,d for corresponding light and SEM micrographs. Figs 20, 21 provide corresponding EDAX element maps.

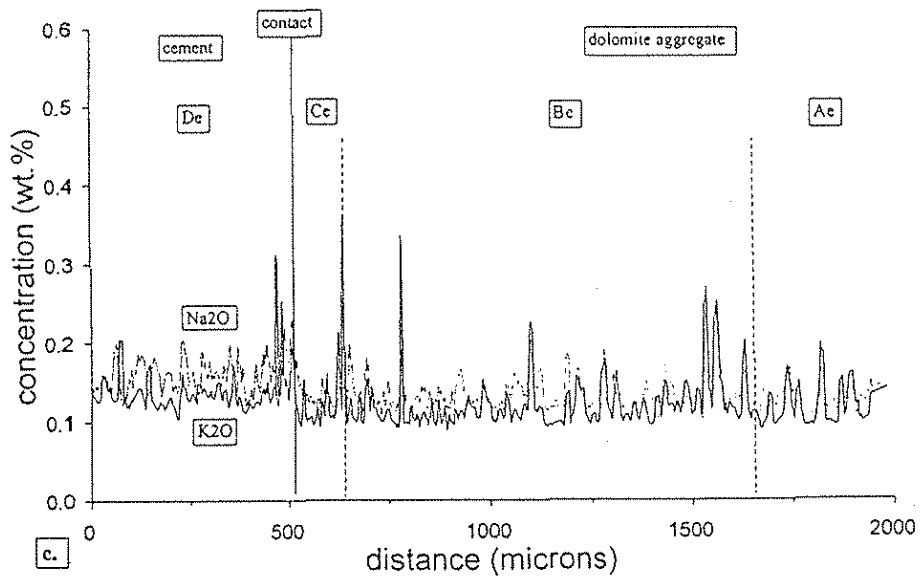
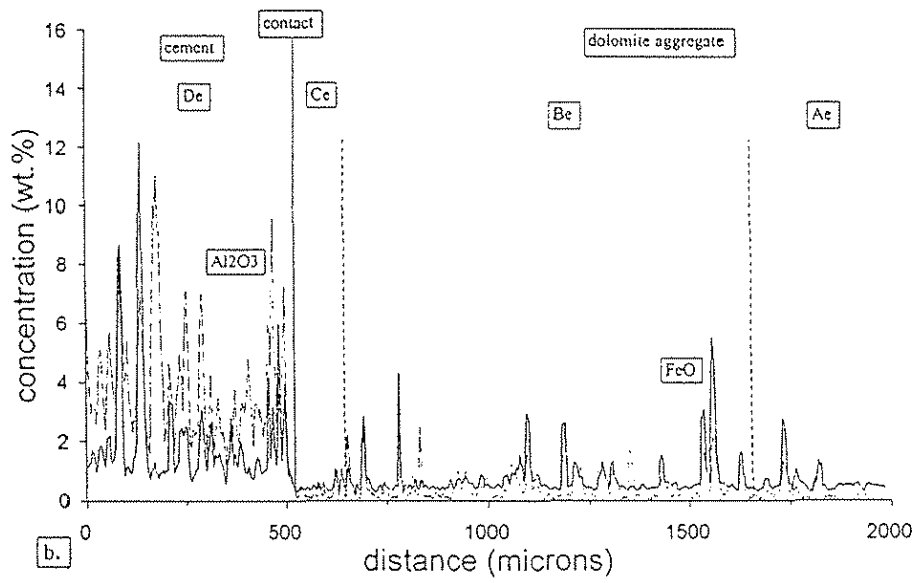
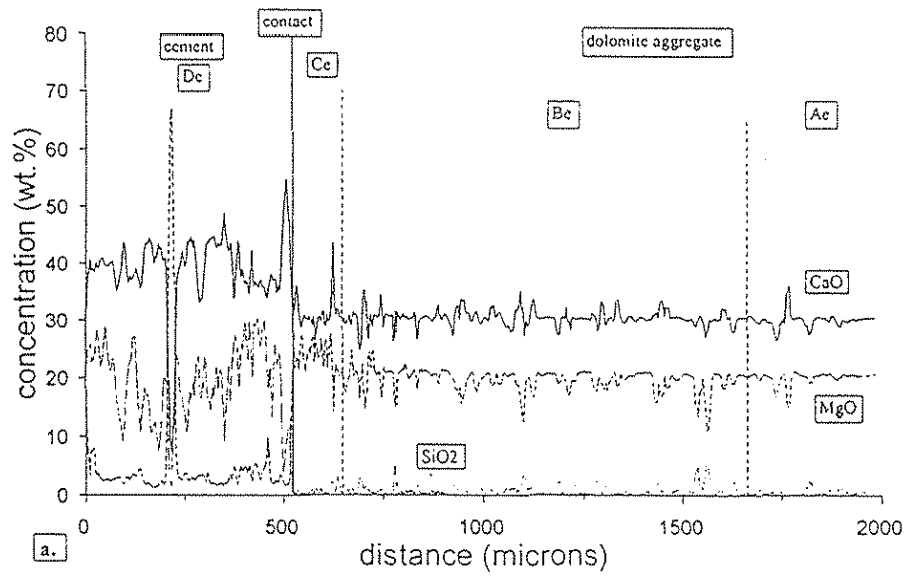


Figure 19

Figure 20.

Fig 20. Experimental decomposition of concrete. EDAX element maps of concrete containing Paralta quarry aggregate after wet/dry cycling in Ca solution. Note the Mg increase in the outer region of the dolomite aggregate which corresponds to that found by electron microprobe analysis, Fig 19.

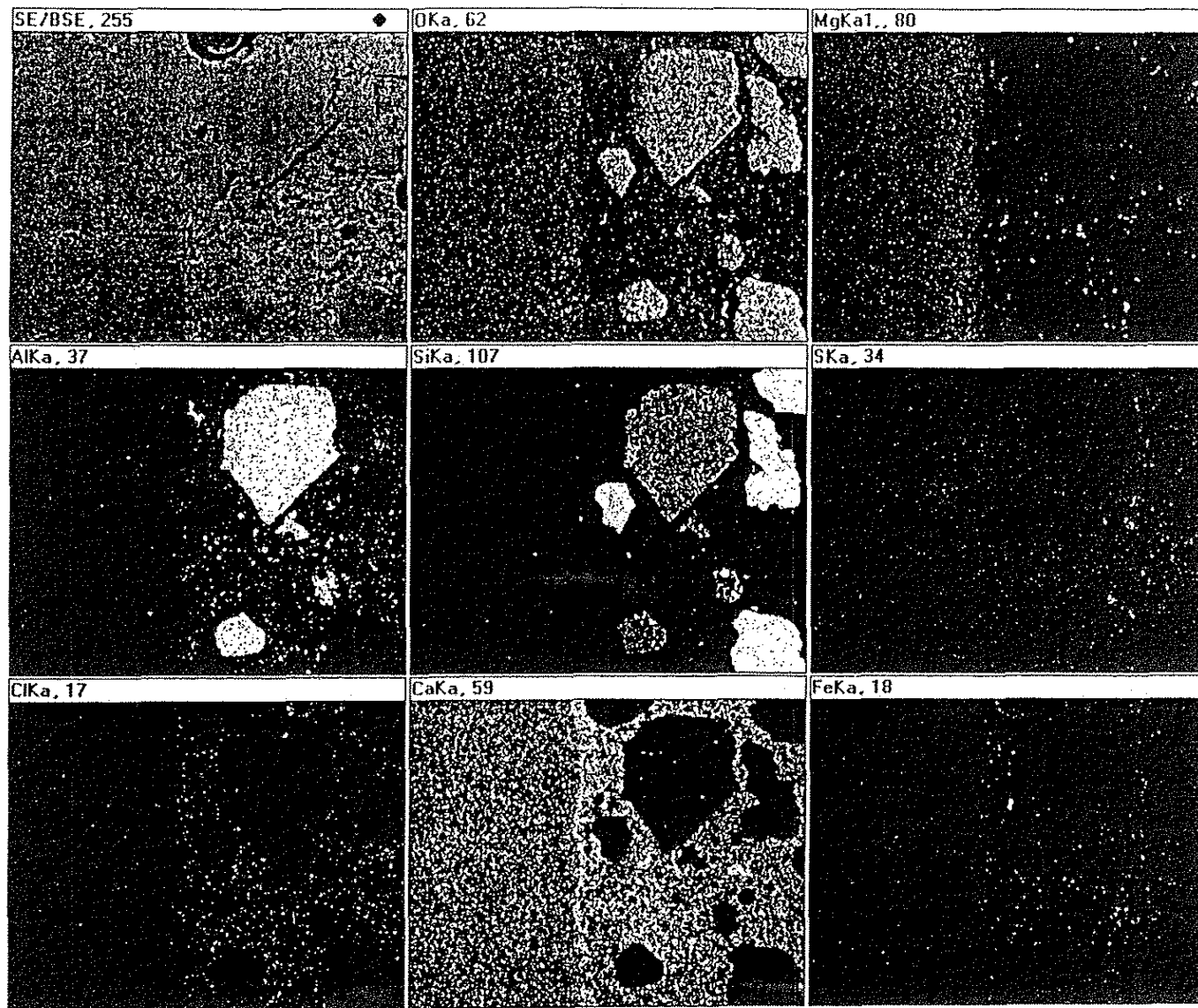
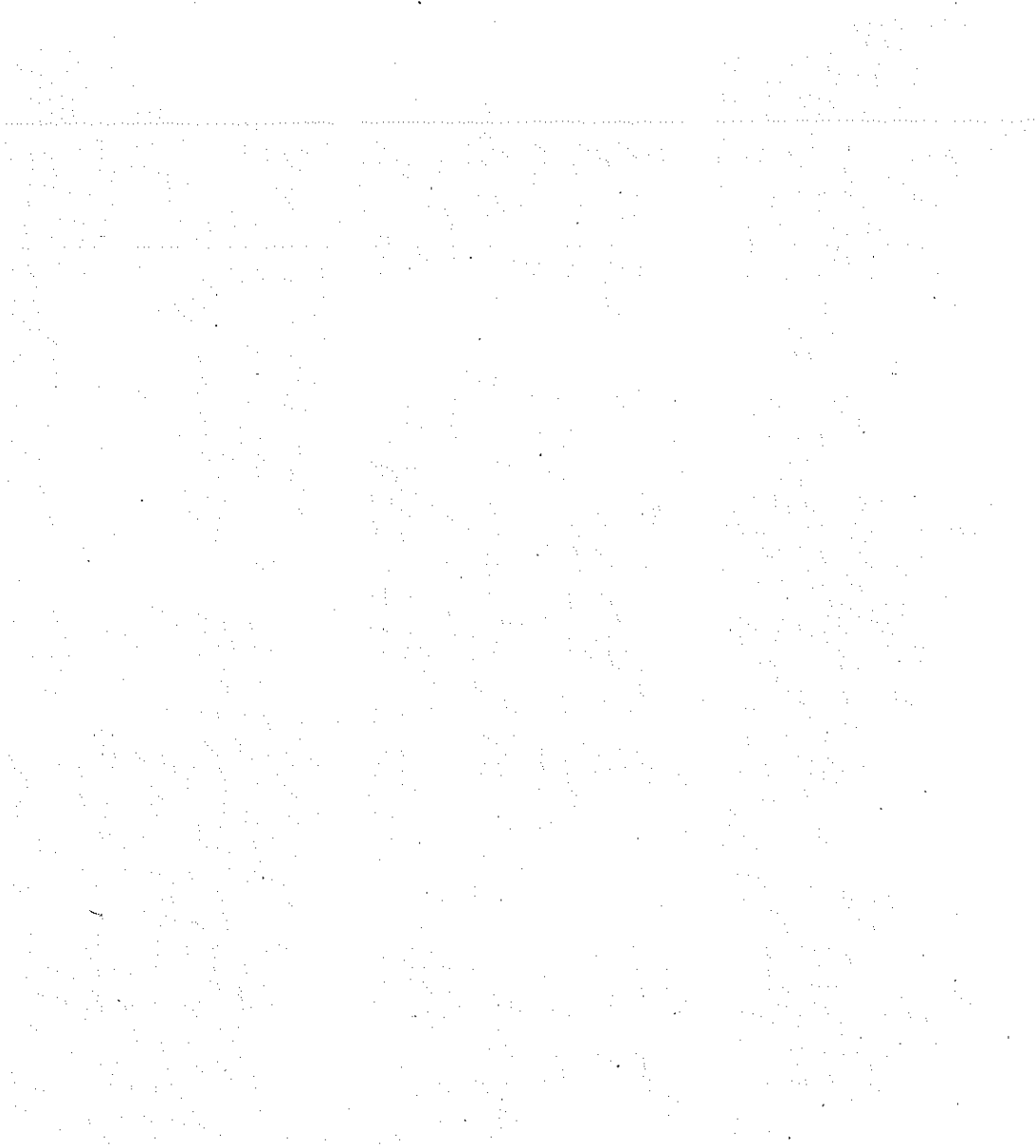


Figure 20

Figure 21.

Fig 21. Experimental decomposition of concrete. EDAX of high magnification of area shown in Fig 20. Calcite and brucite crystals occur in zone Be and Ce, and De is more Ca-rich than zone Ee. Plt XIId gives corresponding SEM photo of area.



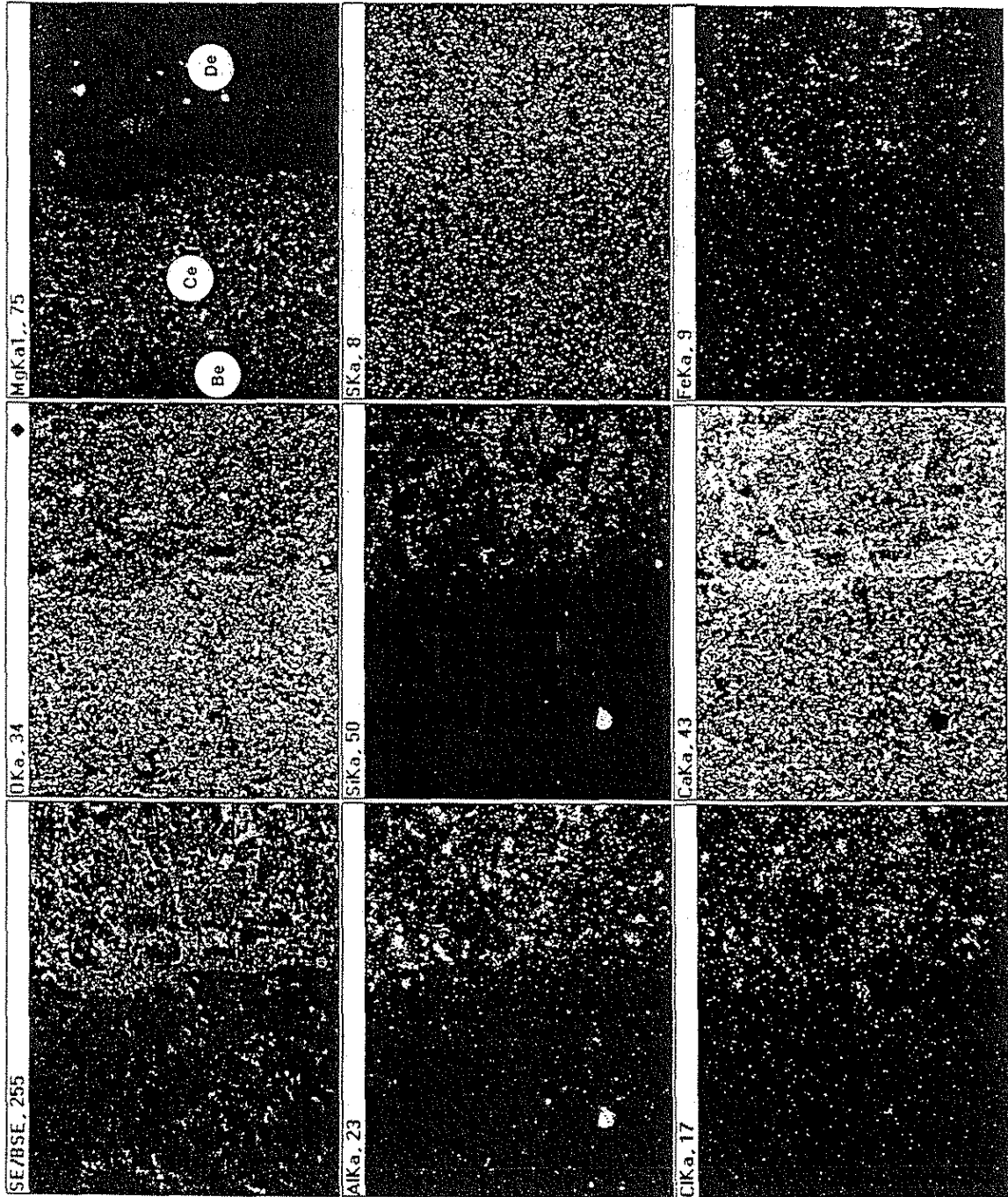


Figure 21

Figure 22.

Fig 22. Experimental decomposition of concrete. Electron microprobe traverse across concrete containing Paralta quarry aggregate after freeze/thaw cycling in Ca solution.

a. CaO and MgO traverse.

b. Na₂O, Al₂O₃ and FeO traverse.

This traverse passed entirely through a small coarse aggregate particle and into paste on both sides. The outer rims at both sides of the dolomite aggregate are enriched in MgO with CaO showing erratic but roughly corresponding decrease in the complex rims. The corresponding SEM view is shown in Plt XIe.

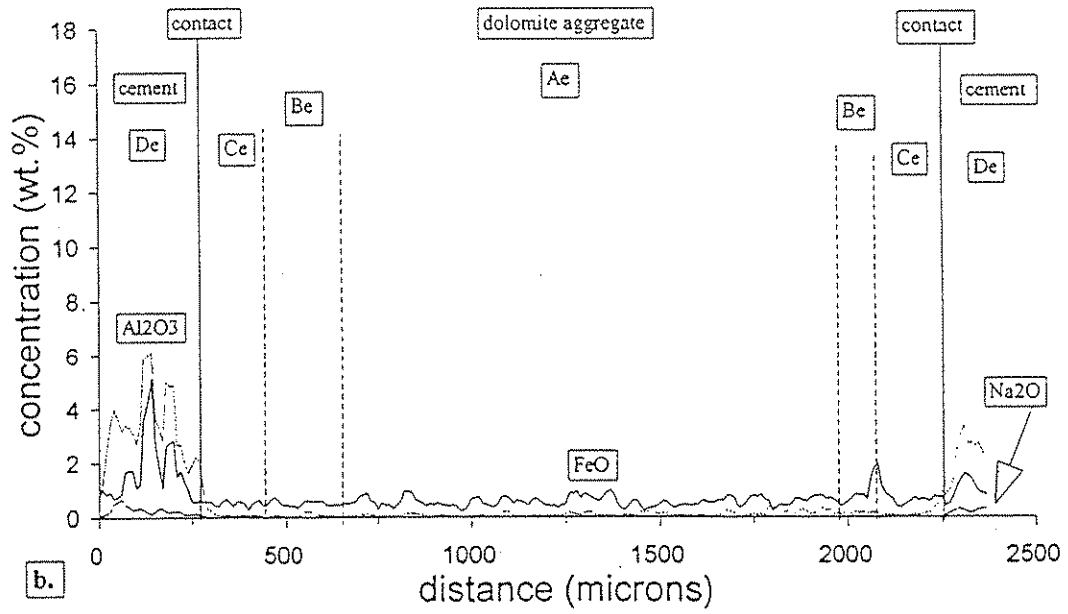
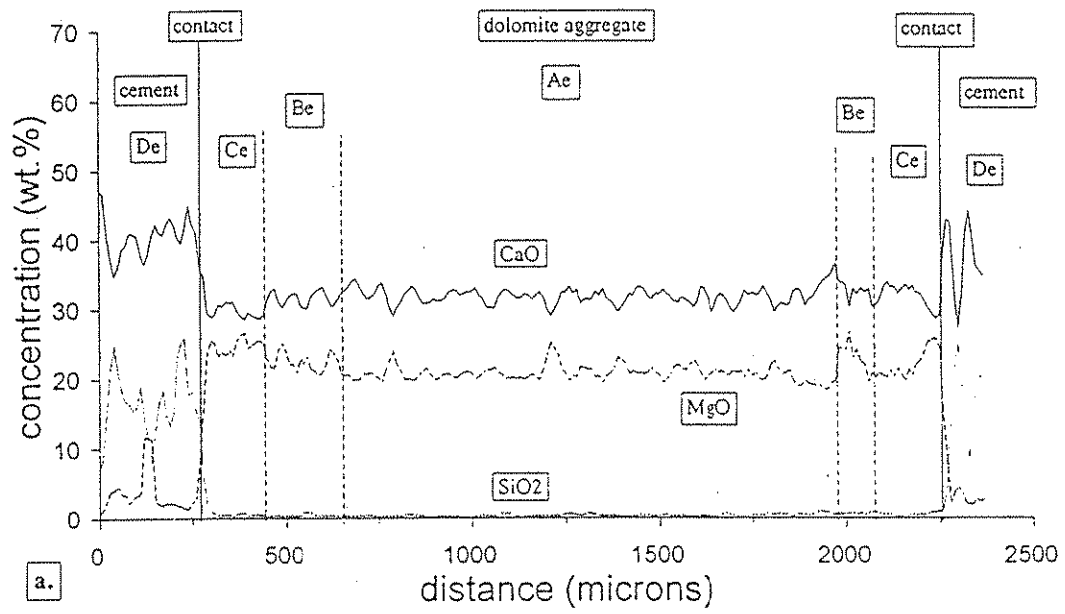


Figure 22

Figure 23.

Fig 23. Experimental decomposition of concrete. Electron microprobe traverse across concrete containing Smith quarry aggregate after wet/dry cycling in Ca solution.

a. CaO and MgO traverse.

b. Al₂O₃ and FeO traverse.

c. K₂O and Na₂O traverse.

The aggregate rim zone does not exhibit the MgO increase that was characteristic of the two previous experimentally decomposed concretes. Plt XIc shows the light micrograph of this area.

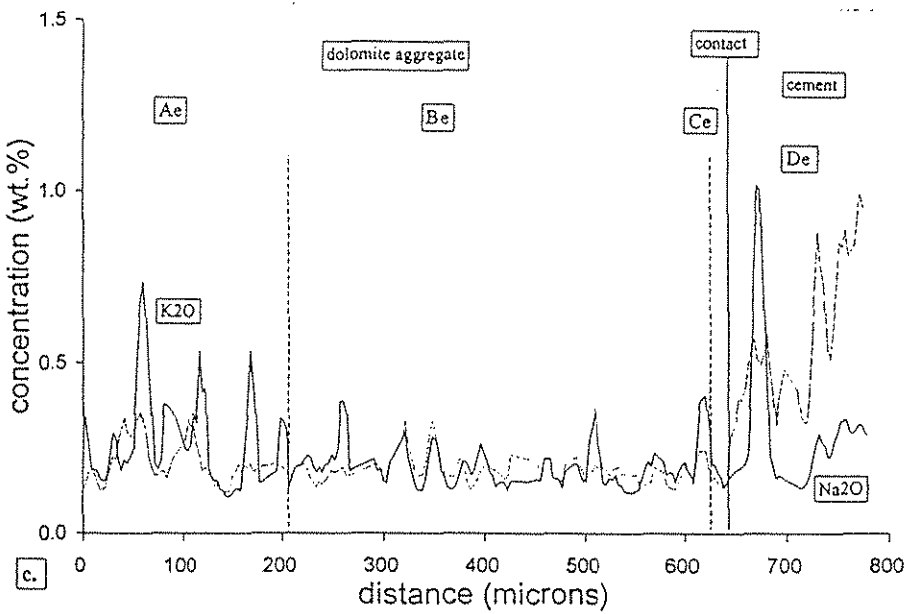
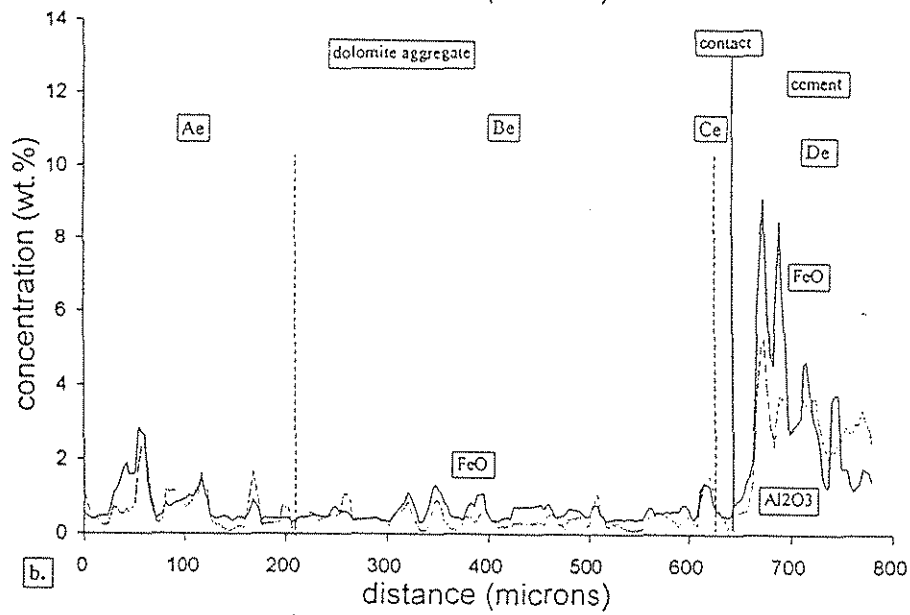
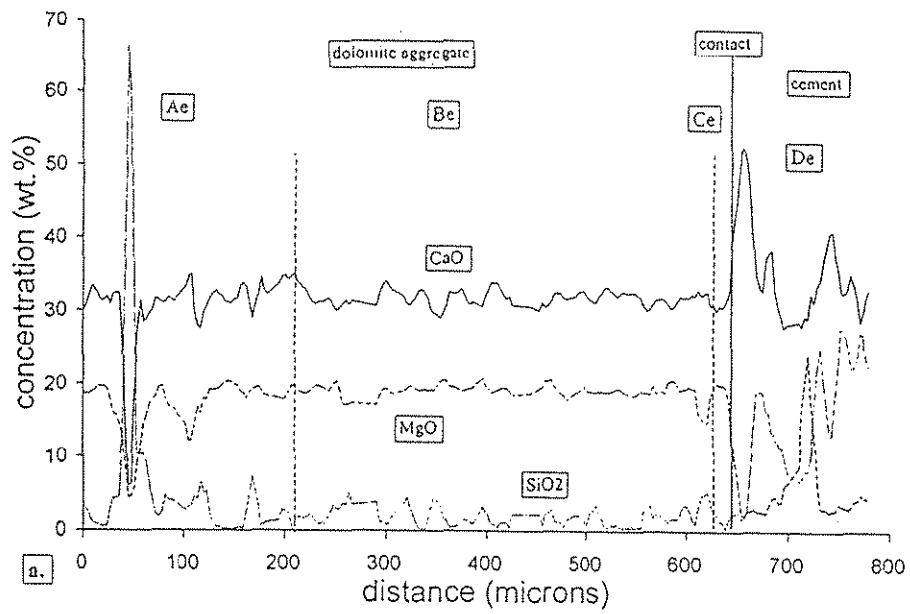


Figure 23

Figure 24.

Fig 24. Experimental decomposition of concrete. Electron microprobe traverse across durable concrete containing Mar-Jo Hills quarry aggregate after wet/dry cycling in Ca solution.

a. CaO and MgO traverse.

b. Na₂O, Al₂O₃ and FeO traverse.

There is no rim development visible in aggregate or paste. Plt XIIa,b shows light micrographs of the area.

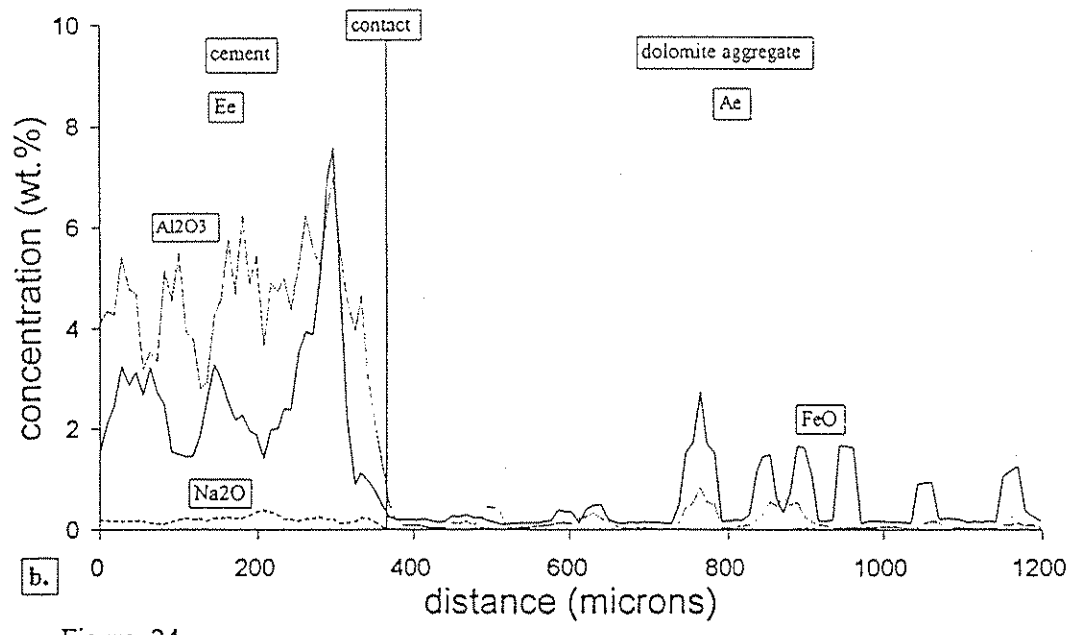
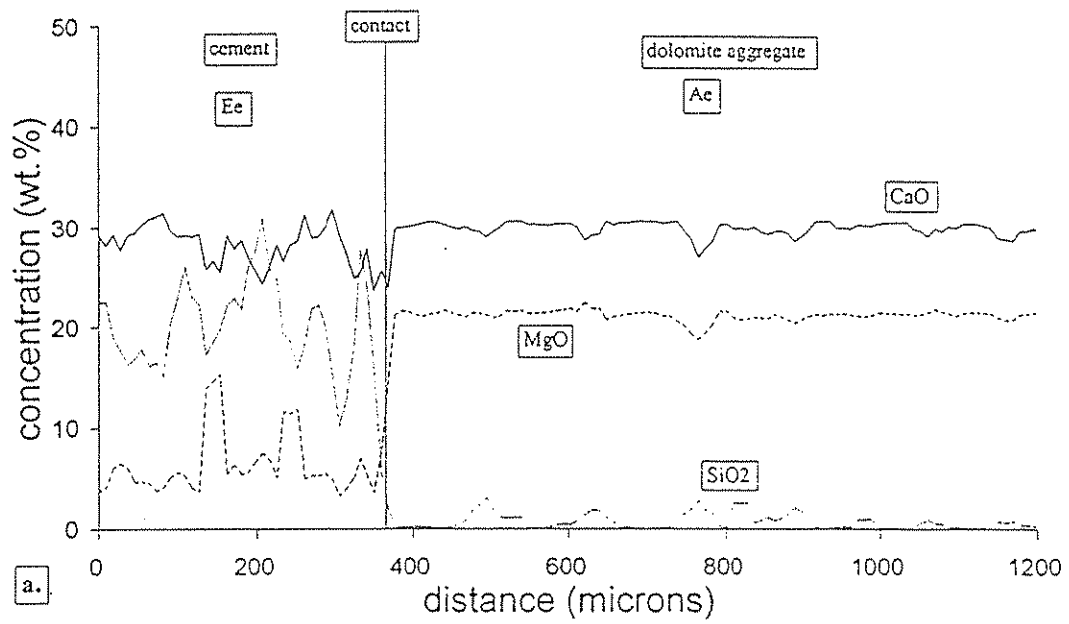


Figure 24

Figure 25.

Fig 25. Experimental decomposition of concrete. Electron microprobe traverse across concrete containing Mar-Jo Hills quarry aggregate after freeze/thaw cycling in Ca solution.

a. CaO and MgO traverse.

b. Na₂O, Al₂O₃ and FeO traverse.

There is no rim development visible in aggregate or paste. Plt XIIc,d shows light micrographs of the area.

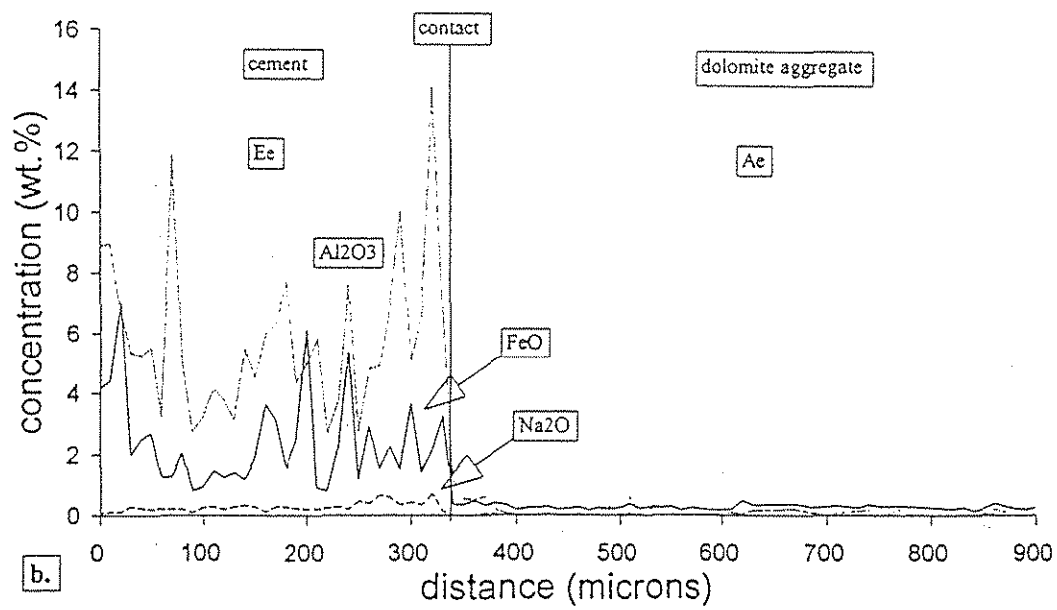
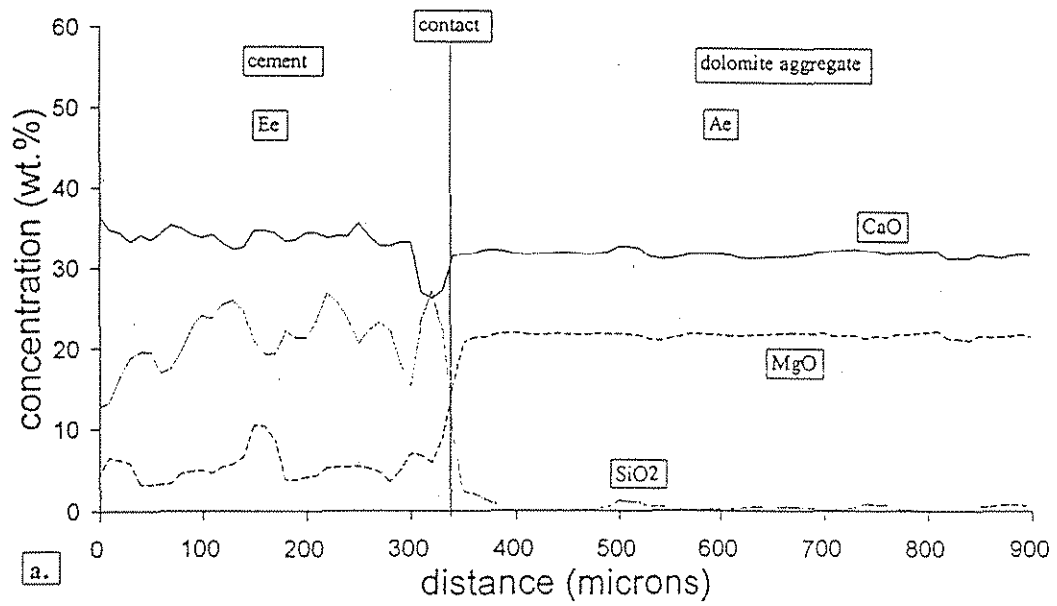


Figure 25

Figure 26.

Fig 26. Experimental decomposition of concrete. Electron microprobe traverse across concrete containing Mar-Jo Hills quarry aggregate after wet/dry cycling in Mg solution.

a. CaO and MgO traverse.

b. Na₂O, Al₂O₃ and FeO traverse.

The dolomite aggregate is relatively uniform in composition across the traverse except for the sharp CaO enrichment near the aggregate-paste boundary. Plt XIIe,f shows light micrographs of the area.

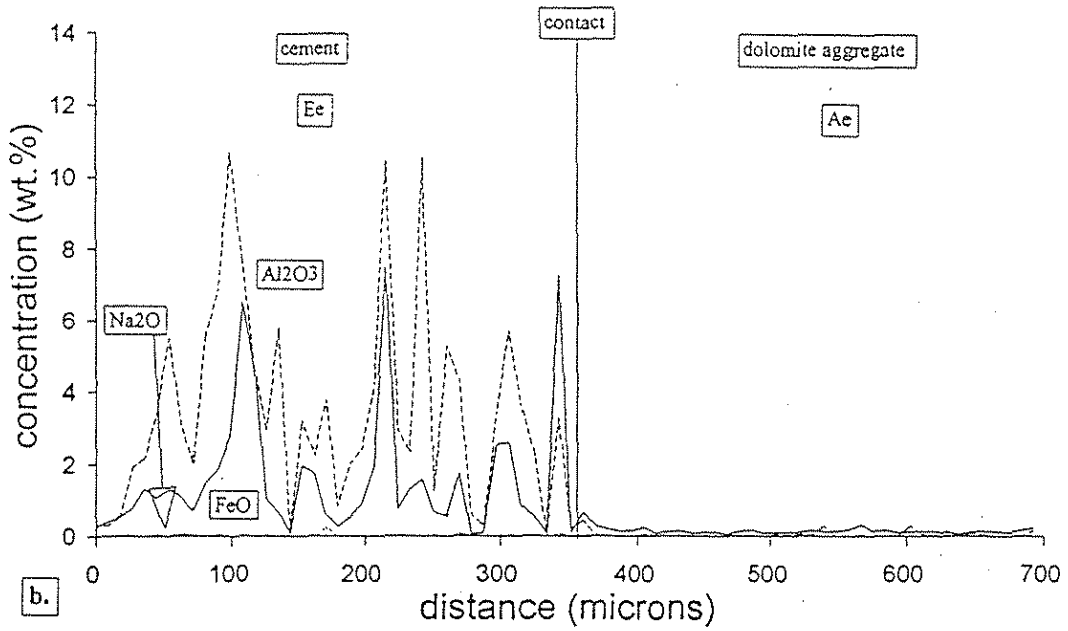
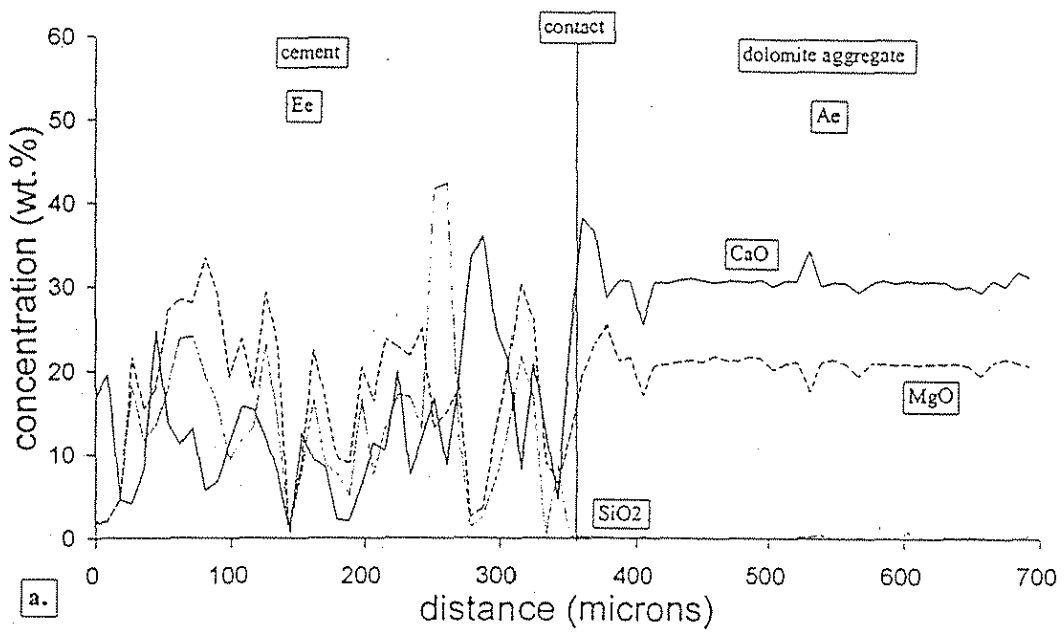


Figure 26

Figure 27.

Fig 27. Experimental decomposition of concrete. EDAX element maps of concrete containing Mar-Jo Hills aggregate after wet/dry cycling in Mg solution. The crack-fills in dolomite are calcite, brucite, and Mg chloride. In the paste, crack and void-filling minerals of various compositions are shown by element concentrations. Calcite (Ca+O), brucite (Mg+O), Mg chloride (Mg + Cl), and possibly gibbsite (Al + O), dolomite (Ca + Mg +O), quartz (Si +O), and minor amounts of an unidentified sulfur-bearing phase. Plt XIIIa shows SEM view of area.

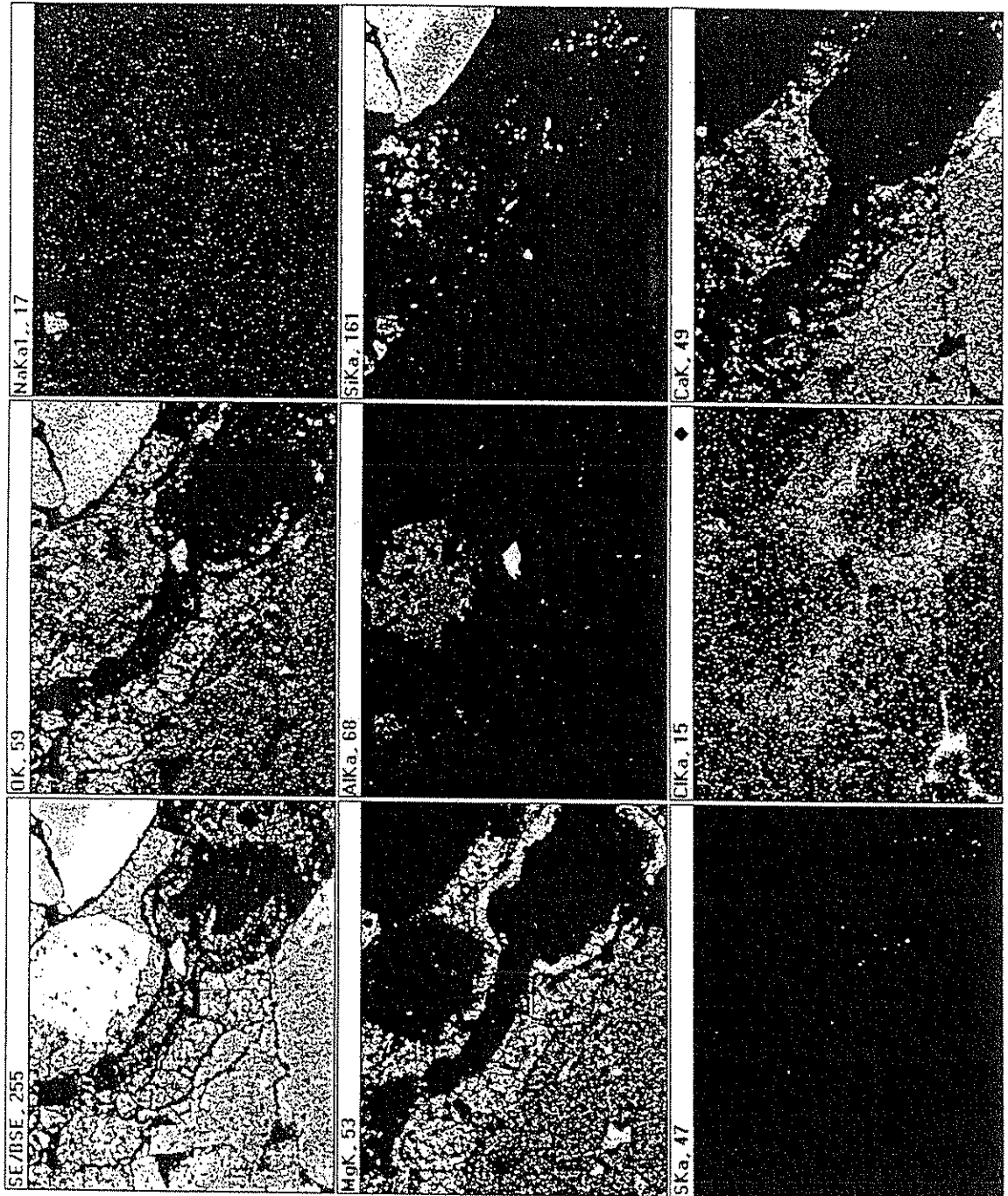


Figure 27

Figure 28.

Fig 28. Experimental decomposition of concrete. EDAX element maps of concrete containing Mar-Jo Hills aggregate after wet/dry cycling in Mg solution. Similar to that of Fig 27, except SEM micrograph of area is given in Plt XIIIb.

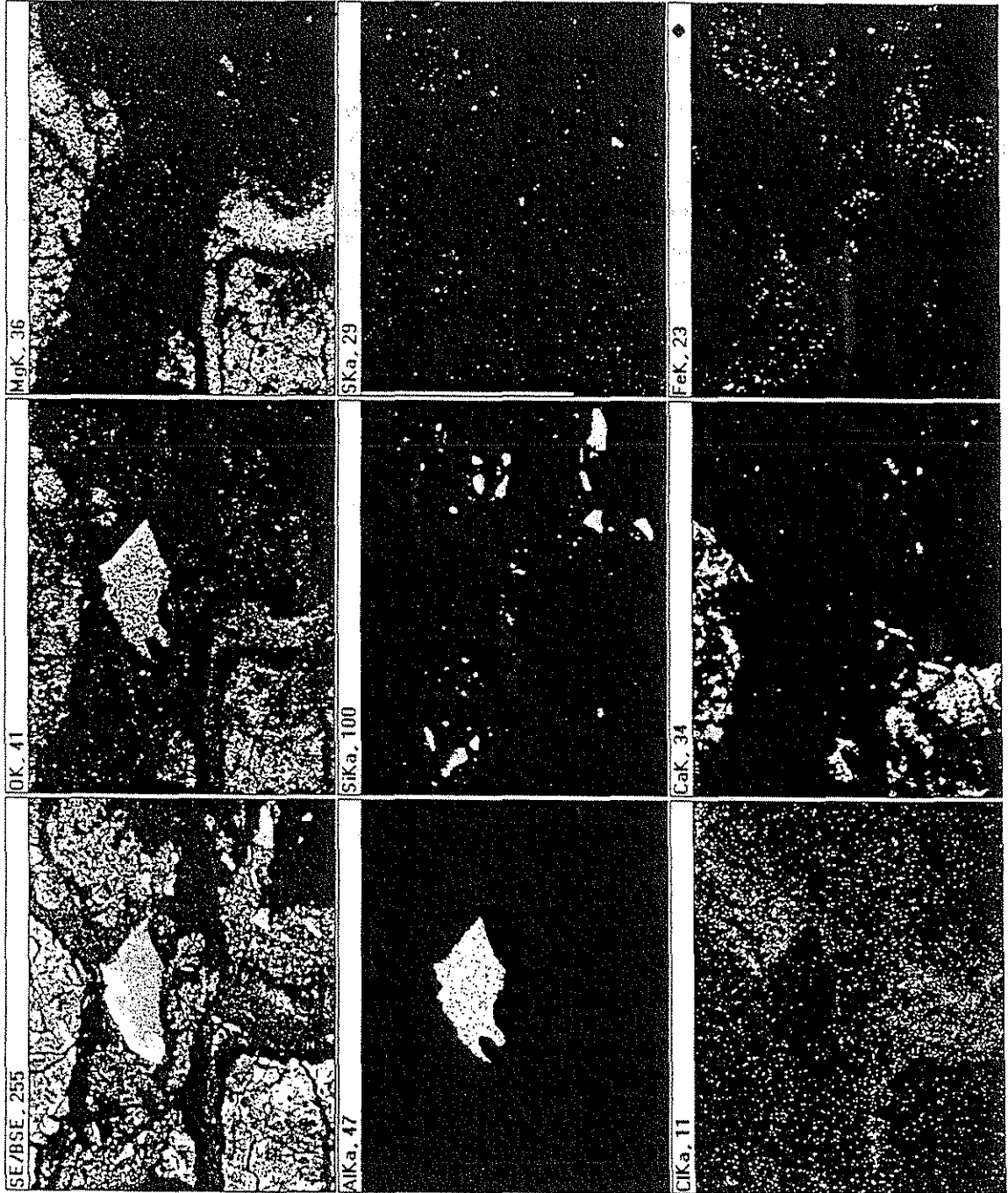


Figure 28

Figure 29.

Fig 29. Experimental decomposition of concrete. Electron microprobe traverse across concrete containing Paralta quarry aggregate after wet/dry cycling in Mg solution.

a. CaO and MgO traverse.

b. Na₂O, Al₂O₃ and FeO traverse.

Dolomite aggregate shows a relatively uniform composition across the traverse, except for a slight magnesium depletion in light-colored dolomite rim, Ce. There is little, if any, corresponding increase in calcium in the rim. The cement paste shows an expected magnesium increase as a result of the treatment. Plt XIVa,b shows corresponding area.

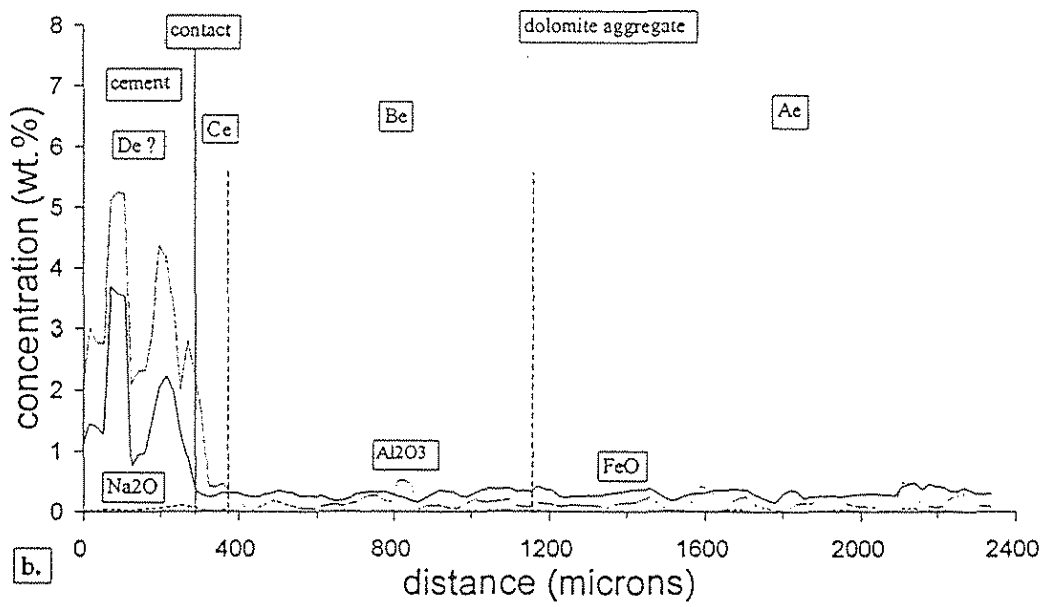
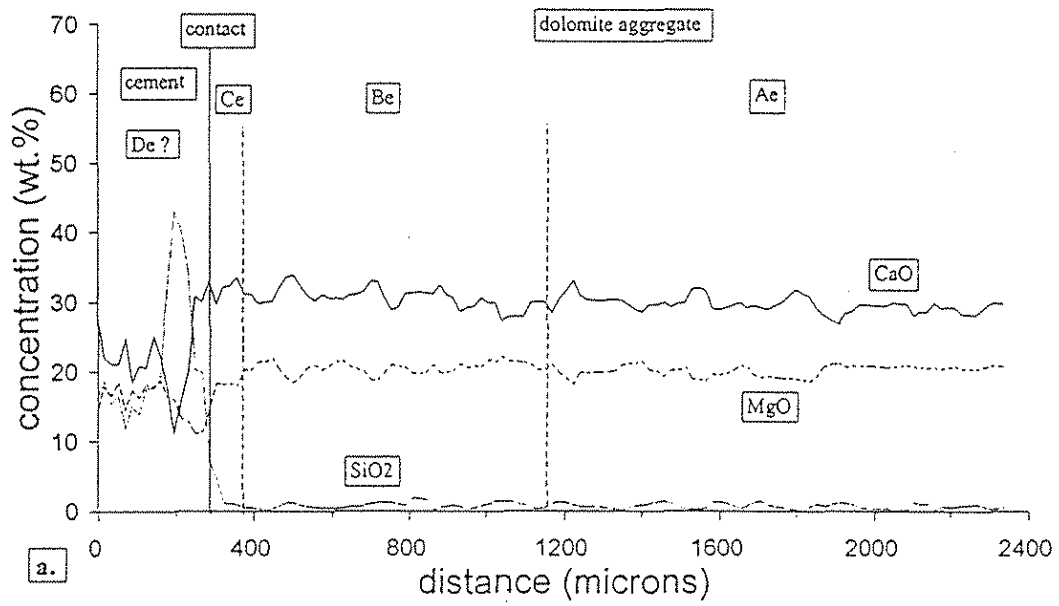


Figure 29

Figure 30.

Fig 30. Experimental decomposition of concrete. EDAX element maps of concrete containing Garrison aggregate after wet/dry cycling in Mg solution. Interstitial voids in dolomite aggregate are filled with brucite, calcite, and magnesium chloride. In the cement there are void and crack fills of brucite, magnesium chloride, and possibly calcite. Plt XIIIe,f shows light micrographs and Plt XIIIf shows SEM view of area.

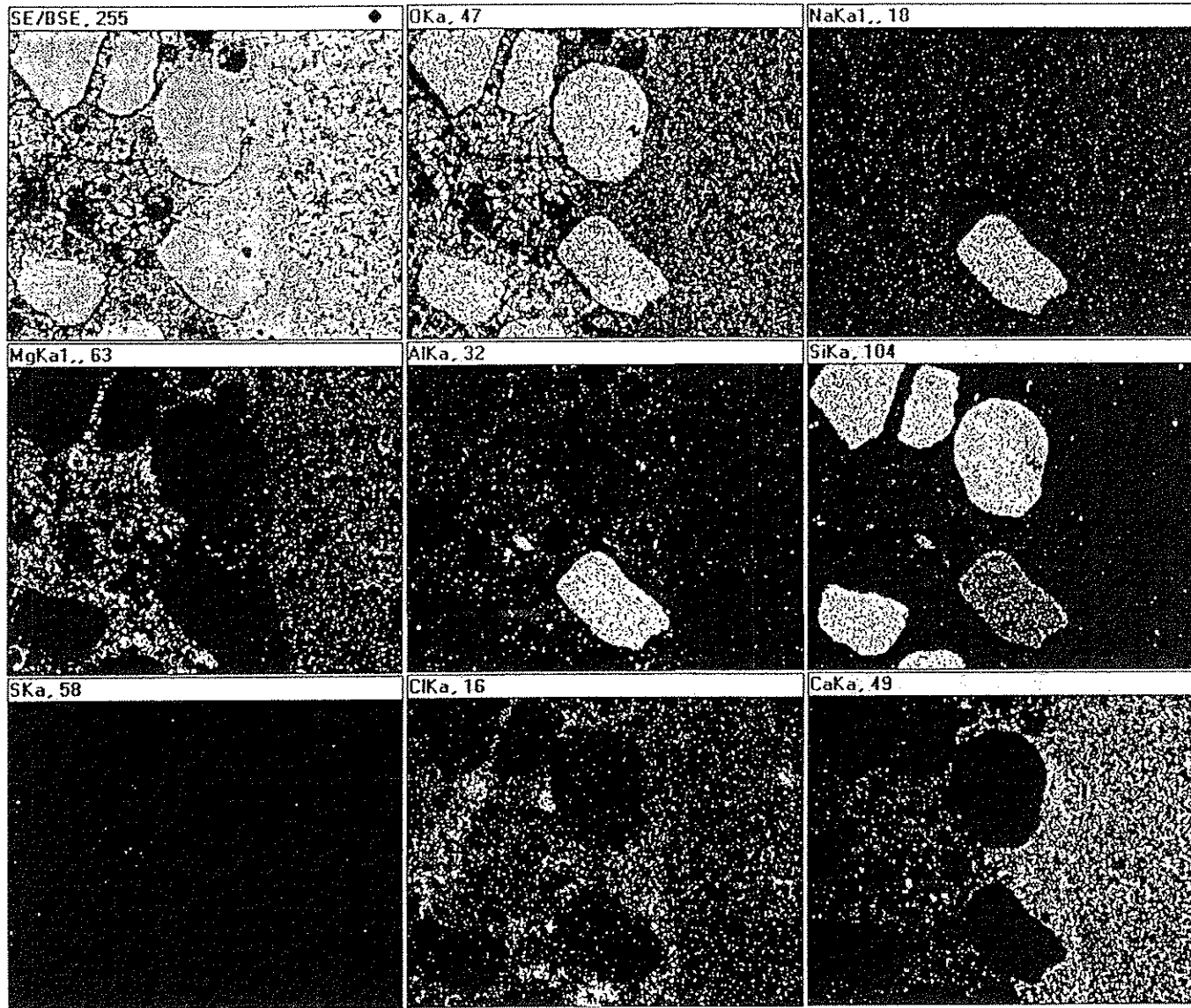


Figure 30

Figure 31.

Fig 31. Experimental decomposition of concrete. Electron microprobe traverse of concrete containing Paralta quarry aggregate after wet/dry cycling in Na solution.

a. CaO and MgO traverse.

b. Na₂O, Al₂O₃ and FeO traverse.

The dolomite has a relatively constant composition across the traverse except in the extreme outer edge of the dark dolomite rim, Be where MgO increases at the expense of CaO. This rim composition change probably was inherited from the untreated concrete. As expected, Na₂O is enriched in the paste as a result of Na treatments.

Note the enrichment of Na in the paste near the aggregate. This location was presumably more permeable to sodium migration into the paste from the experimental Na-brine. Plt XIVc,d provide light micrographs of area, and XIVE,f gives corresponding SEM view.

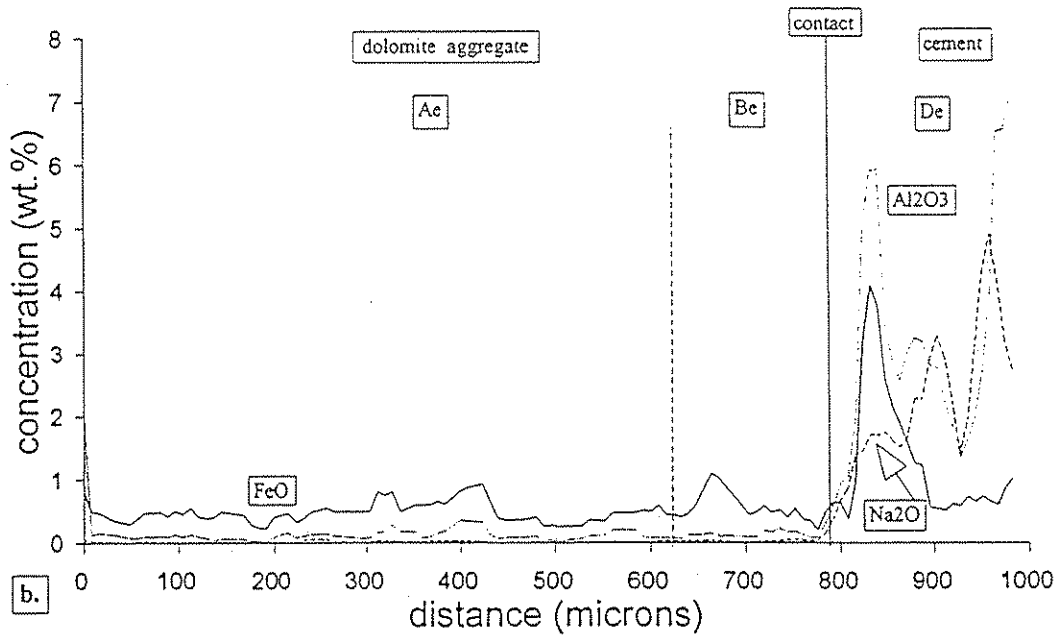
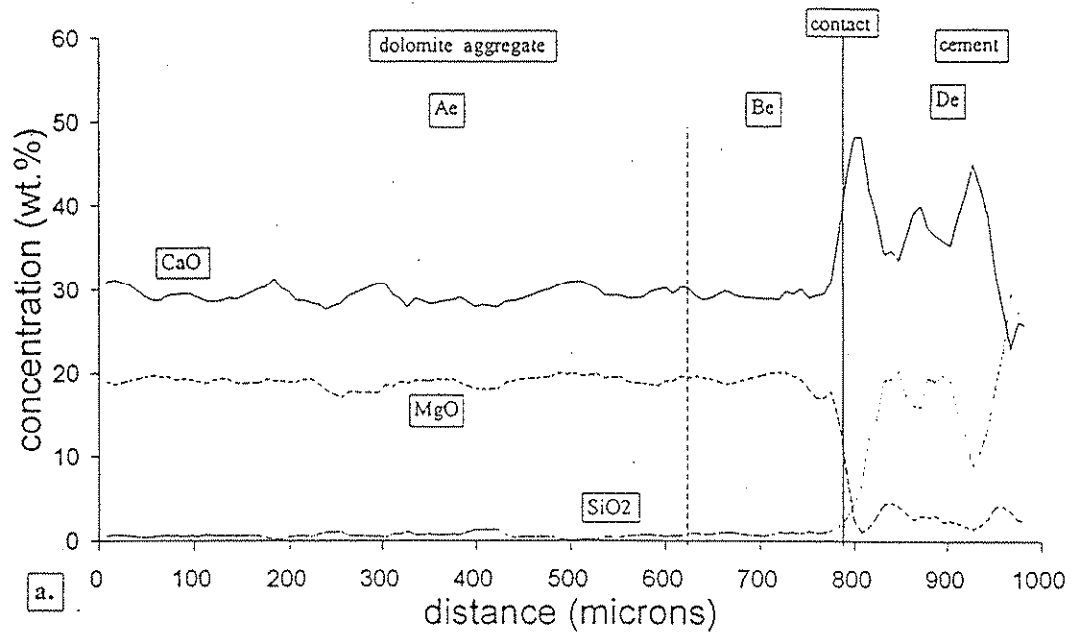


Figure 31

Figure 32.

Fig 32. Experimental decomposition of concrete. EDAX element maps of concrete containing Paralta aggregate after wet/dry cycling in Na solution. Interstitial voids in the dolomite aggregate are filled with brucite and calcite. The experimentally altered cement and its light-colored reaction rim contains brucite and sodium chloride. The light-colored rim paste in contact with the aggregate is strongly enriched in calcium. Plt XIVc, d provide light micrographs of area, and XIVE,f gives corresponding SEM view.

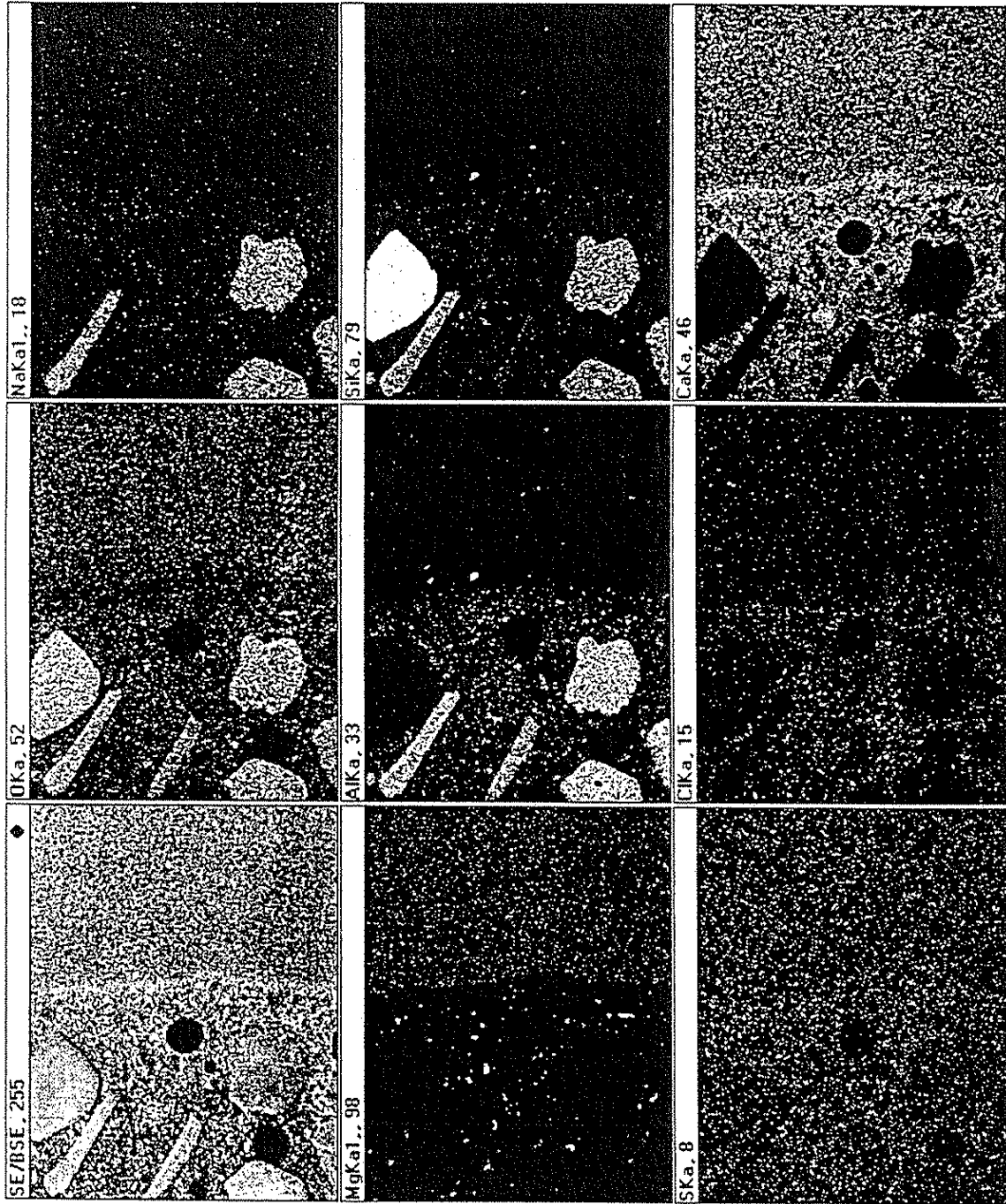


Figure 32